VIBRATION ANALYSIS OF COMPOSITE BEAMS USING HIERARCHICAL FINITE ELEMENT METHOD

Amit K. Nigam

A Thesis

in

The Department

of

Mechanical & Industrial Engineering

Presented in Partial Fulfillment of the Requirements
for the Degree of Master of Applied Science at
Concordia University
Montreal, Quebec, Canada

October, 2002

ABSTRACT

VIBRATION ANALYSIS OF COMPOSITE BEAMS USING HIERARCHICAL FINITE ELEMENT METHOD

Amit K. Nigam

The conventional finite element formulation has limitations in performing the dynamic analysis of composite beams. The discretization necessary for obtaining solutions with acceptable accuracy in the determination of dynamic response parameters leads to discontinuities in stress and strain distributions. The hierarchical finite element formulation provides us with the advantages of using fewer elements and obtaining better accuracy in the calculation of natural frequencies, displacements and stresses. The hierarchical finite element formulation for uniform and variable-thickness composite beams is developed in the present work. Two sub-formulations of hierarchical finite element method viz. polynomial and trigonometric sub-formulations have been developed. The efficiency and accuracy of the developed formulation are established in comparison with closed-form solutions for uniform composite beams. The static response of uniform composite beams is evaluated using the hierarchical finite element method. The dynamic response of variable-thickness composite beams is calculated based on the developed formulation. A detailed parametric study encompassing the influences of boundary conditions, laminate configuration, taper angle and the type of taper on the

dynamic response of the beam is performed. The NCT-301 graphite-epoxy composite material is considered in the analysis and in the parametric study.

Acknowledgements

It is a genuine pleasure for me to be able to take this opportunity to acknowledge the numerous people without whom this work would not have been possible. First and foremost, I want to express my most sincere gratitude to Dr. Rajamohan Ganesan. Throughout my research, he provided me endless support that I consider to be unparalleled by other research advisors. Above and beyond this, he afforded me his time, patience, and tolerance in addition to his keen, incisive insight and guidance. In short, Dr. Ganesan enhanced the value and experience of my graduate research immeasurably, and for this I thank him.

I would be amiss to neglect to mention how much I appreciate my time sharing an office with Shashank Venugopal and Vijay Kowda. Not only are they the ideal officemates, but are also good friends. We have shared a chemistry in our office like no other, and we have all had tremendous fun. I will always look back on the time we shared with a smile.

Outside of my research environment, there have been a few people whose aspirations and encouragement kept my spirits up throughout my indentured servitude to Concordia University. I wish to thank my mom, Suman Nigam and my father Dr. Mohan S. Nigam. Their confidence in me helped me face the slings and arrows of the M.A.Sc. program with decisive certainty. My mother has pushed me to excel academically for as long as I can remember, and I am as proud to present to her this accomplishment as she is to see it. I love them both dearly.

TABLE OF CONTENTS

LIST OF FIGURES

LIST OF TABLES

Nomenclature

E	Young's modulus
I	mass moment of inertia
W	transverse deflection, as a function of X or x only
θ	slope of the beam (function of x)
w	transverse deflection, as a function of X and time 't'
w_m	amplitude of the hierarchical function applied to transverse displacement
θ_m	amplitude of the hierarchical function applied to rotation
w_r	amplitude of the hierarchical function applied to transverse displacement
θ_r	amplitude of the hierarchical function applied to rotation
A_r	amplitude of the polynomial term
r_1	variable defining the coefficients of the hierarchical terms added to transverse displacement
r_2	variable defining the coefficients of the hierarchical terms added to rotation
m_1	variable defining the coefficients of the hierarchical terms added to transverse displacement
m_2	variable defining the coefficients of the hierarchical terms added to rotation
p	p co-ordinate system
q	q co-ordinate system

ψ	rotation of the longitudinal axis
$\bar{\gamma}$	mean shear deformation angle
ϕ	modal matrix
$\bar{\theta}$	taper angle of the variable-thickness beam
b	laminate width
ε_x°	strain component in the x direction on the reference plane
κ_x	curvature in the x direction
ρ	mass density of the laminate material
A	area of cross-section of the laminate
$\bar{m}$	mass per unit length
q'	distributed transverse load (function of X and t)
L	beam span
l	beam element length
ξ	non-dimensional co-ordinate
t	time
λ	square of the natural frequency, ω
τ	arbitrary function of time
v	weight function
[N]	interpolation function matrix
Q_i	generalized force matrix
[K]	beam element stiffness matrix
[M]	beam element mass matrix

$[K_q]$	element stiffness matrix in the in the q co-ordinate system
$[M_q]$	element mass matrix in the in the q co-ordinate system
$[K_p]$	element stiffness matrix in the in the p co-ordinate system
$[M_p]$	element mass matrix in the in the p co-ordinate system
K_t	constant used in the closed form solution of beams
[F]	equivalent nodal force vector
[Q]	ply stiffness in the laminate co-ordinates
$[\overline{Q}]$	transformed ply stiffness matrix
$[C']$	ply stiffness in the laminate reference
[A]	laminate axial stiffness matrix (relating normal and shear forces per unit width to mid-plane strain components)
[B]	bending-stretching coupling matrix
[D]	laminate bending or flexural stiffness matrix (relating bending and twisting moments per unit width to curvatures)
N_x	in-plane force resultant
M_x	bending moment resultant
$b\,D_{11}$	laminate flexural rigidity
D_{11}^*	first element in $[D]^{-1}$
G_{12}	in-plane shear modulus
G_{23}	out-of-plane shear modulus
[H]	transverse shear stiffness of the laminate

[F]	shear stiffness of the laminate
k	shear correction factor
t_p	ply thickness
m	slope of the centerline of a ply in the tapered laminate
g	intercept of the centerline of a ply in the tapered laminate
v_{12}	poisson's ratio between the fiber direction (1) and the transverse direction (2)
ω	natural frequency of the beam
{d}	global degrees of freedom vector
[T]	transformation matrix
h	laminate height
U_j	common variable for all nodal variables (degrees of freedom) in local co-ordinates
P_n	modal force
	non-dimensional frequency
nTm	refers to solutions with n beam elements and m trigonometric terms in each element
nPm	refers to solutions with n beam elements and m polynomial terms in each element

Chapter 1

INTRODUCTION

1.1 Dynamic Analysis in Mechanical Design

Mechanical components and structures are subjected to forces of time dependent nature. Analysis and design of such components and structures subjected to dynamic loads involve consideration of time-dependant inertial forces and dissipation forces in addition to time-dependant elastic forces. A dynamic analysis does not have a single solution as in the case of static problem. Instead, the analyst must establish a succession of solutions corresponding to all times of interest in the response history.

One of the ways in which a component or structure can get damaged or become useless is through a dynamic response to time-dependant loads, resulting in too large deflections or too high stresses or fatigue damage. The dynamic loading on a structure can vary from a recurring cyclic loading of the same magnitude to the other extreme of a short time intense non-recurring load, termed as shock or impact loading. A number of different types of dynamic loads exist between these two extremes of harmonic oscillation and impact loading. In both the cases, the free vibration response of the component becomes a controlling aspect.

1.2 Composite Materials and Structures in Mechanical Design

Basically, a composite material consists of two or more constituent materials or phases that have significantly different macroscopic behavior and a distinct interface between each constituent (on the microscopic level). This includes the continuous fiber-reinforced laminated composites that are of primary concern herein, as well as a variety of composites not specifically addressed.

The term composites is usually referred to materials that are combinations of two or more organic or inorganic components, of which one serves as the matrix and the other as fibers. Individual fiber is usually stiffer and stronger than the matrix. The central concept behind composites is that the fibers and the matrix can blend into a new material with properties that are better than those of the constituent parts. In addition, by changing the orientation of the fibers, the composites can be optimized for strength, stiffness, fatigue, heat and moisture resistance, etc. It is therefore feasible to tailor the material to meet specific needs. Composite materials also have much higher strength to weight and stiffness to weight ratios than the conventional materials.

Tapered composites are formed by terminating or dropping off some of the plies in primary structures. Their elastic tailoring properties and potential for creating more significant weight savings than commonly used laminated components allow an increasing use of tapered composites in commercial and military aircraft applications. A typical example is a helicopter yoke, where a progressive variation in the thickness of the

yoke is required to provide high stiffness at the hub and relative flexibility at the mid-length of the yoke to accommodate flapping. The first commercial composite rotor-blade yoke assembly made from glass-fiber/epoxy composite was fabricated at Bell Helicopter Textron. Constructed completely from S-2 glass, the dual yoke assemblies in the Bell 430 helicopter endure several times more flight hours than traditional titanium or steel yokes, and also provide improved safety. Much more tolerance to damage than conventional materials and the elimination of corrosion are also displayed by these composite components. Other applications include composite-aircraft wing skins, helicopter flex-beams, flywheels, etc.

1.3 Finite Element Method in Mechanical Design

The analysis of laminated composite beams is usually based on three approaches, classical theory of elasticity, theory of mechanics of materials, and variational methods. The governing equations of motion are generally nonlinear partial differential equations, which are extremely difficult to solve in the closed form. The availability and sophistication of modern digital computers has made possible the extensive use of the finite element method for analyzing complex structures. Finite Element Method (FEM) is one of the most powerful numerical analysis tools in the engineering and physical sciences. In spite of its tremendous potential, the FEM has some drawbacks too. Specially for the analysis of uniform and tapered composite beams, the conventional FEM lacks on some counts. The Hierarchical Finite Element Method (HFEM), provides us with critical advantages of using fewer elements and obtaining better accuracy in the calculation of

natural frequencies, displacements and stresses of uniform and thickness-tapered composite beams.

1.4 Literature Survey

In the following sub-sections a comprehensive and up-to-date literature survey on relevant topics is presented. Important works done on the dynamic analysis of composite beams by analytical, experimental and finite element methodologies have been chronicled. Details for both the uniform and thickness-tapered composite beams have been presented. After a brief history of the hierarchical finite element method, seminal works on the HFEM analysis of beams and plates are given. Finally, the works on the HFEM analysis of composite beams have been presented, though the quantity of such works is of course very limited.

1.4.1 Dynamic analysis of composite beams

There is a wealth of literature available for the vibration analysis of laminated plates and shells. In comparison, study on the analysis of laminated beams has been scarce despite their applicability in important structures such as turbine blades, helicopter blades, robot arms, etc. Also, the analysis of laminated beams has been restricted to eigenvalue analysis.

Abarcar and Cunniff [1] obtained experimental results for the natural frequencies and the mode shapes of cantilevered beams with solid cross-sections made out of graphite-epoxy and boron-epoxy composites. They also clearly established that there is

interaction between bending and twisting. Teoh and Huang [2] made a theoretical analysis of the vibration of composite beams based on a Timoshenko beam model. Teh and Huang [3] extended the work to show that the bending-torsion coupling of orthotropic beams with solid cross-section is dependent on fiber orientation and the wavelength of the mode. The paper by Kapania and Raciti [4] details the developments in the vibration analysis of laminated composite beams. In recent years several authors have tried to predict the natural frequencies of laminated beams of uniform- thickness. Miller and Adams [5] studied the vibration characteristics of orthotropic clamped-free beams using classical lamination theory. Vinson and Sierakowiski [6] have given exact solutions based on classical lamination theory, which neglects the effects of the rotary inertia and shearing deformation. Chen and Yang [7] and Chandrashekhara et al. [8] have carried out the free vibration analysis of composite beams based on first order shear deformation theory. Recently Chandrashekhara and Bangera [9] have studied the free vibration characteristics of laminated composite beams using a third order shear deformation theory. They have corrected generalized force and generalized strain relations to consider the Poisson effect by ignoring the forces in the *y* direction, which is along the breadth of the beam. Their solution involves inversion of certain matrices and is limited to the type of beam theory that the analyst would be using. It would be appropriate to correct stress-strain relations rather than to correct the generalized force and generalized strain relations [10]. Abramovich [11] presented exact solutions based on the Timoshenko-type equations for symmetrically laminated composite beams with ten different boundary conditions. The rotary inertia and shear deformation effects were investigated for simply supported straight beams. Singh and Abdelnassar [12] examined the forced vibration

response of composite beams considering a third order shear deformation theory. Krishnaswamy et al. [13] obtained the governing equations of laminated composite beams using the Hamilton's principle and presented the analytical solutions. Abramovich and Livshits [14] studied the in-plane free vibrations of non-symmetrically laminated cross-ply composite beams based on Timoshenko-type equations. Khedier and Reddy [15] investigated the free vibration of cross-ply laminated beams with arbitrary boundary conditions by the state space approach (matrix transfer method) and higher order shear deformation theory. Eisenberger et al. [16] used the dynamic stiffness analysis of laminated beams using a first order shear deformation theory. Abramovich et al. [17] treated vibration of multi-span non-symmetric composite beams. Zappe and Lesiutre [18] presented a smeared laminate model based on the first order shear deformation theory for the dynamic analysis of laminated beams.

The dynamic analysis of uniform and tapered composite beams, using finite element method has been conducted only in few existing works and the number of such works is substantially less as compared to the works on the analysis of laminated plates. A review of the literature (see, eg., [4]) indicates this clearly. Yuan and Miller [19,20] have developed beam finite elements. The models include separate rotational degrees of freedom for each lamina but do not require additional axial or transverse degrees of freedom beyond that necessary for a single lamina. A set of higher order theories with C° finite elements having five, six and seven degrees of freedom per node for the analysis of composite and sandwich beams have been presented by Manjunatha and Kant [21]. An interlaminar stress continuity theory via the multi-layer approach has been presented by

Lee and Liu [22]. This theory satisfies the continuity equations of both interlaminar shear stresses and interlaminar normal stresses at a composite interface. Shi, Lam and Tay [23] discuss an efficient finite element modeling technique based on the higher order theories for the analysis of composite beams. They illustrate how to choose the proper strain expressions to formulate accurate elements under the same number of nodal degrees of freedom. Shi and Lam [24] present a new finite element based on the third order beam theory. They use Hamilton's principle to obtain the variational consistent equation of motion in matrix form corresponding to the third order shear deformation theory. They also study the influence of mass components resulting from the higher order displacements on the frequencies of flexural vibrations. Hodges et al. [25] solved the equations of motion using a mixed finite element and an exact integration method.

The effect of non-uniformity has been discussed by several authors. The paper by Karabalis and Beskos [26] contains a comprehensive list of references on the subject. Venkatesh and Rao [27] developed a curved element based on the classical lamination theory. The element has two nodes and eight degrees of freedom per node. The bending, stretching and twisting actions can be modeled by this element. Nabi and Ganesan [28] developed a general finite element code based on the first order shear deformation theory. Oral [29] has formulated a three-node finite element with six degrees of freedom per node, three displacements and three independent rotations for a linearly tapered symmetrically laminated composite beam using first order shear deformation theory. This element is obtained from a five-node parent element by constraining the shear angle variation along the length to be linear. Rao and Ganesan [30,31] considered the harmonic

response of tapered composite beams by using a finite element model based on a higher order shear deformation theory. They include the Poisson's effect and also consider the effects of in-plane and rotary inertia. More broadly, a detailed review of the recent advances in the study of tapered laminated composite structures is given in the paper by He, Hoa and Ganesan [32]. This review article focuses mainly on the stress analysis, fracture behavior and the optimization for static response of tapered composite plates.

1.4.2 Hierarchical Finite Element Method (HFEM)

The finite element method has been serving as a powerful tool for the analysis of structures. The finite element method in general, is a special case of the Rayleigh-Ritz method, with the main difference between the two lying in the choice of admissible functions used in the series representation of the solution [33]. The standard Finite Element method consists of dividing the domain of interest into a number of smaller – although not necessarily identical–convex sub-domains called Finite Elements. The solution is then approximated by locally admissible polynomial functions, which are piecewise smooth only over each individual sub-domain.

There are various procedures that exist for the refinement of the finite element solutions. Broadly these fall into two categories: The first, and the most common, involves refining the mesh while keeping the degree of the elements fixed. This is termed as the *h*-version of the finite element method, or simply the finite element method. The second method involves keeping the mesh size constant and letting the degree of the approximating polynomial to tend to infinity [34,35]. This approach is better known as the *p*- version of the finite element method or the Hierarchical Finite Element Method

(HFEM). Clearly, the HFEM has much in common with the classical Rayleigh–Ritz method; however, greater versatility and improved rates of convergence always result, since local (as opposed to global) admissible displacement functions are used [36].

Hierarchical functions were initially introduced by Zienkiewicz et al. [37] with the objective of introduction of p-graded meshes in an *a priori* chosen manner. Initial applications included the analysis of the nuclear reactor vessels [38]. Subsequently, new and useful families of p-type elements were introduced by Peano et al. [34,39-40]. Explicit discussion of hierarchical functions has been done by Zienkiewicz et al. [41]. The use of non-uniform p-refinement in finite element method done hierarchically was initiated by Kelly et al. [42] and Gago et al. [43]. These papers as parts I and II respectively, deal with error analysis and adaptive processes applied to finite element calculations. In part I, they derive the basic theory and methods of deriving error estimates for second order problems. In part II, they provide in detail a strategy for adaptive refinement and concentrate on the p-convergent methods. It is shown that an extremely high rate of convergence is reached in practical problems using such procedures. They also present applications to realistic stress analysis and potential problems. Babuska et al. [35] describe the mathematical aspect of the convergence of the finite element solution for p-refinement. Szabo [44] showed that uniform p-refinement also allows the global energy norm error to be approximately extrapolated by three consecutive solutions.

The transition of the hierarchical finite element method from the developmental stages to the application stages has been rather arduous. In general, it offers superior performance to the h-version, but it took a long time for its merits to be recognized at the commercial level [45]. Polynomial functions are more common in the finite element analysis. With regards to the HFEM, Legendre polynomials in the Rodrigues form are quite popular. They have, for example been applied to linear analysis of plates in references [46,47] and to non-linear dynamic analysis of beams and plates in the frequency domain in references [48-52]. In these references, it has been shown that convergence is achieved with far fewer degrees of freedom in the HFEM than that in the h-version of the FEM. Bardell et al. [53] applied the h-p method to study linear vibrations of shells.

Beam eigenfunctions, exact solutions of the linear problems, are hyperbolic-trigonometric or only trigonometric, depending on the boundary conditions. Since the non-linear mode shape is either similar (though generally different) to a linear mode, or to a combination of linear modes [52], a beam element built with these eigenfunctions should require a reduced number of degrees of freedom for accuracy in dynamic analysis. Another advantage of these functions is that the linear stiffness matrices and the mass matrices are diagonal, and therefore they are well-conditioned and they have several computational benefits. Also, since higher order polynomials are ill-conditioned [54], some researchers advised the use of trigonometric displacement shape functions [54-59].

The idea of using trigonometric terms in the finite element method is not new. Pian [60] described the concept of using more co-ordinates than the element nodal displacements in deriving element stiffness matrices. Krahula and Polhemus [59] used the Fourier series for a rectangular plane stress element. The desirability of using higher order finite elements for vibration problems has been shown by many authors. Thomas and Documaci [60] have shown that high order finite elements yield improved results for the vibration of tapered beams. Dawe [61] suggested that an increase in efficiency would result in the vibration analysis of plates using the Mindlin theory, if finite elements of order higher than those used in previous Timoshenko beam models were utilized. Houmat [55] investigated linear plate vibration by the HFEM and compared trigonometric shape functions with Legendre Polynomials. The trigonometric HFEM was found to yield better accuracy with less d.o.f for *s-s-s-s* and *s-f-s-f* plates (*s*, *f* and *c* stand for simply supported, free and clamped boundary conditions respectively). For fully clamped and free plates both sets of shape functions yield the same accuracy with the same number of d.o.f. Leung and Chan [56] used polynomials and trigonometric functions to analyze linear vibrations of beams and plates and found that accuracy is achieved with a reduced number of shape functions. Beslin and Nicolas [57] proposed a set of hierarchical trigonometric functions to predict flexural motion of plate-like structures in the medium frequency range. Barrette et al. [62] have used the trigonometric functions of Beslin as local trail functions to conduct the vibration analysis of stiffened plates by Hierarchical FEM.

Han et al. [63] have extended Bardell's [36] model of HFEM for free vibration analysis of plates, to geometrically non-linear static analysis of symmetrically laminated

rectangular plates. They also extended their analysis to the linear free and forced vibration analysis of symmetrically laminated rectangular plates [48,49]. Ribeiro and Petyt [52] conducted the non-linear vibration analysis of laminated plates using the hierarchical finite element method and the harmonic balance method.

1.5 Scope and Objectives of the Thesis

The objectives of the present thesis are, (1) to develop and evaluate the hierarchical finite element formulation for the static and dynamic analysis of composite beams; (2) to analyze the thickness-tapered composite beams for dynamic response using the developed hierarchical finite element formulation; and, (3) to conduct a detailed parametric study of tapered composite beams. The influences of damping are not included in the analyses.

Hierarchical finite element formulations are developed, viz. the trigonometric and polynomial formulations. Both the formulations are analyzed for their performance in the static and dynamic analysis of uniform beams. The more accurate formulation among the two is then applied for the analysis of thickness-tapered composite beams. The developed methodology not only gives more accurate and faster convergence, but also, uses less number of elements, which is extremely advantageous in the analysis of composite structures. Finally, a detailed parametric study of thickness-tapered composite beams is conducted.

1.6 Layout of the Thesis

The present chapter provided a brief introduction and literature survey regarding the hierarchical finite element method and the dynamic analysis of composite beams.

In chapter 2 the hierarchical finite element method is developed and applied to the dynamic analysis of isotropic beams. Both the hierarchical sub-formulations, viz. trigonometric and polynomial formulations are developed and validated using closed form solutions. Finally a detailed comparison is made between the conventional and the hierarchical finite element formulations.

Chapter 3 gives the application of hierarchical finite element method to uniform and thickness-tapered composite beams. The static and dynamic analysis of uniform composite beams is performed and finally, the dynamic analysis of thickness-tapered composite beams is performed.

Chapter 4 is devoted to the parametric study, which includes the effects of the boundary conditions, the laminate configuration, taper angle and the type of taper on the natural frequencies of the tapered beams.

Chapter 5 brings the thesis to its end by providing the conclusions of the present work and some recommendations for future work.

Chapter 2

Dynamic Analysis Of Isotropic Beams Using Hierarchical Finite Element Method

2.1 Introduction

Beams are the most common structural components found in civil, mechanical and aerospace structures. A beam is a rod-like structural member that can resist transverse loading applied between its supports. In practical structures beam members can take up a great variety of loads, including biaxial bending, transverse shears, axial forces and even torsion. Such complicated actions are typical of spatial beams, which are used in three-dimensional frameworks and are subjected to forces applied along arbitrary directions. A plane beam resists primarily loading applied in one plane and has a cross-section that is symmetric with respect to that plane. A beam is prismatic if the cross-section is uniform. Our study is primarily based on straight, prismatic and plane beams.

Mathematical Models: Beams are actually three-dimensional solids. One-dimensional mathematical models of plane beams are constructed on the basis of beam theories. All such theories involve some form of approximation that describes the behavior of the cross-sections in terms of quantities evaluated at the longitudinal axis. More precisely,

the kinematics of a plane beam is completely defined if the following functions are given: the transverse displacement $W(X)$ and the cross-section rotation $\theta_z(X) = (X)$, where X denotes the longitudinal co-ordinate in the reference configuration. (Figure 2.1)

Two beam models are in common use in structural mechanics:

Euler-Bernoulli (EB) Model. This is also called *classical beam theory* or the *engineering beam theory.* This model accounts for bending moment effects on stresses and deformations. Transverse shear forces are recovered from equilibrium but their effect on beam deformations is neglected. Its fundamental assumption is that cross-sections remain plane and normal to the deformed longitudinal axis. The rotation occurs about a neutral

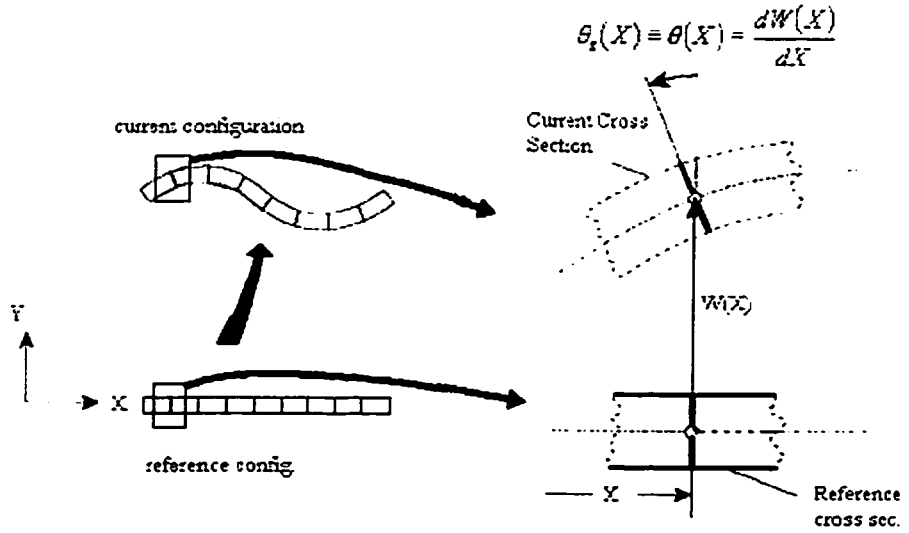

Figure 2.1 Beam kinematics for EB model. In the Timoshenko model, (X) is not constrained by normality

axis that passes through the centroid of the cross-section. The rotation, (X) and the displacement, W(X) are related as indicated in Figure 2.1.

Timoshenko Model. This model corrects the classical beam theory by including first-order shear deformation effects. In this theory, cross-sections remain plane and rotate about the

same neutral axis as the EB model, but do not remain normal to the deformed longitudinal axis. The deviation from normality is produced by a transverse shear that is assumed to be constant over the cross-section.

Both the EB and Timoshenko models are based on the assumptions of small deformations and linear elastic isotropic material behavior. In addition both models neglect changes in dimensions of the cross-sections as the beam deforms.

To carry out the finite element analysis of a framework structure, beam members are idealized as the assembly of one or more finite elements, as illustrated in Figure 2.2. The most common elements used in practice have two end nodes. The I^{st} node has two degrees of freedom: the nodal displacement W_1, and the nodal rotation θ_1 about the *Z-axis*, positive counterclockwise and expressed in radians (Figure 2.3). The cross-section rotation from the reference to the current configuration is called θ in both models. In the EB model this is the same as the rotation ψ of the longitudinal axis. In the Timoshenko model, the difference $\bar{\gamma} = \psi - \theta$ is used as a measure of mean shear deformation. These angles are illustrated in Figure 2.4.

C^1 Versus C^o Beam Element: In the Finite Element Method, a Euler-Bernoulli model such as the one shown in Figure 2.3(a) is called a C^1 beam because this is the kind of mathematical continuity achieved in the longitudinal direction when a beam member is divided into several elements (Figure 2.2). On the other hand the Timoshenko element shown in Figure 2.3(b) is called a C^o beam element because both transverse

displacement, as well as the rotation, preserve only C^o continuity [64]. It would be easy to mistake the C^o element unsuitable for the practical use. And indeed the kinematics looks strange. The shear deformation implied by the drawing appears to grossly violate the basic assumptions of beam behavior. Furthermore, a huge amount of shear energy would be required to keep the element straight as depicted.

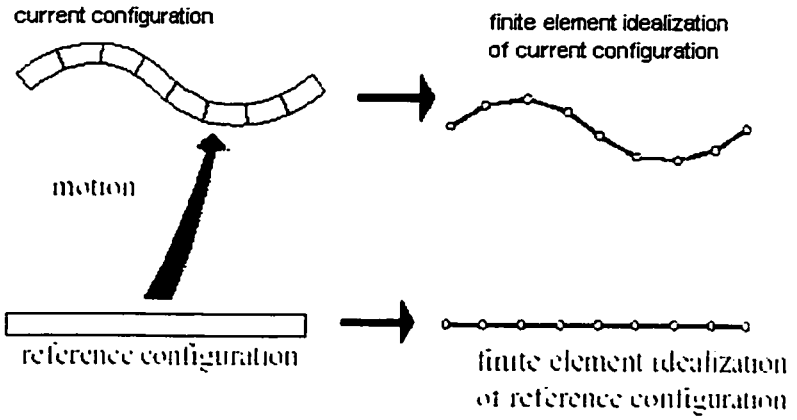

Figure 2.2 Idealization of a beam member as an assembly of finite elements

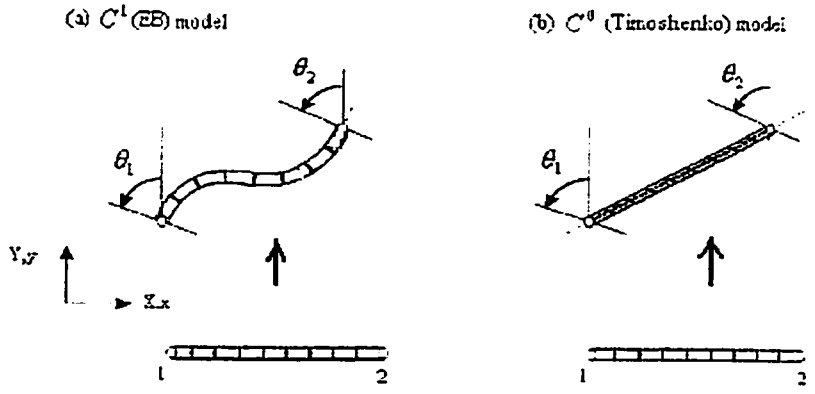

Figure 2.3 Two-node beam elements have six DOFs, regardless of the model used

If the two-node element of Figure 2.3(b) were constructed with actual shear properties and exact integration, an overstiff model results. This phenomenon is well known in the

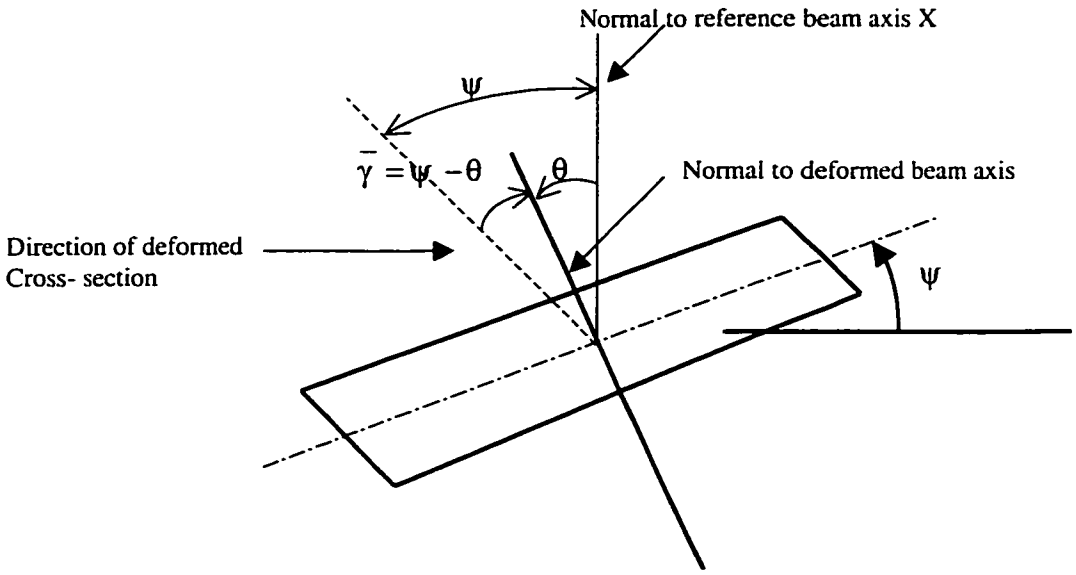

Figure 2.4 Definition of total section rotation θ and EB section rotation ψ in the Timoshenko beam model.

FEM literature and receives the name of *shear locking* [65]. To avoid locking while retaining the element simplicity it is necessary to use certain computational schemes. The most common are:

1. Selective integration for the shear energy.

2. Residual energy balancing.

As a result of the application of the aforementioned schemes the beam element behaves like a EB beam although the underlying model is Timoshenko's. This represents a curious paradox: shear deformation is used to simplify the kinematics, but then most of the shear is removed to restore the correct stiffness. As a result, the name "C^o element" is more appropriate than "Timoshenko element" because capturing the actual shear deformation is not the main objective.

2.2 The Conventional Finite Element Formulation

2.2.1 Weak Formulation based on the Euler – Bernoulli Theory

In the Euler – Bernoulli beam theory the transverse deflection w of the beam is governed by the fourth order differential equation [65].

$$\frac{\partial^2}{\partial X^2}\left(b\frac{\partial^2 w}{\partial X^2}\right)+\rho A\frac{\partial^2 w}{\partial t^2}-q'(X,t)=0 \qquad \text{for } 0< X <L \tag{2.1}$$

where b = b(X) and w is the dependant variable. The function b = EI is the product of the modulus of elasticity, E, and the moment of inertia, I, of the beam. ρ is the mass density of the material, A is the area of cross-section of the beam, q' is the transversely distributed load and w is the transverse deflection of the beam. In addition to satisfying Equation (2.1), w must also satisfy appropriate boundary conditions; since the equation is of fourth order, four boundary conditions are needed to solve it. The weak formulation of the equation will provide the form of these four boundary conditions.

The weak form in solid mechanics problems can be obtained either by the principle of virtual work or from the governing differential equations. Here we obtain the weak form by making use of Equation (2.1). The approach of the seperation of variables is applied for $w(X,t)$ and it can be expressed as the product of two functions – one in spatial co-ordinate 'X'and the other in time 't' as,

$$w(X,t)=W(X)\tau(t)=W(X)e^{i\omega t} \tag{2.2}$$

where ω will correspond to the frequency of free vibration of the beam.

Using Equation (2.2), the weak form for an element of length, l, that is obtained is as follows [65],

$$\int_0^l \left(\frac{d^2v}{dx^2} EI \frac{d^2W}{dx^2} - \lambda \rho A v W - vq' \right) dx + \left[v \frac{d}{dx}\left(EI \frac{d^2W}{dx^2} \right) - \frac{dv}{dx} EI \frac{d^2W}{dx^2} \right]_0^l = 0 \tag{2.3}$$

where, $\lambda = \omega^2$ and x is the local co-ordinate for the element.

2.2.2 Interpolation Functions

The conventional formulation for the Euler-Bernoulli beam element proceeds ahead of the variational form derived above, by the determination of the interpolation functions. The variational form in Equation (2.3) requires that the interpolation functions of an element be continuous with non zero derivatives up to order two. As discussed in the introduction, this element is named as the C^1 element. Also, the approximation of the primary variables over a finite element should be such that it satisfies the interpolation properties (i.e. it satisfies the essential boundary conditions of the element), viz.

$$W(x_e) = W_1; \qquad W(x_{e+1}) = W_2; \; \theta(x_e) = \theta_1; \qquad \theta(x_{e+1}) = \theta_2; \tag{2.4}$$

where x_e and x_{e+1} define a typical element (see Figure 2.5) and $x_{e+1} = x_e + l$. In satisfying the essential boundary conditions in Equation (2.4), the approximation automatically satisfies the continuity conditions. Hence, we pay attention to the

satisfaction of Equation (2.4), which forms the basis of the interpolation procedure. Since there are four boundary conditions in an element (2 per node), a four-parameter polynomial is selected for W:

$$W(x) = c_1 + c_2 x + c_3 x^2 + c_4 x^3 \tag{2.5}$$

In accordance with the assumption of the EB beam theory, the expression for $\theta(x)$ will be,

$$\theta(x) = \frac{dW(x)}{dx} = c_2 + 2c_3 x + 3c_4 x^2 \tag{2.6}$$

Since the polynomial should satisfy the essential boundary conditions, the following expressions can be obtained,

$$W(0) = W_1 = c_1 \tag{2.7}$$
$$\theta(0) = \theta_1 = c_2 \tag{2.8}$$
$$W(l) = W_2 = c_1 + c_2 l + c_3 l^2 + c_4 l^3 \tag{2.9}$$
$$\theta(l) = \theta_2 = c_2 + 2c_3 l + 3c_4 l^2 \tag{2.10}$$

The above equations can be put in the matrix form as,

$$\begin{Bmatrix} W_1 \\ \theta_1 \\ W_2 \\ \theta_2 \end{Bmatrix} = \begin{bmatrix} 1 & 0 & 0 & 0 \\ 0 & 1 & 0 & 0 \\ 1 & l & l^2 & l^3 \\ 0 & 1 & 2l & 3l^2 \end{bmatrix} \begin{Bmatrix} c_1 \\ c_2 \\ c_3 \\ c_4 \end{Bmatrix} \tag{2.11}$$

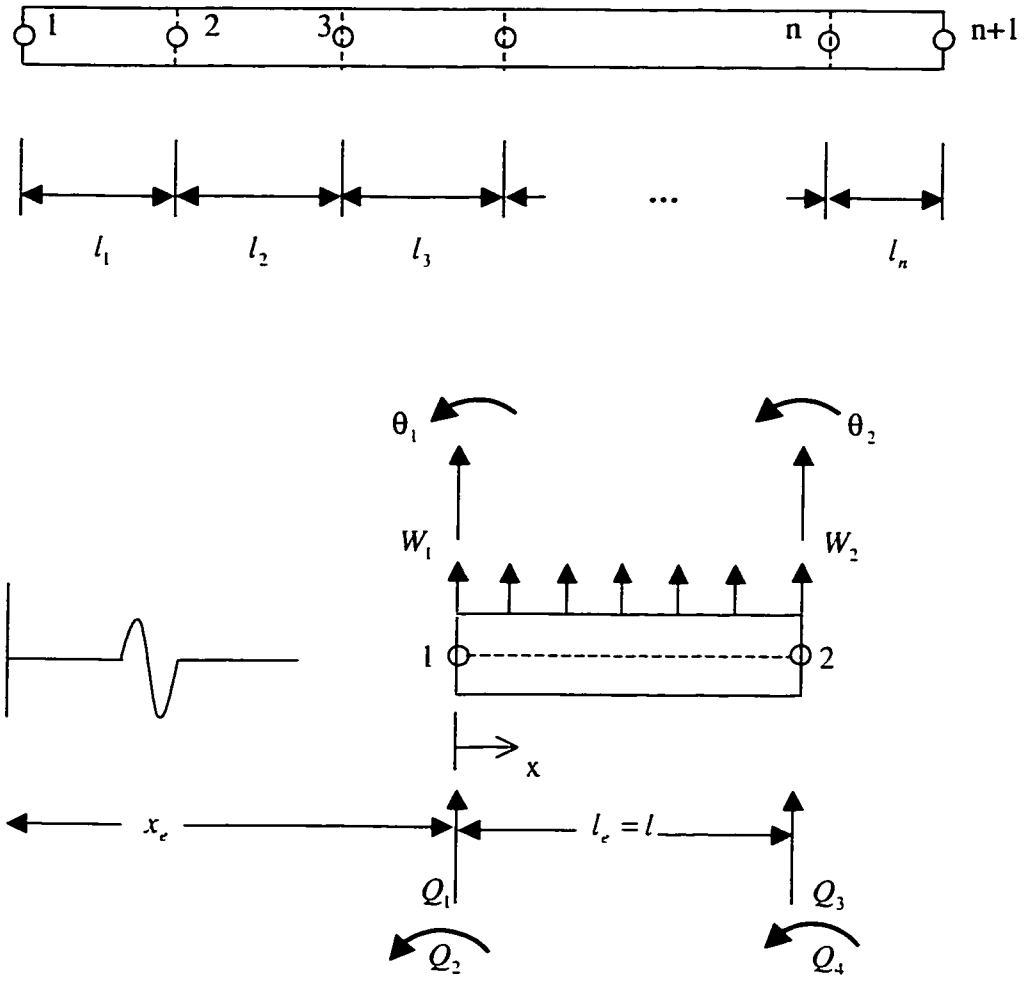

Figure 2.5 Finite element discretization and a typical element

Inverting this matrix and obtaining c_j in terms of $W_1, \theta_1, W_2, \theta_2$ and substituting the results into Equation (2.5) we will obtain,

$$W(x) = N_1 W_1 + N_2 \theta_1 + N_3 W_2 + N_4 \theta_2 \tag{2.12}$$

where,

$$N_1 = 1 - \frac{3x^2}{l^2} + \frac{2x^3}{l^3} \tag{2.13}$$

$$N_2 = x - \frac{2x^2}{l} + \frac{x^3}{l^2} \tag{2.14}$$

$$N_3 = \frac{3x^2}{l^2} - \frac{2x^3}{l^3} \tag{2.15}$$

$$N_4 = -\frac{x^2}{l} + \frac{x^3}{l^2} \tag{2.16}$$

These interpolation functions satisfy the following relationships:

$$N_1\big|_{x=0} = 1 \qquad N_i\big|_{x=0} = 0 \quad (i \neq 1) \tag{2.17}$$

$$N_3\big|_{x=l} = 1 \qquad N_i\big|_{x=l} = 0 \quad (i \neq 3) \tag{2.18}$$

$$\left.\frac{dN_2}{dx}\right|_{x=0} = 1 \qquad \left.\frac{dN_i}{dx}\right|_{x=0} = 0 \quad (i \neq 2) \tag{2.19}$$

$$\left.\frac{dN_4}{dx}\right|_{x=l} = 1 \qquad \left.\frac{dN_i}{dx}\right|_{x=l} = 0 \quad (i \neq 4) \tag{2.20}$$

$i = 1,2,3,4.$

It is critical to note the procedure and conditions for the formulation of the interpolation functions in the case of conventional FEM. We would make relevant changes in this formulation to obtain the Hierarchical FEM formulation.

Generation of the Finite Element Model:

The Finite Element Model of the governing differential Equation (2.1) is obtained by substituting the finite element interpolation functions for W, and the interpolation functions N_i in Equations (2.13-2.16) for the weight function v in the weak form given by Equation (2.3). Since there are four nodal variables, four different choices are used for v , i.e. $v = N_{1..4}$ to obtain a set of four algebraic equations.

The i^{th} equation will be:

$$\sum_{j=1}^{4}\int_0^l \left(EI\frac{d^2N_i}{dx^2}\frac{d^2N_j}{dx^2} - \lambda\rho A N_i N_j - N_i q' \right) dx + \left(-Q\right) = 0 \tag{2.21}$$

or,

$$\sum_{j=1}^{4}\left\{ \int_0^l \left(EI\frac{d^2N_i}{dx^2}\frac{d^2N_j}{dx^2} - \lambda\rho A N_i N_j \right) dx \right\} U_j - \int_0^l N_i q' dx - Q = 0 \tag{2.22}$$

This equation can be written as,

$$\sum_{j=1}^{4}\left[K_{ij} - \lambda M_{ij}\right] U_j - F_i = 0 \tag{2.23}$$

where,

$$U_1 = W\big|_{x=0} \qquad U_3 = W\big|_{x=l}$$

$$U_2 = \left.\frac{dW}{dx}\right|_{x=0} \qquad U_4 = \left.\frac{dW}{dx}\right|_{x=l}$$

Hence,

$$K_{ij} = \int_0^l EI \frac{d^2N_i}{dx^2} \frac{d^2N_j}{dx^2} dx \tag{2.24}$$

$$M_{ij} = \int_0^l \rho A N_i N_j dx \tag{2.25}$$

$$F_i = \int_0^l N_i q' dx + Q_i \tag{2.26}$$

$$Q = \begin{bmatrix} \left[\frac{d}{dx}\left(EI\frac{d^2W}{dx^2}\right)\right]_{x=0} \\ -\left[EI\frac{d^2W}{dx^2}\right]_{x=0} \\ -\left[\frac{d}{dx}\left(EI\frac{d^2W}{dx^2}\right)\right]_{x=l} \\ \left[EI\frac{d^2W}{dx^2}\right]_{x=l} \end{bmatrix} \tag{2.27}$$

Here K_{ij} is the coefficient of the stiffness matrix, M_{ij} is the coefficient of the mass matrix, and F_i is the force vector.

Now by making use of the MATHEMATICA® software, we obtain the stiffness, mass and the force matrices for a Euler-Bernoulli beam element having 4 degrees of freedom (DOF).

$$[K] = \frac{EI}{l^3} \begin{bmatrix} 12 & 6l & -12 & 6l \\ & 4l^2 & -6l & 2l^2 \\ & & 12 & -6l \\ sym & & & 4l^2 \end{bmatrix} \tag{2.28}$$

$$[M]=\frac{\rho Al}{420}\begin{bmatrix} 156 & 22l & 54 & -13l \\ & 4l^2 & 13l & -3l^2 \\ & & 156 & -22l \\ & & & 4l^2 \end{bmatrix} \tag{2.29}$$

$$[F_i]=\frac{q'l}{12}\begin{bmatrix} 6 \\ l \\ 6 \\ -l \end{bmatrix}+\begin{bmatrix} Q_1 \\ Q_2 \\ Q_3 \\ Q_4 \end{bmatrix} \tag{2.30}$$

It can easily be verified that the terms $\frac{q'l}{12}\begin{bmatrix} .. \\ .. \end{bmatrix}$ in Equation (2.30) represent the "work equivalent" forces and moments at nodes 1 and 2 due to the uniformly distributed load over the element. When q' is a complicated function of x, the mechanics of material type approach becomes less appealing, whereas Equation (2.22) provides a straightforward way of determining the "generalized work equivalent force" components.

2.2.3 Formulation for the Timoshenko Beam Element

The basic assumptions for the Timoshenko Beam theory and its contrast with the Euler-Bernoulli Theory have been explained in detail in the introduction. This theory takes into account the effect of shear deformation. We will now proceed with the formulation for the Timoshenko Theory.

The co-ordinate system used to define the geometry of a 2-node Timoshenko beam element is shown in Figure 2.6. The x co-ordinate and the non-dimensional ξ co-ordinate are related by the equation,

$$\xi = x/l \tag{2.31}$$

The potential energy, PE, and the kinetic energy, KE, of the prismatic Timoshenko beam element are [64],

$$PE = \frac{1}{2}\left[EI\int_0^1 \left(\frac{1}{l}\frac{d\theta}{d\xi} \right)^2 l d\xi + kGA\int_0^1 \left(\theta - \frac{1}{l}\frac{dw}{d\xi} \right)^2 l d\xi \right] \tag{2.32}$$

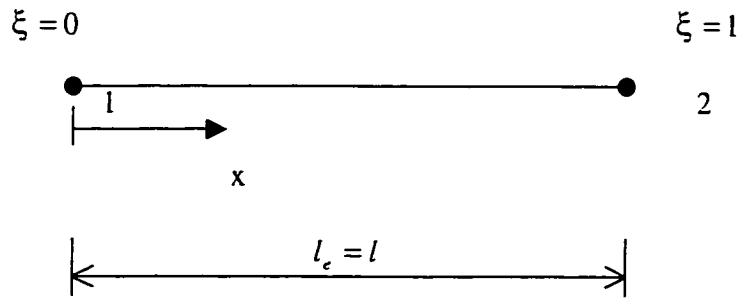

Figure 2.6 The two-node Timoshenko (linear) element showing element co-ordinates.

$$KE = \frac{\rho\omega^2}{2}\left[A\int_0^1 w^2 l d\xi + I\int_0^1 \theta^2 l d\xi \right] \tag{2.33}$$

Generic displacements for this element are the transverse displacement w and the rotation of beam cross-section θ. A close examination of the terms in the above two equations shows that both w and θ are differentiated only once with respect to ξ. Since the primary variables are the dependent unknowns themselves (and do not include their derivatives), the Lagrange interpolation of w and θ is appropriate here. The minimum admissible degree of interpolation here is linear, so that $dw/d\xi$ and $d\theta/d\xi$ are not equal to zero.

The variables w and θ do not have the same physical units; they can be interpolated, in general, with different degrees of interpolation. The displacement functions assumed for this element are,

$$w = q_1 + q_3\xi \tag{2.34}$$

$$\theta = q_2 + q_4\xi \tag{2.35}$$

The polynomial terms in the assumed displacement field are used to define the transverse displacements and the rotation of beam cross-section at the two nodes of the element.

The quantities needed to form the element stiffness and the mass matrices are obtained in the matrix form:

$$\{w\}=[C]\{q\};\ \{\theta\}=[D]\{q\};\ \left(\frac{1}{l}\right)\frac{d\theta}{d\xi}=[F]\{q\};\qquad \theta-\left(\frac{1}{l}\right)\frac{dw}{d\xi}=[H]\{q\} \tag{2.36-2.39}$$

where,

$C = [1, 0, \xi, 0]$; $D = [0, 1, 0, \xi]$; $F = [0, 0, 0, 1/l]$;

$H = [0, 1, -1/l, \xi]$; $q^T = [q_1, q_2, q_3, q_4]$

Substituting the above equations in the equations for PE and KE we get,

$$PE = \frac{1}{2}\{q\}^T [K_q]\{q\};\ KE = \frac{1}{2}\omega^2 \{q\}^T [M_q]\{q\} \tag{2.40}$$

where, $[K_q]$ and $[M_q]$ are, respectively, the element stiffness and mass matrices, expressed in the q co-ordinate system as

$$[K_q] = EI\int_0^l [F]^T [F] l d\xi + kGA\int_0^l [H]^T [H] l d\xi\ ;\ M_q = \rho A\int_0^l [C]^T [C] l d\xi + \rho I\int_0^l [D]^T [D] l d\xi \tag{2.41}$$

The element stiffness matrix, $[K_q]$, and the element mass matrix, $[M_q]$, expressed in the q co-ordinate system will be obtained by integrating explicitly the expressions given by the above equation.

A new set of generalized co-ordinates p is chosen in order to satisfy inter-element compatibility. The relation between the p co-ordinates and the q co-ordinates is found by applying the element "boundary conditions" and is

$$[q] = [T][p] \tag{2.42a}$$

where,

$$p^T = [w_1, \theta_1, w_2, \theta_2] \tag{2.42b}$$

The generalized co-ordinates $w_1, \theta_1, w_2, \theta_2$ are the transverse displacement w and the rotation of the beam cross-section θ at the two nodes of the element. The transformation matrix [T] is,

$$T = \begin{bmatrix} 1 & 0 & 0 & 0 \\ 0 & 1 & 0 & 0 \\ -1 & 0 & 1 & 0 \\ 0 & -1 & 0 & 1 \end{bmatrix} \tag{2.43}$$

The element stiffness and the mass matrices are transformed to the p co-ordinate system by using the relations

$$[K_p] = [T]^T [K_q][T]; \; [M_p] = [T]^T [M_q][T] \tag{2.44}$$

The element stiffness matrix, $[K_p]$ and the mass matrix, $[M_p]$, are then assembled into the system stiffness and mass matrices by direct summation. We will use the subroutine developed for the assembly of the elements for this purpose, the details of which will be provided in the program development section. After that any of the known techniques that solves a generalized eigenvalue problem can then be used to find the frequencies (eigenvalues) and mode shapes (eigenvectors). In the present study, the Generalized Jacobi method [66] has been used to solve the eigenvalue problem.

2.2.4 Vibration Analysis based on the Conventional Formulation

2.2.4.1 Free Vibration Analysis

The salient aspects of flexural vibration of beams are discussed here. Both the Euler- Bernoulli and the Timoshenko Beam Theories and the corresponding formulations are considered in the application of the conventional Finite Element Method. Upon obtaining the [K] and [M] matrices in both the cases, we can find the natural frequencies

by solving the eigenvalue problem by any of the standard procedures. In this study, the Generalized Jacobi method [66] has been used for the solution of the eigenvalue problem. Exact solutions based on both the theories are available in the literature [67] and they will be used to validate the results obtained using finite element formulation.

The exact solutions, obtained using the **Euler - Bernoulli Theory**, for the transverse vibrations of beams having different boundary conditions are given below: The following legend is common for all the cases;

ω_i - natural frequency of the i^{th} mode; L – length of the beam;

A – area of cross-section of the beam; ρ - mass density of the beam

EI – flexural rigidity of the beam

(i) Simply Supported Beam

$$\omega_i = \frac{i^2\pi^2}{L^2}\sqrt{\frac{EI}{\rho A}} \tag{2.45}$$

(ii) Fixed – Fixed Beam

$$\omega_i = \left(\frac{K_i}{L}\right)^2\sqrt{\frac{EI}{\rho A}} \tag{2.46}$$

where, i = 1,2,3,4,..., and K_i denotes the values of constants given as follows,

$K_1 = 4.732$, $K_2 = 7.853$, $K_3 = 10.996$, $K_4 = 14.137$, and so on [67].

(iii) Fixed – Free Beam

$$\omega_i = \left(\frac{K_i}{L}\right)^2 \sqrt{\frac{EI}{\rho A}} \tag{2.47}$$

where, i = 1,2,3,4,...,and K_i denotes the values of constants given as follows,

$K_1 = 1.875$, $K_2 = 4.694$, $K_3 = 7.855$, $K_4 = 10.996$, and so on.

The exact solution obtained using the **Timoshenko Beam Theory**, for the transverse vibrations of simply-supported beams is given below [67].

(i) Simply Supported Beam

$$\omega_i = \frac{a\pi^2}{\lambda_i^2}\left[1 - \frac{1}{2}\frac{\pi^2 r_g^2}{\lambda_i^2}\left(1 + \frac{E}{kG}\right)\right] \tag{2.48}$$

where,

$$a = \sqrt{\frac{EI}{\rho A}}, \qquad \lambda_i = \frac{L}{i}, \qquad r_g^2 = \frac{I}{A}$$

In the above, EI is the flexural rigidity, ρ is the mass density, L is the length of the beam, A is the cross- sectional area, k is the shear correction factor, I is the moment of inertia of the cross- sectional area with respect to the z axis, i.e. the centroidal axis and i is the index for the frequency.

2.2.4.2 Forced Vibration Analysis

Forced vibration is the motion caused by external force acting on a vibrating system. The system will oscillate with an amplitude that depends upon the amplitude of excitation, the frequency of the driving force and the natural frequency of the system. When the forcing frequency matches the natural frequency of the system, the amplitude will be at its maximum and resonance is said to be taking place.

The solution assumed as standard in this study for the forced vibration of beams is obtained by formulating the dynamic equations for beams with reference to a discrete number of nodal co-ordinates. These co-ordinates are the translational and rotational displacements defined at the nodes of the finite elements of the beam. The dynamic equations for a linear system without considering the damping effects can be conveniently written as,

$$[M]\{\ddot{U}\}+[K]\{U\}=\{F(t)\} \tag{2.49}$$

where, F(t) is the force vector and [M] and [K] are, respectively, the mass and stiffness matrices of the structure. These matrices are assembled using the appropriate superposition (direct method) of the matrices that correspond to each beam segment of the structure.

The solution of the dynamic equations (i.e. the response) of a linear system can be obtained by the modal superposition method. This method requires the determination of the natural frequencies ω_i (i = 1, 2, 3... N), where N is the order of the stiffness matrix,

and the corresponding normal modes which are conveniently written as the columns of the modal matrix $[\phi]$. The linear transformation $\{U\}=[\phi]\{V(t)\}$ applied to the dynamic equations reduces them to a set of independent equations (uncoupled equations) of the form,

$$\ddot{v}_n + \omega_n^2 v_n = P_n(t) \tag{2.50}$$

where, [U] is the matrix of nodal point deflections, $[V]$ is a time dependent vector of generalized displacements, n = 1,2,3,...,N and $P_n(t) = \phi_n^T Q(t)$ is the modal force.

Alternatively, the response is also determined by the numerical integration of the dynamic equations. The linear acceleration methods, namely the Wilson-θ and Newmark - β methods [66] have been employed for this purpose.

2.2.5 Example Applications

In this section a complete set of example problems will be solved using the formulations developed in the preceding sections. It will house sets of examples – one for Euler- Bernoulli Beams and the other for the Timoshenko beams. Solutions are validated by comparing them with the results obtained using the available exact solutions or other approximate methods. Both the fps and SI system of units have been used for the examples. This is done to obtain direct comparison with various references.

2.2.5.1 Free Vibration Analysis of a Euler-Bernoulli Beam

Problem Description

An A-36 steel I beam with a cross-section of type 8I23 and with both ends simply supported [68] is as shown in Figure 2.7. The problem is defined by the following mechanical and geometrical parameters: cross-sectional area (A) = 6.71 in^2; moment of inertia (I) = 64.2 in^4; modulus of elasticity (E) = 30 Mpsi; and mass density of the beam (ρ) = 0.000733 $lbf - \sec^2/in^4$. The beam is modeled using three beam elements. The natural frequencies and mode shapes are sought.

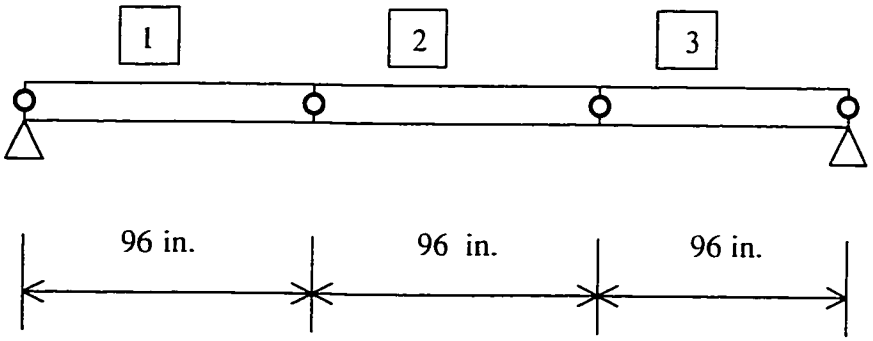

Figure 2.7 Beam discretization for the free vibration problem

The problem is solved by the conventional finite element method. The use of the MATHEMATICA® software is made for symbolic computing.

The first four natural frequencies of the beam obtained by modeling it using 3 beam elements are; ω_1 = **74.519 rad/sec,** ω_2 = **301.36 rad/sec,** ω_3 = **743.81 rad/sec and** ω_4 = **1383.10 rad/sec.**

The first four natural frequencies of the beam obtained by modeling it using 6 beam elements are; ω_1 = **74.459 rad/sec,** ω_2 = **297.52 rad/sec,** ω_3 = **672.79 rad/sec and** ω_4 = **1205.50 rad/sec.**

The natural frequencies of the beam obtained by the closed form solution for a simply-supported beam are; ω_1 = **74.461 rad/sec,** ω_2 = **297.844 rad/sec,** ω_3 = **670.149 rad/sec and** ω_4 = **1191.378 rad/sec.**

Table 2.1 gives a comparison between the results obtained by the current formulation and the results given in the reference [68]. As can be seen the accuracy in higher modes gets better as we refine the mesh which is an essential feature of the conventional finite element method.

Table 2.1 Percentage of error in the natural frequencies of a Euler-Bernoulli beam

Number of Elements	Mode	Present Results	Results given in [68]
3	1	0.08	0.08
	2	1.18	1.18
	3	10.99	11.00
6	1	0.01	0.01
	2	0.08	0.08
	3	0.39	0.39

2.2.5.2 Forced Vibration Analysis of a Euler-Bernoulli Beam

Problem Description

For the fixed – fixed beam [69] shown in the Figure 2.8, (a) the natural frequencies and mode shapes, and (b) the response to a concentrated force of 10000 lb suddenly applied at the center of the beam for 0.1 sec and removed linearly as shown in the Figure 2.9 are sought. A time step of integration $\Delta t = 0.01$ sec is used. The properties of the beam are: length (L) = 200 in.; moment of inertia (I) = 100 in^4; Young's modulus (E) = 6.58 Mpsi; and mass per unit length ($\overline{m}$) = 0.10 $lbf.\sec^2/in^2$. The beam is divided into four elements of equal length as shown in Figure 2.8.

The problem is solved by first obtaining the stiffness and the mass matrices for the beam by the methodology described in the previous sections. Then the Generalized Jacobi Method [66] is applied to obtain the natural frequencies ω_i and the corresponding modal shapes ϕ_i. The ω_i and ϕ_i obtained for the beam are listed below:

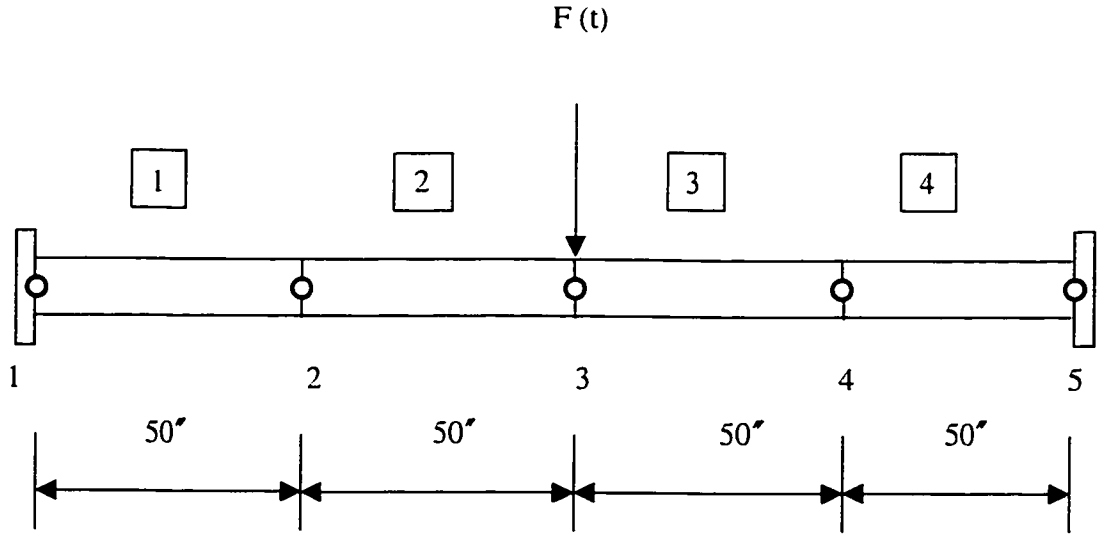

Figure 2.8 Modeling the Fixed – Fixed Beam for the Forced Vibration Analysis

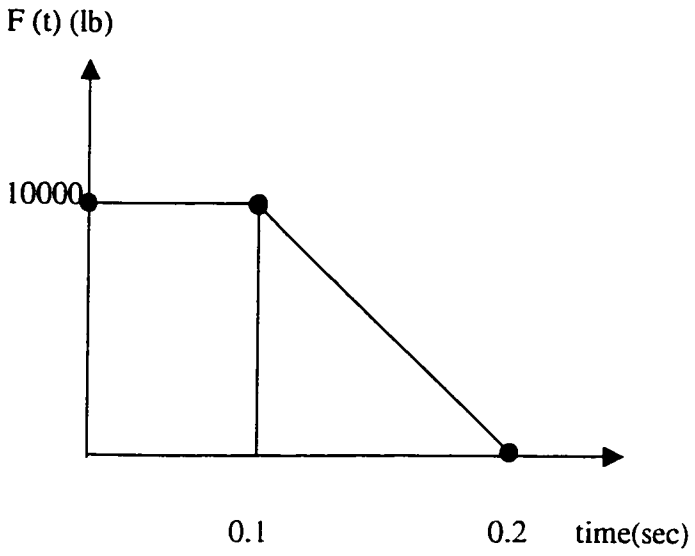

Figure 2.9 Force applied on the beam for forced vibration

The eigenvalues for the fixed – fixed beam obtained by the Generalized Jacobi method [66] are $10^4 \times (0.2064, 1.5933, 6.2710, 22.446, 61.395, 159.39)$.

The eigenvectors obtained by the Generalized Jacobi method for the above problem are listed as follows (by columns).

3.2051×10^{-1}	-1.5157×10^{-1}	1.9352×10^{-1}	1.8579×10^{-1}	-3.2920×10^{-1}	-6.6817×10^{-2}
-7.5434×10^{-3}	2.8917×10^{-2}	5.4203×10^{-3}	4.7578×10^{-2}	-3.5498×10^{-3}	-4.8653×10^{-2}
-3.3013×10^{-1}	2.7393×10^{-16}	3.5606×10^{-1}	3.7361×10^{-16}	-3.7975×10^{-17}	3.1435×10^{-1}
8.3171×10^{-18}	-3.2333×10^{-2}	1.0892×10^{-17}	7.7369×10^{-2}	1.2986×10^{-2}	1.2638×10^{-17}
3.2051×10^{-1}	1.5157×10^{-1}	1.9352×10^{-1}	-1.8579×10^{-1}	3.2920×10^{-1}	-6.6817×10^{-2}
7.5434×10^{-3}	2.8917×10^{-2}	-5.4203×10^{-3}	4.7578×10^{-2}	-3.5498×10^{-3}	4.8653×10^{-2}

The natural frequencies corresponding to the above eigenvalues are ω_1 = **45.432 rad/sec,** ω_2 = **126.23 rad/sec,** ω_3 = **250.42 rad/sec,** ω_4 = **473.77 rad/sec,** ω_5 = **783.55 rad/sec,** ω_6 = **1262.5 rad/sec.**

The solution to the above dynamic analysis problem is obtained by both the methods, viz. direct integration method and the mode superposition method.

Tables 2.2, 2.3, and 2.4 give the maximum values of the responses i.e. displacement, velocity and acceleration respectively over the time specified for all the degrees of freedom in the finite element mesh after applying the boundary conditions.

Table 2.2 Values of maximum displacement for Ex. 2

D.O.F.	MAXIMUM RESPONSE – DISPLACEMENT (inches)		
	WILSON – θ Method (Direct Integration)	*NEWMARK* – β Method (Direct Integration)	Mode Superposition Method
3	0.6502	0.6548	0.6502
4	0.0187	0.0186	0.0187
5	1.2328	1.2421	1.2328
6	0.0000	0.0000	0.0000
7	0.6502	0.6548	0.6502
8	0.0187	0.0186	0.0187

Table 2.3 Values of maximum velocity for Ex. 2

D.O.F.	MAXIMUM RESPONSE – VELOCITY (inches/sec)		
	WILSON –θ Method (Direct Integration)	*NEWMARK* – β Method (Direct Integration)	Mode Superposition Method
3	15.9802	19.8910	15.9798
4	0.5199	0.8798	0.5199
5	27.0415	34.5923	27.0413
6	0.0000	0.0000	0.0000
7	15.9802	19.8910	15.9798
8	0.5199	0.8798	0.5199

Table 2.4 Values of maximum acceleration for Ex.2

D.O.F.	MAXIMUM RESPONSE – ACCELERATION($inches/sec^2$)		
	WILSON –θ Method (Direct Integration)	*NEWMARK* – β Method (Direct Integration)	Mode Superposition Method
3	1279.9089	1599.7288	1279.8960
4	164.9535	193.5179	164.9512
5	1242.5861	2514.4064	1242.5556
6	0.0000	0.0000	0.0000
7	1279.9089	1599.7288	1279.8960
8	164.9535	193.5179	164.9512

The results obtained for the maximum displacement of the forced vibration problem for the fixed-fixed beam of Example 2 are in excellent agreement with those given in reference [69]. We will now analyze the maximum response of the beam in Example 2 for other boundary conditions.

Simply Supported Beam of Ex. 2

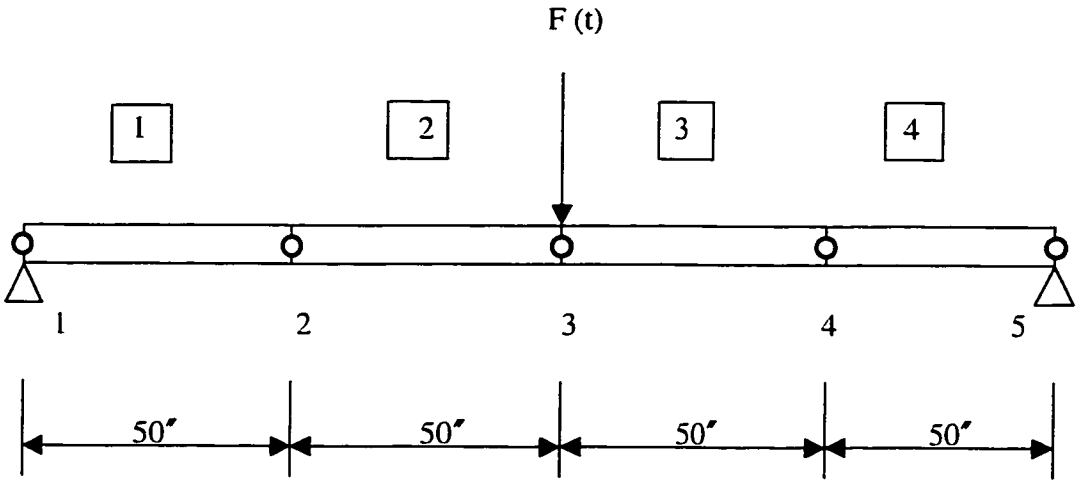

Figure 2.10 Modeling the Simply - Supported beam for the forced vibration analysis

Table 2.5 Values of maximum displacement for Simply-Supported beam in Ex.2

D.O.F.	MAXIMUM RESPONSE – DISPLACEMENT (inches)		
	WILSON $-\theta$ Method (Direct Integration)	*NEWMARK* $-\beta$ Method (Direct Integration)	Mode Superposition Method
1	0.0741	0.0762	0.0741
2	3.3544	3.4154	3.3544
3	0.0534	0.0548	0.0534
4	4.7838	4.8861	4.7838
5	0.0000	0.0000	0.0000
6	3.3544	3.4154	3.3544
7	0.0534	0.0548	0.0534
8	0.0741	0.0762	0.0741

Table 2.6 Values of maximum velocity for Simply-Supported beam in Ex.2

D.O.F.	MAXIMUM RESPONSE – VELOCITY (inches/sec)		
	WILSON –θ Method (Direct Integration)	*NEWMARK* – β Method (Direct Integration)	Mode Superposition Method
1	1.1301	1.3837	1.4415
2	50.7667	53.0035	64.4400
3	0.7957	1.0195	1.0080
4	71.9038	62.9541	90.8140
5	0.0000	0.0000	0.0000
6	50.7667	53.0035	64.4400
7	0.7957	1.0195	1.0080
8	1.1301	1.3837	1.4415

Table 2.7 Values of maximum acceleration for Simply-Supported beam in Ex.2

D.O.F.	MAXIMUM RESPONSE – ACCELERATION($inches/sec^2$)		
	WILSON –θ Method (Direct Integration)	*NEWMARK* – β Method (Direct Integration)	Mode Superposition Method
1	130.0088	256.7592	130.0097
2	1095.9703	2192.6142	1278.8967
3	201.6205	193.7600	201.6223
4	1587.3911	2580.1884	1829.0061
5	0.0000	0.0000	0.0000
6	1095.9703	2192.6142	1278.8967
7	201.6205	193.7600	201.6223
8	130.0088	256.7592	130.0097

Fixed–Free Beam of Ex. 2

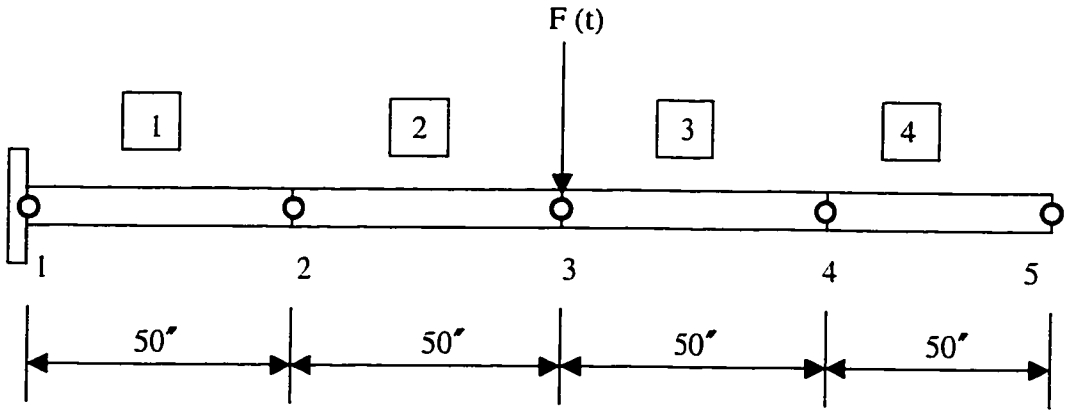

Figure 2.11 Modeling the Fixed – Free Beam for the Forced Vibration Analysis.

Table 2.8 Values of maximum displacement for Fixed-Free beam in Ex.2

D.O.F.	MAXIMUM RESPONSE – DISPLACEMENT (inches)		
	WILSON –θ Method (Direct Integration)	*NEWMARK* – β Method (Direct Integration)	Mode Superposition Method
1	1.1492	1.2583	1.2525
2	0.0415	0.0440	0.0448
3	3.7502	3.9589	3.9999
4	0.0592	0.0605	0.0610
5	6.8302	7.0507	7.1009
6	0.0627	0.0618	0.0621
7	9.9651	10.0752	10.1868
8	0.0627	0.0597	0.0616

Table 2.9 Values of maximum velocity for Fixed-Free beam in Ex.2

D.O.F.	MAXIMUM RESPONSE – VELOCITY (inches/sec)		
	WILSON –θ Method (Direct Integration)	*NEWMARK* – β Method (Direct Integration)	Mode Superposition Method
1	16.2166	20.0637	16.2166
2	0.5613	0.8996	0.5613
3	34.8962	39.5176	37.1797
4	0.4757	0.5040	0.4793
5	49.8044	56.3777	53.7276
6	1.0573	1.4764	1.0470
7	99.5557	106.9976	98.8751
8	1.1825	1.9614	1.1794

Table 2.10 Values of maximum acceleration for Fixed-Free beam in Ex.2

D.O.F.	MAXIMUM RESPONSE – ACCELERATION($inches/sec^2$)		
	WILSON –θ Method (Direct Integration)	*NEWMARK* – β Method (Direct Integration)	Mode Superposition Method
1	1260.2287	1596.9102	1260.2454
2	161.5970	185.2860	161.6018
3	1307.6690	2472.1470	1307.7105
4	17.7090	19.2595	17.7107
5	1062.9925	1594.0649	1062.9907
6	219.8572	237.9279	219.8677
7	2186.7303	4243.5505	2186.8117
8	194.6379	356.0901	194.6579

Tables 2.5 through 2.10 give the maximum response of the beam in Example 2 with different boundary conditions.

2.2.5.3 Free Vibration Analysis of the Timoshenko Beam

Problem Description

For the simply – supported Timoshenko beam shown in the Figure 2.13, the natural frequencies are to be obtained using the application of the conventional FEM. The properties of the beam are: length (L) = 10 ft.; moment of inertia (I) = 0.0278 $ft.^4$; area of cross-section (A) = 1/3 ft^2; Young's modulus (E) = $4.17x10^9 lbf / ft.^2$; shear modulus (G) = $1.649x10^9 lbf / ft.^2$; shear correction factor (k_s) = 0.85 and mass density (ρ) = 15.20 $lbf - \sec^2 / ft.^4$

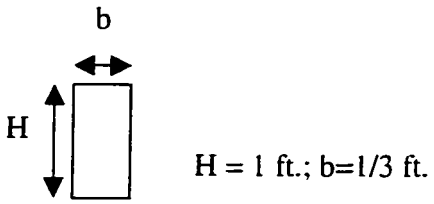

Figure 2.12 The cross-section of the Timoshenko beam

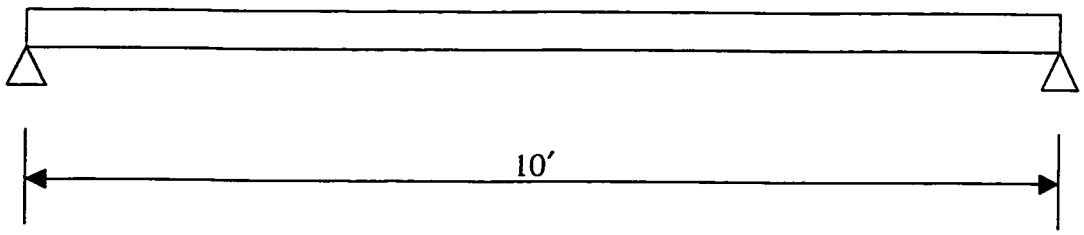

Figure 2.13 Modeling the Simply-Supported Timoshenko beam for the free vibration analysis

As can be seen form the displayed results, since a linear element has been used in the conventional FEM for a Timoshenko beam, the results do not converge rapidly to the exact solution, even when 25 elements are employed for modeling the beam. When quadratic elements are employed, the values of frequencies converge to the exact solution more rapidly.

Table 2.11 Natural frequencies of the Timoshenko beam modeled using linear elements

MODE	EXACT SOLUTION (rad/sec)	NUMBER OF ELEMENTS ; (DOF)*			
		10 ; (20)	20 ; (40)	25 ; (50)	30; (60)!
1	**464.52**	541.36	484.67	477.53	467.15
2	**1765.38**	2120.50	1865.70	1834.30	1812.36
3	**3624.44**	4639.00	3974.00	3894.40	3888.61

* Numbers in parenthesis refer to the number of system degrees of freedom *excluding the restrained ones.*

! results obtained by taking into considering the shear locking effect

2.3 The Hierarchical Finite Element Method (HFEM)

2.3.1 Trigonometric Hierarchical Formulation

As has been mentioned in the previous chapter (section 1.3), the HFEM has inherent advantages over the conventional FEM. Hence in order to understand the method better and to apply it to obtain greater numerical efficiency, it has been the object of attention for researchers in recent past.

In the formulation of the finite element model using the conventional formulation, we assumed a cubic displacement function for W (Equation 2.5). In the hierarchical formulation, we modify the approximating function, (i) by adding trigonometric functions and (ii) by adding polynomial functions. We shall study both these cases simultaneously and ascertain the pros and cons of them as we proceed in our analysis.

2.3.1.1 Formulation Based on Euler – Bernoulli Theory

The co-ordinate system used to define the geometry of a two-node Euler-Bernoulli beam element is shown in Figure 2.14. The x co-ordinate and the non-dimensional co-ordinate ξ are related by the equation,

$$\xi = x/l \tag{2.51}$$

The transverse displacement W, of the above beam element is expressed as,

$$W(\xi) = c_1 + c_2\xi + c_3\xi^2 + c_4\xi^3 + \sum_{r=1}^{N} c_{r+4} Sin[\delta_r \xi] \tag{2.52}$$

where $\delta_r = r\pi$, r= 1,2,3....N

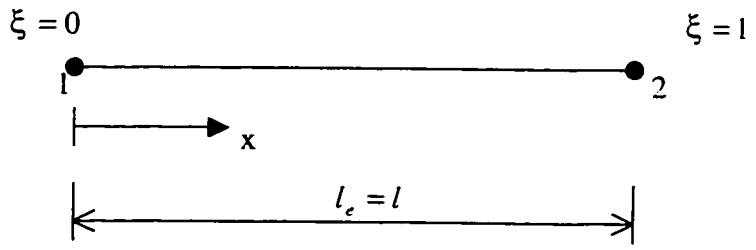

Figure 2.14 The two-node Euler-Bernoulli beam element showing element co-ordinates

and c_i are coefficients to be determined.

The element degrees of freedom in this case are the same as in the conventional case, viz. transverse displacement (W) and slope ($\theta = \partial W/\partial x$), the rotation of the beam cross- section). The polynomial terms in the assumed displacement field are used as before to define the element nodal degrees of freedom and the trigonometric terms are used to give additional freedom to the interior of the element. The above equation can be written in the matrix form as,

$$W(\xi) = [g][c] \tag{2.53}$$

where,

$$g = [1, \xi, \xi^2, \xi^3, Sin[\delta, \xi]] \tag{2.54}$$

$$c = [c_1, c_2, c_3, c_4, c_{r+4}]^T \tag{2.55}$$

Now, upon evaluating W and the product $l\theta$, at node 1 (i.e. x = 0, ξ = 0) and at node 2 (x = l, ξ =1) we get the following matrix,

$$\begin{Bmatrix} W_1 \\ l\theta_1 \\ W_2 \\ l\theta_2 \\ W_{r+4} \end{Bmatrix} = \begin{bmatrix} 1 & 0 & 0 & 0 & 0 \\ 0 & 1 & 0 & 0 & \delta_r \\ 1 & 1 & 1 & 1 & 0 \\ 0 & 1 & 2 & 3 & (-1)^r \delta_r \\ 0 & 0 & 0 & 0 & 1 \end{bmatrix} \begin{Bmatrix} c_1 \\ c_2 \\ c_3 \\ c_4 \\ c_{r+4} \end{Bmatrix} \tag{2.56}$$

The above matrix can be written in the following form,

$$[p] = [h][c] \tag{2.57}$$

$$[c] = [h]^{-1}[p] \tag{2.58}$$

Upon substitution of [c] in Equation (2.53) we get,

$$W = [g][h]^{-1}[p] \tag{2.58a}$$

or,

$$W = [N][p] \tag{2.58b}$$

Interpolation Function Matrix.

where, $[N] = [g][h]^{-1}$ (2.58c)

$$= [1, \xi, \xi^2, \xi^3, Sin[\delta_r \xi]] \; [h]^{-1} \tag{2.58d}$$

Hence the individual interpolation functions would be,

$$\begin{aligned} N_1 &= 1 - 3\xi^2 + 2\xi^3 \\ N_2 &= \xi - 2\xi^2 + \xi^3 \\ N_3 &= 3\xi^2 - 2\xi^3 \\ N_4 &= -\xi^2 + \xi^3 \end{aligned} \tag{2.59}$$

and the trigonometric hierarchical shape functions are,

$$N_{r+4} = -\delta_r \xi + \left(2\delta_r + (-1)^r \delta_r\right)\xi^2 + \left(-\delta_r - (-1)^r \delta_r\right)\xi^3 + Sin[\delta_r \xi] \tag{2.60}$$

$$where \delta_r = r\pi, r = 1,2,3....N$$

Hence, the displacement field for the element, in terms of the nodal degrees of freedom and the hierarchical degrees of freedom, can now be written as,

$$W = N_1 W_1 + N_2(l\theta_1) + N_3 W_2 + N_4(l\theta_2) + \sum_{r=1}^{N} N_{r+4} W_{r+4} \tag{2.61}$$

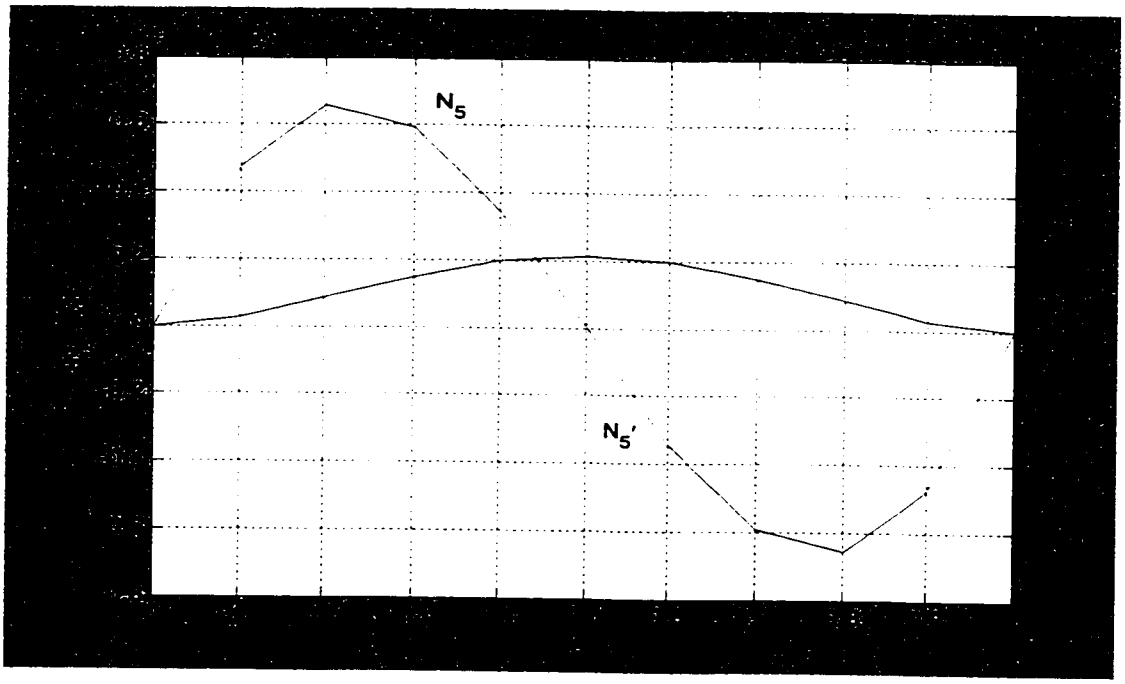

Figure 2.15 The first trigonometric hierarchical shape function (N_5) and its derivative (N_5')

The values of N_1, N_2, N_3 and N_4 at $\xi = 0$ (x = 0) and at $\xi = 1$ (x = l) are the same as given in Equations (2.17) – (2.20).

The hierarchical term(s) N_{r+4} has the values as follows at each node.

$N_{r+4} = 0 \qquad at \quad \xi = 0 \quad and \quad \xi = 1$

$N'_{r+4} = 0 \qquad at \quad \xi = 0 \quad and \quad \xi = 1$

Figures 2.15 – 2.18 show the values of the trigonometric hierarchical shape functions N_5, N_6, N_7, N_8 and their derivatives at various locations within the element. These functions provide zero displacement and zero slope at each node. This feature is highly significant, since these functions only provide additional freedom to the interior of the element and do not affect the element's nodal degrees of freedom.

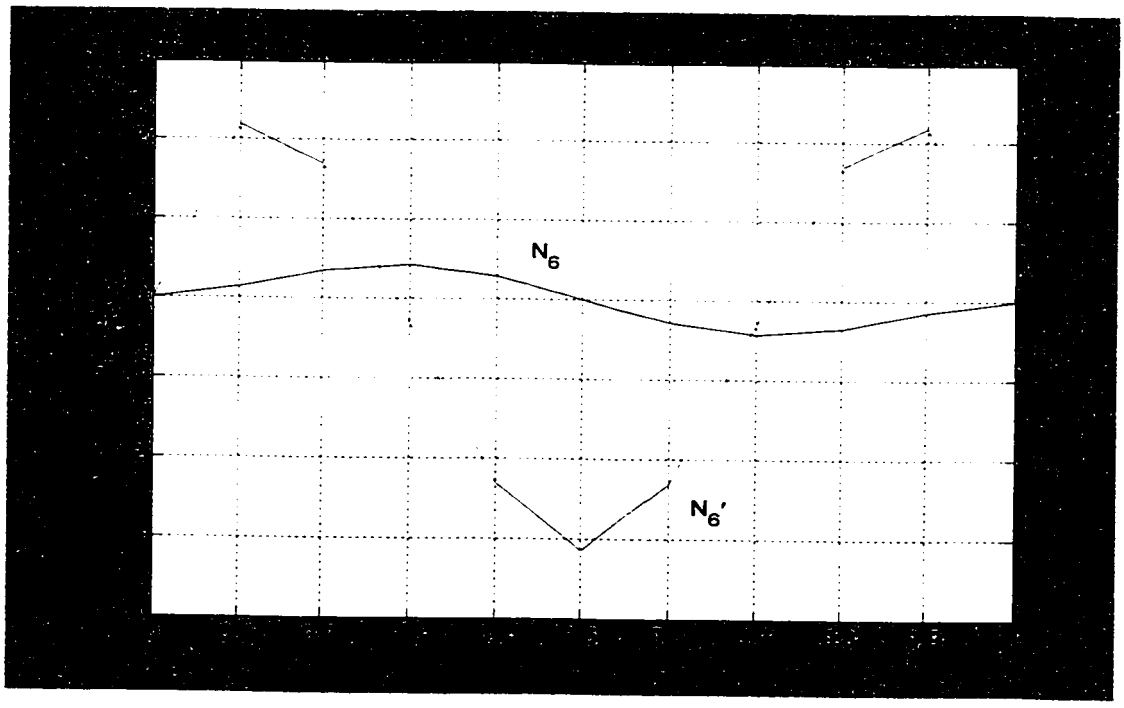

Figure 2.16 The second trigonometric hierarchical shape function (N_6) and its derivative (N'_6)

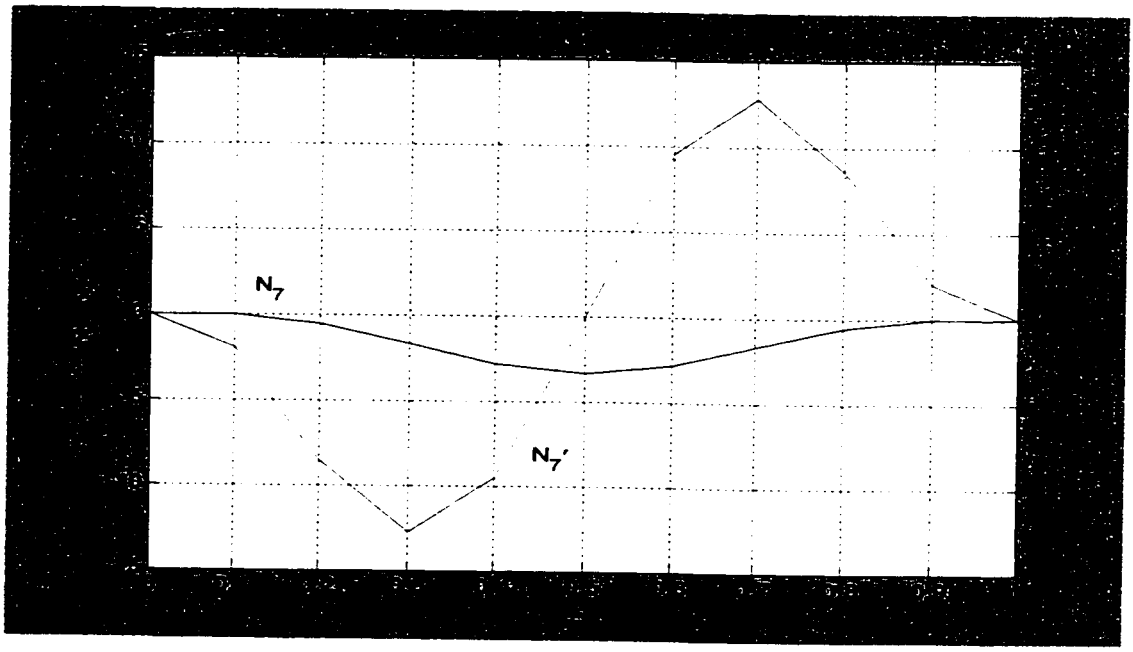

Figure 2.17 The third trigonometric hierarchical shape function (N_7) and its derivative (N_7')

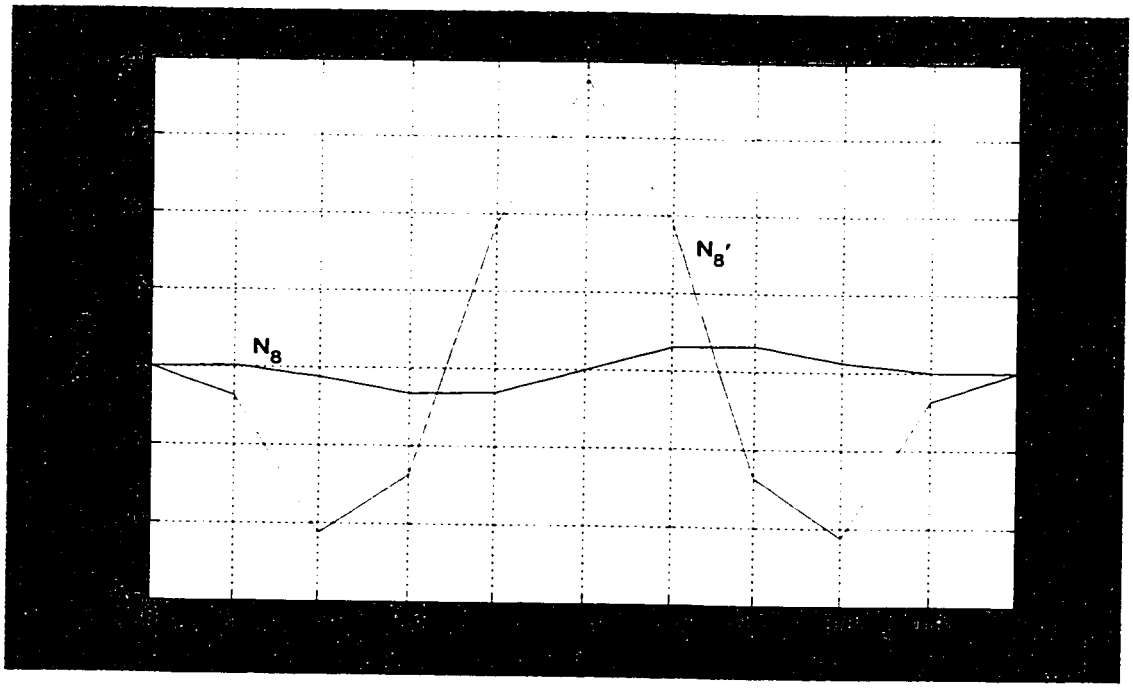

Figure 2.18 The fourth trigonometric hierarchical shape function (N_8) and its derivative (N_8')

Generation of the Finite Element model

To generate the finite element model using the trigonometric HFEM, we use the weak form as given in Equation (2.3) and make suitable changes for the non-dimensional co-ordinate system that we have chosen for this formulation.

$$\sum_{j=1}^{n}\left\{\frac{1}{l^3}\int_0^1\left(EI\frac{d^2N_i}{d\xi^2}\frac{d^2N_j}{d\xi^2}\right)d\xi-\int_0^1\lambda\rho AN_iN_jld\xi\right\}W_j-\int_0^1N_iqld\xi-Q_i=0 \qquad (2.62)$$

Accordingly,

$$K_{ij}=\frac{1}{l^3}\int_0^1\left(EI\frac{d^2N_i}{d\xi^2}\frac{d^2N_j}{d\xi^2}\right)d\xi \qquad (2.63)$$

$$M_{ij}=\int_0^1\left(\rho AN_iN_jl\right)d\xi \qquad (2.64)$$

The element stiffness matrix and the mass matrix are then assembled into the system stiffness matrix and the mass matrix by the usual overlay procedure.

2.3.1.2 Formulation Based on Timoshenko Theory

The Trigonometric Hierarchical finite element formulation for the Timoshenko beam element will involve changes to the displacement and rotation (displacement and rotation fields are independent in the Timoshenko element) fields that are similar to that corresponding to the conventional formulation based on the Euler –Bernoulli theory.

Hence, in this case the displacement and the rotation fields are modified as follows

$$w = q_1 + q_3\xi + q_{m1}Sin[\delta_m\xi] \tag{2.65}$$

$$\theta = q_2 + q_4\xi + q_{m2}Sin[\delta_m\xi] \tag{2.66}$$

where $\delta_m = m\pi$, $\quad m = 1,2,3.... M$

and $\xi = x/l$

In the Equations (2.65) and (2.66), m_1 and m_2 define the coefficients of the hierarchical terms added to the displacement and rotation expressions and are defined as;

$$m_1 = 2m + 3; \quad m_2 = m_1 + 1$$

The potential energy (PE) and the kinetic energy (KE) of the prismatic Timoshenko beam element remain the same as in the conventional case.

$$PE = \frac{1}{2}\left[EI\int_0^1 \left(\frac{1}{l}\frac{d\theta}{d\xi}\right)^2 ld\xi + kGA\int_0^1 \left(\theta - \frac{1}{l}\frac{dw}{d\xi}\right)^2 ld\xi \right] \tag{2.67}$$

$$KE = \frac{\rho\omega^2}{2}\left[A\int_0^1 w^2 ld\xi + I\int_0^1 \theta^2 ld\xi \right] \tag{2.68}$$

It is imperative to mention here that if the polynomial terms are used by themselves they will be sufficient to describe the displacement and the rotation of the beam cross-section within the element. The additional trigonometric sine term allows for better description of the transverse displacement and the rotation of the beam cross-

section within the element. Inter-element compatibility is achieved by matching the generalized co-ordinates at the element end nodes.

The quantities needed to form the element stiffness and mass matrices are obtained in the matrix form and are given as follows:

$$\{w\}=[C]\{q\};\ \{\theta\}=[D]\{q\};\ \left(\frac{1}{l}\right)\frac{d\theta}{d\xi}=[F]\{q\};\qquad \theta-\left(\frac{1}{l}\right)\frac{dw}{d\xi}=[H]\{q\} \tag{2.69-2.72}$$

where,

$$C=[1,\ 0,\ \xi,\ 0,\ Sin[\delta_m\xi],\ 0];\qquad D=[0,\ 1,\ 0,\ \xi,\ 0,\ Sin[\delta_m\xi]]; \tag{2.73}$$

$$F=[0,\ 0,\ 0,\ 1/l,\ 0,\ \left(\frac{\delta_m}{l}\right)Cos[\delta_m\xi]]; \tag{2.74}$$

$$H=[0,\ 1,\ -1/l,\ \xi,\ -\left(\frac{\delta_m}{l}\right)Cos[\delta_m\xi],\ Sin[\delta_m\xi]]; \tag{2.75}$$

$$q^T=[q_1,q_2,q_3,q_4,q_{m1},q_{m2}] \tag{2.76}$$

Substituting the above equations in the equations for PE and KE we get,

$$PE=\frac{1}{2}\{q\}^T[K_q]\{q\};\qquad KE=\frac{1}{2}\omega^2\{q\}^T[M_q]\{q\} \tag{2.77}$$

where, $[K_q]$ and $[M_q]$ are, respectively, the element stiffness and mass matrices, expressed in the q co-ordinate system as,

$$[K_q] = EI\int_0^1 [F]^T[F]\,d\xi + kGA\int_0^1 [H]^T[H]\,d\xi\,;\ [M_q] = \rho A\int_0^1 [C]^T[C]\,d\xi + \rho I\int_0^1 [D]^T[D]\,d\xi \tag{2.78}$$

The element stiffness matrix, $[K_q]$, and the mass matrix, $[M_q]$, expressed in the q co-ordinate system will be obtained by integrating explicitly the expressions given above. A new set of generalized co-ordinates p is chosen in order to satisfy inter-element compatibility. The relation between the p co-ordinates and the q co-ordinates is found by applying the element "boundary conditions" and is given by,

$$[q] = [T][p] \tag{2.79}$$

where,

$$p^T = [w_1, \theta_1, w_2, \theta_2, \ldots, w_m, \theta_m] \tag{2.79a}$$

and the generalized co-ordinates w_1, θ_1, w_2 and θ_2 correspond to the transverse displacement w and the rotation of the beam cross-section θ at the two nodes of the element. The generalized co-ordinates w_m and θ_m are the amplitudes of the trigonometric functions for the transverse displacement w and the rotation of the beam cross-section θ in the interior of the element. The transformation matrix T for M=1 is,

$$T = \begin{bmatrix} 1 & 0 & 0 & 0 & 0 & 0 \\ 0 & 1 & 0 & 0 & 0 & 0 \\ -1 & 0 & 1 & 0 & 0 & 0 \\ 0 & -1 & 0 & 1 & 0 & 0 \\ 0 & 0 & 0 & 0 & 1 & 0 \\ 0 & 0 & 0 & 0 & 0 & 1 \end{bmatrix} \tag{2.80}$$

As can be seen from the above matrix, the transformation matrix is composed of a fixed 4 x 4 block and a variable number of diagonal 2 x 2 blocks and zero coefficients outside these blocks. Hence, the above matrix is for M = 1. The order N of the matrix T depends on the number of trigonometric terms M chosen. The matrix T is simply found by expanding it along the diagonal with as many 2 x 2 blocks as the number of terms used. The order N of the element stiffness, mass and transformation matrices is,

$$N = 2M + 4 \tag{2.81}$$

The element stiffness and mass matrices are transformed to the p co-ordinate system by using the relations

$$[K_p] = [T]^T [K_q][T] : \ [M_p] = [T]^T [M_q][T] \tag{2.82}$$

The element stiffness matrix,$[K_p]$ and the mass matrix, $[M_p]$, are then assembled into the system stiffness and mass matrices by overlay procedure. We will use the subroutine developed for the assembly of the elements for this purpose, the details of which will be provided in the program development section. After that any of the known techniques that solves a generalized eigenvalue problem can then be used to find the

frequencies (eigenvalues) and mode shapes (eigenvectors). In the present study, the Generalized Jacobi method [66] has been used to solve the eigenvalue problem.

2.3.2 Polynomial Hierarchical Formulation

In place of trigonometric functions that were used in the previous section, in this section we use polynomials that increase the degree of approximation of the displacement and rotation fields. The choice of the polynomials is governed by certain aspects. The chosen set should be complete. Polynomials that have the property that the set of functions corresponding to an approximation of lower order constitutes a subset of the set of functions corresponding to a higher order approximation are particularly desirable. Also, the chosen function should not contribute to the displacement values at the element nodes. There is a wide array of polynomials that can be chosen from. In this work we have chosen the following set:

$$f_r(x) = x^{r+1}(x-l)^{r+1} \qquad r = 1.2....M \tag{2.83}$$

where l is the element length.

This function is chosen on the above mentioned basis and it fulfills the criteria when applied to the displacement field as we shall see in the following formulations.

2.3.2.1 Formulation Based on Euler – Bernoulli Theory

The displacement field for the beam element is written as follows for this formulation,

$$\mathrm{W}(x) = N_1 W_1 + N_2 \theta_1 + N_3 W_2 + N_4 \theta_2 + \sum_{r=1}^{M} N_{r+4} A_r \tag{2.84}$$

where,

$$N_{r+4} = x^{r+1}(x-l)^{r+1} \qquad r = 1,2,\ldots M \tag{2.85}$$

and A_r are the coefficients of the polynomial hierarchical terms.

The polynomial hierarchical shape functions are chosen such that,

$$N_{r+4} = 0 \qquad at \quad x = 0 \quad and \quad x = l$$

$$N'_{r+4} = 0 \qquad at \quad x = 0 \quad and \quad x = l$$

The above equations illustrate that the function provides zero displacement and zero slope at each end of the element. Again, it is important to mention that this property is highly significant, since these modes contribute only to the internal displacement field of the element, and do not therefore affect (i.e. over restrain) the displacement at the nodes.

Now the weak form for the beam element remains as follows:

$$\int_0^l \left(\frac{d^2 v}{dx^2} EI \frac{d^2 w}{dx^2} - \lambda \rho A v w - v q' \right) dx + \left[v \frac{d}{dx}\left(EI \frac{d^2 w}{dx^2} \right) - \frac{dv}{dx} EI \frac{d^2 w}{dx^2} \right]_0^l = 0 \tag{2.86}$$

Let us take the case when there is just 1 polynomial term that is added and hence the finite element equations correspond to an element having 5 DOF's. We will make the substitutions for W and the weight function, υ, in the weak form given above in Equation (2.86).

Hence, we get,

$$\sum_{j=1}^{5} \left\{ \int_0^l \left(EI \frac{d^2 N_i}{dx^2} \frac{d^2 N_j}{dx^2} - \lambda \rho A N_i N_j \right) dx \right\} w_j - \int_0^l N_i q' dx - Q_i = 0 \tag{2.87}$$

$$\sum_{j=1}^{5}\left[K_{ij}-\lambda M_{ij}\right]w_j - F_i = 0 \tag{2.88}$$

where,

$$K_{ij} = \int_0^l EI\frac{d^2N_i}{dx^2}\frac{d^2N_j}{dx^2}dx \tag{2.89}$$

$$M_{ij} = \int_0^l \rho A N_i N_j dx \qquad F_i = \int_0^l N_i q' dx + Q_i \tag{2.90}$$

By the addition of one polynomial hierarchical term, the stiffness matrix in Equation (2.89) can be written in a matrix form as,

$$\begin{bmatrix} K_{11} & K_{12} & K_{13} & K_{14} & K_{15} \\ K_{21} & K_{22} & K_{23} & K_{24} & K_{25} \\ K_{31} & K_{32} & K_{33} & K_{34} & K_{35} \\ K_{41} & K_{42} & K_{43} & K_{44} & K_{45} \\ K_{51} & K_{52} & K_{53} & K_{54} & K_{55} \end{bmatrix}\begin{Bmatrix} W_1 \\ \theta_1 \\ W_2 \\ \theta_2 \\ A_1 \end{Bmatrix} = \begin{Bmatrix} q_1' \\ q_2' \\ q_3' \\ q_4' \\ q_5' \end{Bmatrix} + \begin{Bmatrix} Q_1 \\ Q_2 \\ Q_3 \\ Q_4 \\ 0 \end{Bmatrix} \tag{2.91}$$

By making use of the MATHEMATICA® code to solve for individual terms in the stiffness and mass matrices, we get the following,

$$[K] = \frac{EI}{l^3}\begin{bmatrix} 12 & 6l & -12 & 6l & 0 \\ & 4l^2 & -6l & 2l^2 & 0 \\ & & 12 & -6l & 0 \\ & & & 4l^2 & 0 \\ sym & & & & \frac{4l^8}{5} \end{bmatrix} \tag{2.92}$$

$$[M]=\frac{\rho Al}{420}\begin{bmatrix} 156 & 22l & 54 & -13l & 7l^4 \\ & 4l^2 & 13l & -3l^2 & \frac{3l^5}{2} \\ & & 156 & -22l & 7l^4 \\ & & & 4l^2 & -\frac{3l^5}{2} \\ sym & & & & \frac{2l^8}{3} \end{bmatrix} \tag{2.93}$$

2.3.2.2 Formulation Based on the Timoshenko Beam theory

In the formulation of the Polynomial Hierarchical FEM for the Timoshenko beam element, the displacement and the rotation fields are modeled as follows:

$$w = q_1 + q_3 x + q_{r1}[x^{r+1}(x-l)^{r+1}] \tag{2.94}$$

$$\theta = q_2 + q_4 x + q_{r2}[x^{r+1}(x-l)^{r+1}] \tag{2.95}$$

where

r_1 and r_2 define the coefficients of the hierarchical terms added to the displacement and rotation expressions in Equations (2.94) and (2.95) and are defined as

$r_1 = 2r+3$; $\quad r_2 = r_1 + 1 \qquad$ r = 1,2,3.... R

The equations for the potential energy (PE) and the kinetic energy (KE) of the prismatic Timoshenko beam element remain the same as in the conventional case:

$$PE = \frac{1}{2}\left[EI\int_0^l \left(\frac{d\theta}{dx}\right)^2 dx + kGA\int_0^l \left(\theta - \frac{dw}{dx}\right)^2 dx \right] \tag{2.96}$$

$$KE = \frac{\rho\omega^2}{2}\left[A\int_0^l w^2 dx + I\int_0^l \theta^2 dx \right] \tag{2.97}$$

From Equations (2.91) and (2.92) we get:

$$\{w\} = [C]\{q\}\ ; \{\theta\} = [D]\{q\};\ \frac{d\theta}{dx} = [F]\{q\};\qquad \theta - \frac{dw}{dx} = [H]\{q\} \tag{2.98-2.101}$$

where,

$$C = [1, 0, x, 0, x^{r+1}(x-l)^{r+1}, 0];\qquad D = [0, 1, 0, x, 0, x^{r+1}(x-l)^{r+1}]; \tag{2.102}$$

$$F = [0, 0, 0, 1, 0, [(r+1)\{x^{r+1}(x-l)^r + x^r(x-l)^{r+1}\}]]; \tag{2.103}$$

$$H = [0, 1, -1, x, -[(r+1)\{x^{r+1}(x-l)^r + x^r(x-l)^{r+1}\}], [x^{r+1}(x-l)^{r+1}]]; \tag{2.104}$$

$$q^T = [q_1, q_2, q_3, q_4, q_{r1}, q_{r2}] \tag{2.105}$$

Substituting the above equations in the equations for PE and KE we get,

$$PE = \frac{1}{2}\{q\}^T[K_q]\{q\};\quad KE = \frac{1}{2}\omega^2\{q\}^T[M_q]\{q\} \tag{2.106}$$

where, $[K_q]$ and $[M_q]$ are, respectively, the element stiffness and mass matrices, expressed in the q co-ordinate system as

$$[K_q] = EI\int_0^l [F]^T[F]dx + kGA\int_0^l [H]^T[H]dx;\quad [M_q] = \rho A\int_0^l [C]^T[C]dx + \rho I\int_0^l [D]^T[D]dx \tag{2.107}$$

The element stiffness matrix, $[K_q]$, and the mass matrix, $[M_q]$, expressed in the q co-ordinate system will be obtained by integrating explicitly the expressions given above. A new set of generalized co-ordinates p is chosen in order to satisfy inter-element compatibility. The relation between the p co-ordinates and the q co-ordinates is found by applying the element "boundary conditions" and is given by:

$$[q] = [T][p] \tag{2.108}$$

where,

$$p^T = [w_1, \theta_1, w_2, \theta_2, \ldots, w_r, \theta_r] \tag{2.108a}$$

The generalized co-ordinates $w_1, \theta_1, w_2, and\ \theta_2$ correspond to the transverse displacement w and the rotation of the beam cross-section θ at the two nodes of the element. The generalized co-ordinates $w_r\ and\ \theta_r$ are the amplitudes of the polynomial functions for the transverse displacement w and the rotation of the beam cross-section θ in the interior of the element. The transformation matrix T for R = 1 is.

$$T = \begin{bmatrix} 1 & 0 & 0 & 0 & 0 & 0 \\ 0 & 1 & 0 & 0 & 0 & 0 \\ -1/l & 0 & 1/l & 0 & 0 & 0 \\ 0 & -1/l & 0 & 1/l & 0 & 0 \\ 0 & 0 & 0 & 0 & 1 & 0 \\ 0 & 0 & 0 & 0 & 0 & 1 \end{bmatrix} \tag{2.109}$$

As in the case of the trigonometric HFEM, the transformation matrix is composed of a fixed 4 x 4 block and a variable number of diagonal 2 x 2 blocks and zero coefficients outside these blocks. Hence, the above matrix is for R = 1. The order N of the matrix T

depends on the number of polynomial terms R chosen. The matrix T is simply found by expanding it along the diagonal with as many 2 x 2 blocks as the number of terms used. The order N of the element stiffness, mass and transformation matrices is,

$$N = 2R + 4 \tag{2.110}$$

The element stiffness and the mass matrices are transformed to the p co-ordinate system by using the relations

$$[K_p] = [T]^T [K_q][T]; \qquad [M_p] = [T]^T [M_q][T] \tag{2.111}$$

The element stiffness matrix, $[K_p]$, and the mass matrix, $[M_p]$, are then assembled into the system stiffness and mass matrices by direct summation. We will use the subroutine developed for the assembly of the elements for this purpose, the details of which will be provided in the program development section. After that any of the known techniques that solves a generalized eigenvalue problem can then be used to find the frequencies (eigenvalues) and mode shapes (eigenvectors). In the present study, the Generalized Jacobi method [66] has been used to solve the eigenvalue problem.

2.3.3 Example Applications

In this section, we will apply the hierarchical finite element method developed to the examples that were solved in section 2.2.5 using the conventional FEM. We will then compare the results of the HFEM with the results of the conventional FEM and the exact solutions.

2.3.3.1 Free Vibration analysis of a Euler-Bernoulli Beam

Ex. 1 Problem Description

An A-36 steel I beam with a cross-section of type 8I23 and with both ends simply supported is as shown in Figure 2.19 [68],. The problem is defined by the following parameters: cross-sectional area (A) = 6.71 in^2; moment of inertia (I) = 64.2 in^4; modulus of elasticity (E) = 30 Mpsi and mass density of the beam (ρ) = 0.000733 $lbf - \sec^2/in^4$. The beam is modeled using only one hierarchical beam element. The natural frequencies and mode shapes are sought.

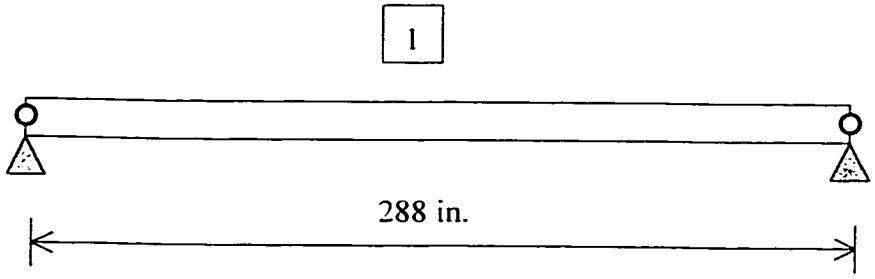

Figure 2.19 Beam modeled by just one hierarchical finite element

We will analyze this problem both by the use of the trigonometric and the polynomial hierarchical finite elements. The following tables will give us the results when we model the whole beam by just one element and with increasing number of hierarchical terms.

Table 2.12 Natural frequencies obtained by using different numbers of trigonometric hierarchical terms with just 1 element

S.NO	DOF* (1 ELEMENT)	ω_1	ω_2	ω_3	ω_4
1	5	74.4665	378.7304	946.2915	-
2	6	74.4665	297.8446	946.2914	1816.2973
3	7	74.4666	297.8446	670.1510	1816.2973
4	8	74.4669	297.8446	670.1510	1191.38
5	9	74.4666	297.8446	670.1511	1191.3826
6	**Exact Solution**	**74.4611**	**297.8444**	**670.1499**	**1191.3776**

*4 conventional DOF + additional trigonometric hierarchical DOF.

Table 2.13 Natural frequencies obtained by using different numbers of polynomial hierarchical terms with just 1 element

S.NO	DOF* (1 ELEMENT)	ω_1	ω_2	ω_3	ω_4
1	5	74.4657	378.730	946.2914	-
2	6	74.4599	378.7261	684.1498	4450.492
3	7	74.4599	302.59	378.7034	669.3930
4	8	74.4598	294.15	378.585	669.365
5	9	59.0023	294.128	377.856	672.479
6	Exact Solution	**74.4611**	**297.8444**	**670.1499**	**1191.3776**

* 4 conventional DOF + additional polynomial hierarchical DOF.

The results shown above give the solution of the free vibration problem stated above. As opposed to the conventional FEM solution we have modeled the whole beam by using just one element and we have varied the numbers of hierarchical terms associated with this one element. Both the trigonometric and the polynomial cases have been presented here and their comparison with the exact solution is also given.

As can be seen from the values in the Tables 2.12 and 2.13, the rate of convergence to the exact solution is much faster in the trigonometric case than in the polynomial case. Also, in the polynomial case the results do not converge to exact solutions on increasing the number of hierarchical terms in the element. This could be attributed to the fact, that the addition of hierarchical terms basically tries to make the deformed shape of the beam element as it would be in the actual deformation. It lends extra freedom to the inside of the element so that the element is more effective in depicting the actual shape of the deformation. This is what makes the element more efficient. The modification in the shape, so that it depicts the actual shape, is brought about by these hierarchical terms.

In our case of the present example, we see that the polynomial terms that we have added to the one element modeling our beam do not converge to the exact solution. The probable reason for this could be that the polynomial terms are not sufficiently effective to alter the deformation inside the element and make it efficient enough to model the behavior of the whole beam. Also, with increasing number of polynomial terms, the

degree of the approximating function is such that the resulting stiffness and the mass matrices become ill-conditioned. Hence, their correct eigenvalue solution is not possible.

It remains to be seen that how do the values converge when we use more than 1 element. We have already seen that in the trigonometric case we achieved absolute convergence just by one element. We had to add trigonometric hierarchical terms to the element to get convergence till the fourth frequency. In the polynomial case we didn't achieve this if there is just 1 element, then there is a limit to the number of polynomial hierarchical terms that we can attach to it to avoid the matrices getting ill–conditioned. Hence, we see how does the formulation fare when we take more than 1 element. Table 2.14 gives us the details when we use more than 1 element to model the beam and with varying number of degrees of freedom (i.e. hierarchical terms).

Table 2.14 Comparison of the two formulations with varying DOF and number of elements

DOF$^{\Omega}$/ Element	HFEM TYPE	NO. OF Elements	FREQUENCIES (ω, RAD / SEC)			
5	T	2	74.467	297.844	689.91	1514.932
		3	74.463	297.96	670.15	1211.01
	P	2*	74.576	330.58	484.14	703.50
		3	74.465	297.96	670.35	1212.2
6	T	2	74.462	297.84	670.91	1191.4
		3	74.464	297.91	670.15	1199.4
	P	2	74.464	297.85	689.06	1514.9
		3	74.465	297.96	670.15	1210.6
7	T	2	74.461	297.84	670.28	1191.4
		3'	-	-	-	-
	P	2	74.464	297.85	689.06	1514.9
		3*	76.929	328.89	754.96	1076.9
8	T	2'	-	-	-	-
		3'	-	-	-	-
	P	2*	74.464	297.85	689.06	1514.9
		3*	-	-	-	-
Exact Solution			**74.4611**	**297.8444**	**670.1499**	**1191.3776**

T – Trigonometric Formulation, P – Polynomial formulation
- 4 conventional DOF + additional hierarchical DOF.
! - The exact solution was already obtained, hence further cases are not considered.
*** - The matrix solution was inaccurate since the matrices became Positive Indefinite. Generalized Jacobi Method was used.**

As evident from Table 2.14 and as mentioned before, the trigonometric formulations fare very well. The highlighted portions shown in Table 2.14 indicate that with the addition of 2 trigonometric hierarchical terms (six degrees of freedom per element), and using 2 elements we converge to the exact answer. Hence, further addition of the hierarchical terms when we are using 2 elements to model the beam is not required. In the case of using the polynomial formulation, when we use 2 elements to model the beam and have 2 polynomial hierarchical terms added to each element (six degrees of freedom per element), we get closest to the exact answer. Adding any further hierarchical terms to the elements does not increase the accuracy but tends to make the matrices ill – conditioned. Also, adding further elements does not increase the accuracy. Table 2.16 gives us an idea about how much error is associated with each value with respect to the exact solution.

It would be important to mention here that the errors associated with other formulations of finite element method viz. the conventional FEM and the advanced finite element method [70]. The advanced FEM has 8 DOF per element, where apart from w and θ, the shear force and the bending moment are also considered as the nodal degrees of freedom. It gives better results than the conventional finite element formulation.

Table 2.15 Errors in the natural frequencies in the conventional formulation and the advanced formulation

No. Of Elements ↓	Error (%) by Formulation Method					
	CONVENTIONAL METHOD			ADVANCED METHOD [70] (8 DOF)		
$\omega \longrightarrow$	ω_1	ω_2	ω_3	ω_1	ω_2	ω_3
2	0.39	10.99	23.99	0.09	0.66	1.15
3	0.08	1.18	10.99	0.03	0.20	1.15
4	0.03	0.39	1.83	0.01	0.09	0.28
5	0.01	0.17	0.79	0.01	0.05	0.15

Table 2.16 Error associated with the cases considered in Table 2.14

DOF$^{\Omega}$/ Element	HFEM TYPE	NO. OF Elements	ERROR (%)			
5	T	2	0.008	-0.0017	2.95	21.35
		3	0.003	0.0372	-0.0016	1.62
	P	2*	0.1543	11.103	-27.683	-69.35
		3	0.005	0.0372	0.028	1.72
6	T	2	0.003	0.0001	0.111	0.0019
		3	0.004	0.0205	-0.0016	0.6689
	P	2	0.004	0.0003	2.926	21.35
		3	0.005	0.0372	-0.0016	1.59
7	T	2	0.000	0.0001	0.0178	0.0019
		3'	-	-	-	-
	P	2	0.004	0.0003	2.926	21.35
		3*	-	-	-	-
8	T	2'	-	-	-	-
		3'	-	-	-	-
	P	2*	0.004	0.0003	2.926	21.35
		3*	-	-	-	-
Exact Solution			**74.4611**	**297.8444**	**670.1499**	**1191.377**

T – Trigonometric Formulation, P – Polynomial formulation
- 4 conventional terms + additional polynomial hierarchical terms.
! - The exact solution was already obtained, hence further cases are not considered.
*** - The matrix solution was inaccurate since the matrices became Positive Indefinite. Generalized Jacobi Method was used.**

As is evident from the Tables 2.15 and 2.16 the trigonometric hierarchical FEM gives much better accuracy with less number of elements than the conventional and the advanced formulations. The polynomial hierarchical formulation also gives better results than the conventional formulation and is at par with the advanced formulation except for the cases when the matrices get ill-conditioned. In that case other polynomials can be used in place of this one which can give better results.

2.3.3.2 Forced Vibration analysis of a Euler-Bernoulli Beam

Ex. 2 Problem Description

For the fixed – fixed beam [69] shown in the Figure 2.20, (a) the natural frequencies and mode shapes, and (b) the response to a concentrated force of 10000 lb suddenly applied at the center of the beam for 0.1 sec and removed linearly as shown in the Figure 2.21 are sought. A time step of integration t = 0.01 sec is used. The properties of the beam are length (L) = 200 inches, moment of inertia (I) = 100 in^4, modulus of elasticity (E) = 6.58 Mpsi, and mass per unit length ($\overline{m}$) = 0.10 $lbf.\sec^2/in^2$. The beam is divided into four elements of equal length as shown in Figure (2.20).

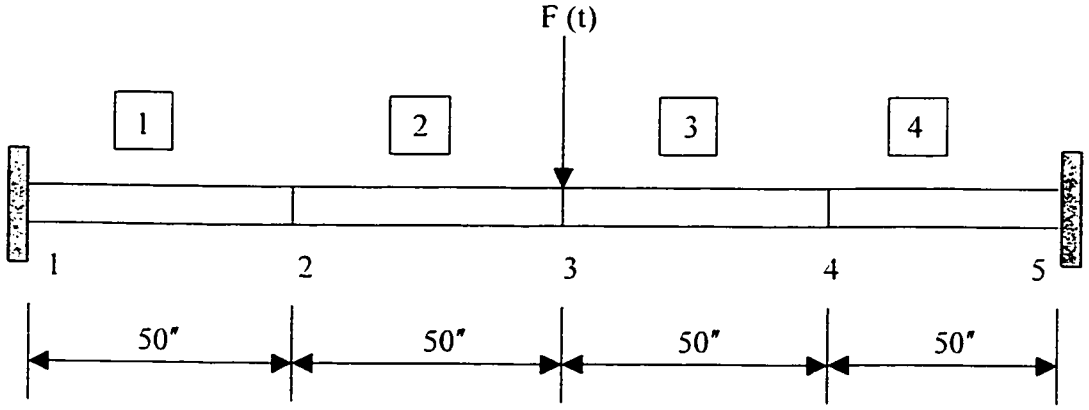

Figure 2.20 Modeling the Fixed – Fixed Beam for the forced vibration analysis using HFEM

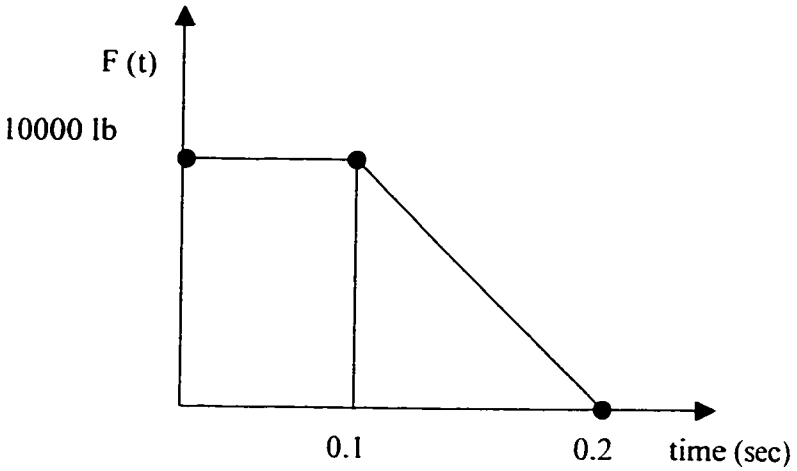

Figure 2.21 Force Applied on the beam for forced vibration

The solution of the forced vibration problem involves the solution of the following equation:

$$[K]\{U\}+[M]\{\ddot{U}\}=[F] \tag{2.112}$$

where [F] is the nodal force matrix. In the forced vibration case, we intend to find the response to the excitation that this beam is subjected to by the application of the force. As we did in the conventional formulation case, we will use the mode superposition method and the direct integration techniques, viz. Wilson - θ method and the Newmark - β method to obtain the solution once the [K] and [M] matrices are obtained by the hierarchical FEM – using both trigonometric and the polynomial functions.

It should be noted that the same problem was solved for the maximum deflection in section 2.2.5 by using the conventional FEM. In the present solution we intend to apply the HFEM to obtain the [K] and [M] for the beam and then proceed with the

solution for the maximum deflection. In the original problem, the discretization of the beam was given as in Figure 2.20. For the HFEM, as given in Figure 2.22, we model the beam using two hierarchical elements, each having one hierarchical term as internal degree of freedom. In the figure, the numbers in bold parenthesis denote the nodal degrees of freedom (DOF), and the numbers in bold italics denote the hierarchical DOF added to the element. The results for the maximum deflection are obtained by the application of the HFEM and are given in the following tables. They are compared with the results in reference [69] and the errors associated with them are given in Tables 2.17 –2.19.

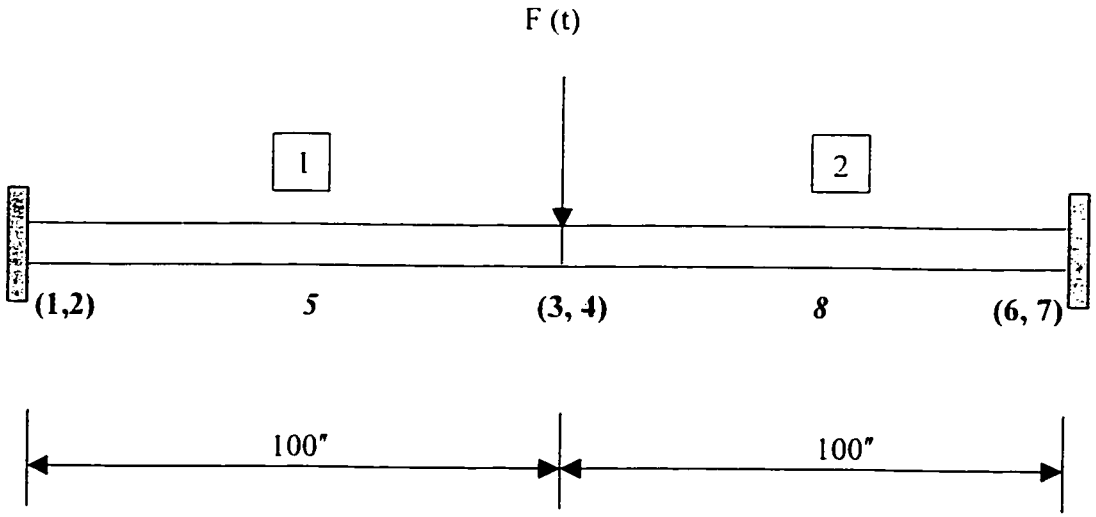

Figure 2.22 Modeling the Fixed – Fixed Beam for the forced vibration analysis using hierarchical method – 1 hierarchical term per element

Formulation using Trigonometric functions:

(i) Maximum Response of the beam in Ex. 2 by modeling with 2 elements, each element having five degrees of freedom (DOF)

Table 2.17 Maximum response of the beam in Ex. 2 using hierarchical finite element

Node	Results in Reference [69] (Mode Superposition)	Solution Using Wilson-θ Method (Error)	Solution Using Newmark-β Method (Error)
3	1.2430	1.2494 (0.52%)	1.2510 (0.64%)
4	0.0000	0.0020 (0.2%)	0.0013 (0.13%)

(ii) Maximum Response of the beam in Ex. 2 by modeling the beam with 2 elements, each element having six degrees of freedom (DOF)

Table 2.18 Maximum response of the beam in Ex. 2 using hierarchical finite element

Node	Results in Reference [69] (Mode Superposition)	Solution Using Wilson-θ Method (Error)	Solution Using Newmark-β Method (Error)
3	1.2430	1.2323 (-0.86 %)	1.2422 (-0.06 %)
4	0.0000	0.0000 (0. 0%)	0.0000 (0.0 %)

Formulation using Polynomial functions:

(i) Maximum Response of the beam in Ex. 2 by modeling the beam with 2 elements, each element having six degrees of freedom (DOF)

Table 2.19 Maximum response of the beam in Ex. 2 using hierarchical finite element

Node	Results in Reference [69] (Mode Superposition)	Solution Using Wilson-θ Method (Error)	Solution Using Newmark-β Method (Error)
3	1.2430	1.2326 (-0.84 %)	1.2406 (-0.19 %)
4	0.0000	0.0000 (0. 0%)	0.0000 (0.0 %)

2.3.3.3 Free Vibration Analysis of the Timoshenko Beam

Ex.3 Problem Description

For the simply – supported Timoshenko beam shown in Figures 2.23 and 2.24, the natural frequencies are to be obtained using the application of the HFEM. The properties of the beam are: length (L) = 10 ft.; moment of inertia (I) = 0.0278 ft^4; area of cross-section of the beam (A) = 1/3 ft^2; modulus of elasticity (E) = $4.17x10^9 lbf/ft^2$; shear modulus (G) = $1.649x10^9 lbf/ft^2$; shear correction factor (k_s) = 0.85 and mass density (ρ) = 15.20 $lbf - \sec^2/ft^4$.

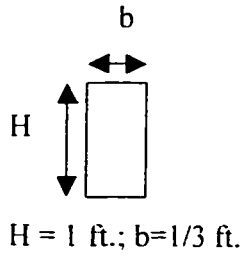

Figure 2.23 Cross-section of a Timoshenko beam

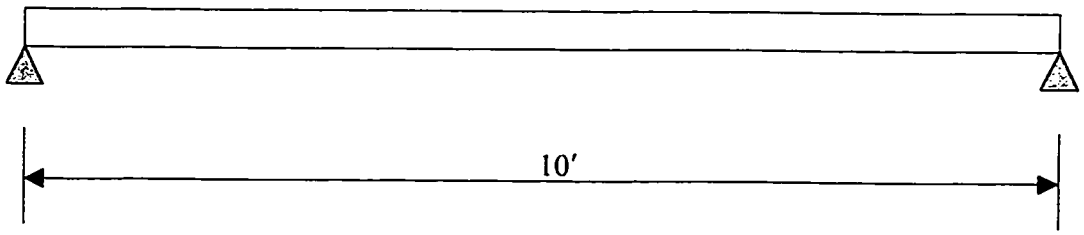

Figure 2.24 Simply-Supported Timoshenko beam for the free vibration analysis using HFEM

The hierarchical FEM formulation developed for the Timoshenko beam is applied to the above problem. Both the trigonometric and the polynomial formulations have been put to use and their results have been compared with the exact solution. Tables 2.20 and

2.21 give us the results for both the formulations. In these tables, nTm refers to the solution with n elements in the complete beam and m trigonometric terms (m/2 each for w and θ) in each element. This notation applies to the polynomial terms as well. The numbers in the parenthesis refer to the number of system degrees of freedom excluding the restrained ones.

Table 2.20 Natural frequencies of a Timoshenko beam using Trigonometric formulation

Mode	Exact Solution	1T4 (6)	2T4 (12)	2T8 (20)	3T8 (30)	4T8 (40)	5T8 (50)
1	**464.52**	469.05	476.99	467.54	466.24	465.61	465.26
2	**1765.38**	2369.20	1788.10	1780.00	1783.30	1781.60	1780.60
3	**3624.44**	-*	4101.90	3797.50	3756.50	3760.20	3758.20
4	**5578.14**	-*	7174.10	6239.10	6224.40	6195.60	6199.50

*Only 2 nodal degrees of freedom associated in this case.

Table 2.21 Natural frequencies of a Timoshenko beam using Polynomial Formulation

Mode	Exact Solution	4P4 (24)	4P8 (40)	6P6 (48)	10P6 (80)	20P6 (160)
1	**464.52**	534.88	493.69	483.75	471.46	466.31
2	**1765.38**	2108.70	1938.80	1868.30	1808.80	1785.50
3	**3624.44**	4680.70	4294.40	4007.90	3834.10	3771.90
4	**5578.14**	7993.60	7174.80	6772.50	6362.60	6228.70

* During the application of the Jacobi Method for the eigenvalue solution, the diagonal terms become negative at a point during iteration – hence, the solution was computed at that point and therefore might not be exact.

In both the trigonometric and the polynomial formulations, the solution involves modeling the Timoshenko beam with increasing number of elements and hierarchical terms in each element. It should be noted that the basic element considered here is linear, hence a large number of elements are required to obtain accurate answers. The results for the same problem are obtained by the conventional FEM and are listed in Table 2.11. Comparison of these results with those obtained by the conventional FEM and the exact solution shows that both the hierarchical formulations fare better than the conventional FEM. The trigonometric formulation gives the best performance both in terms of less number of elements and less trigonometric hierarchical terms. The polynomial formulation on the other hand, requires more elements and more hierarchical terms per element to achieve accuracy.

2.4 Program Organization for FEA and Computation of Vibration Response

In the development of the program, care has been taken to use descriptive variable names for every variable, for example, *nnode* represents the number of nodes in an element, *ndofn* represents the number of degrees of freedom per node, and so on. The program has been divided into segments to accomplish different tasks. This has been done to allow for fluent comprehension of the program. The various tasks performed by different routines are as follows:

- The master program : MAIN
- The Timoshenko analysis program : TIMO
- Compute the transformation matrix : TRANMAT
- Compute laminate stiffness matrices : ELEFREX
- Compute element stiffness matrix : ELESTF
- Compute element mass matrix : ELEMAS
- Assemble element stiffness and mass matrices : ASSMAT
- Calculate Eigenvalues and Eigenvectors : EIGVAL
- Compute dynamic displacements and rotations using Mode-Superposition method : FORVIBMS
- Compute dynamic displacements and rotations using Wilson- θ method : FORVIBWT
- Compute dynamic displacements and rotations using Newmark- β method : FORVIBNB
- Compute deformations for static analysis : FORVIBST

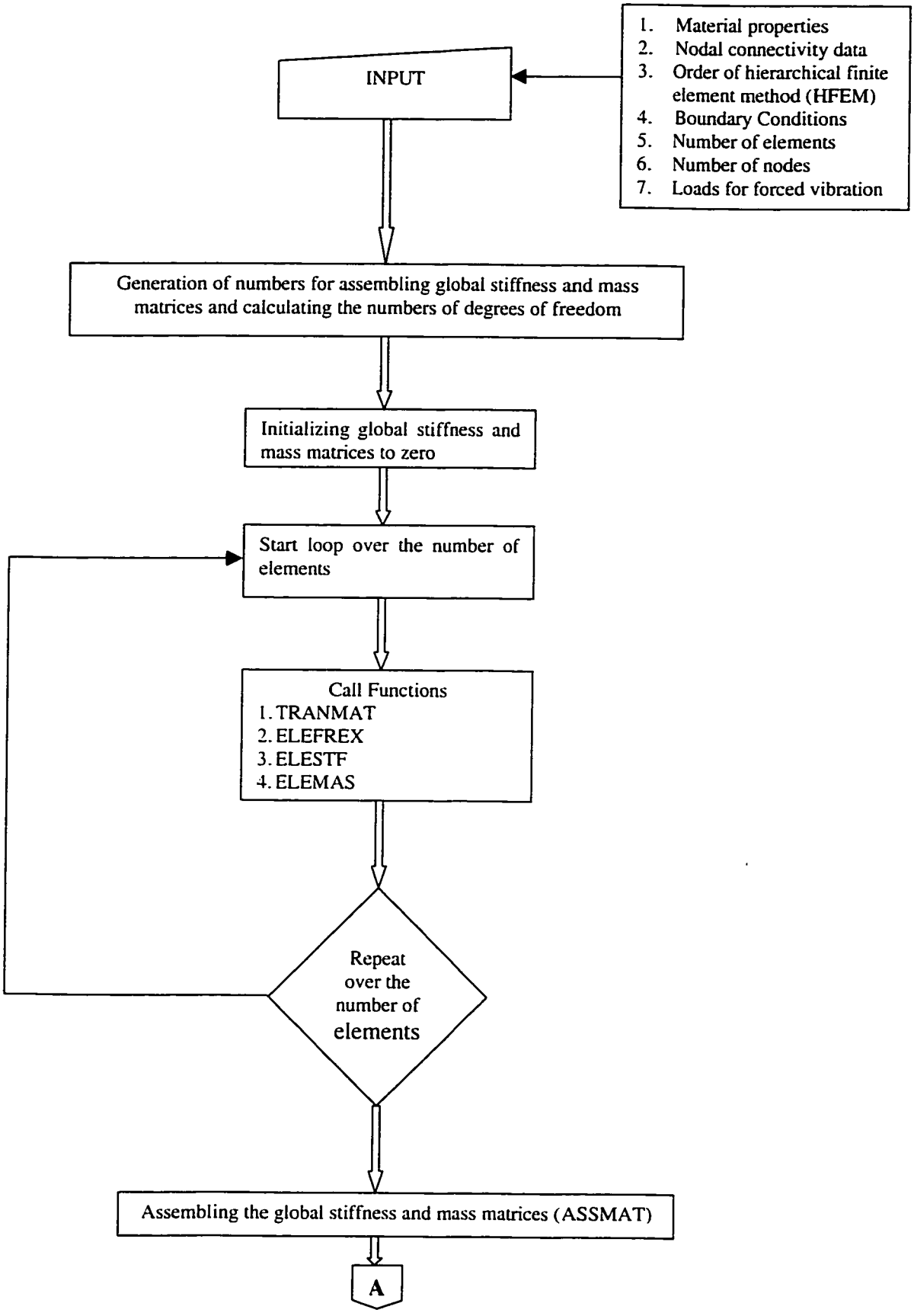
INPUT
1. Material properties
2. Nodal connectivity data
3. Order of hierarchical finite element method (HFEM)
4. Boundary Conditions
5. Number of elements
6. Number of nodes
7. Loads for forced vibration
Generation of numbers for assembling global stiffness and mass matrices and calculating the numbers of degrees of freedom
Initializing global stiffness and mass matrices to zero
Start loop over the number of elements
Call Functions
1. TRANMAT
2. ELEFREX
3. ELESTF
4. ELEMAS
Repeat over the number of elements
Assembling the global stiffness and mass matrices (ASSMAT)
A

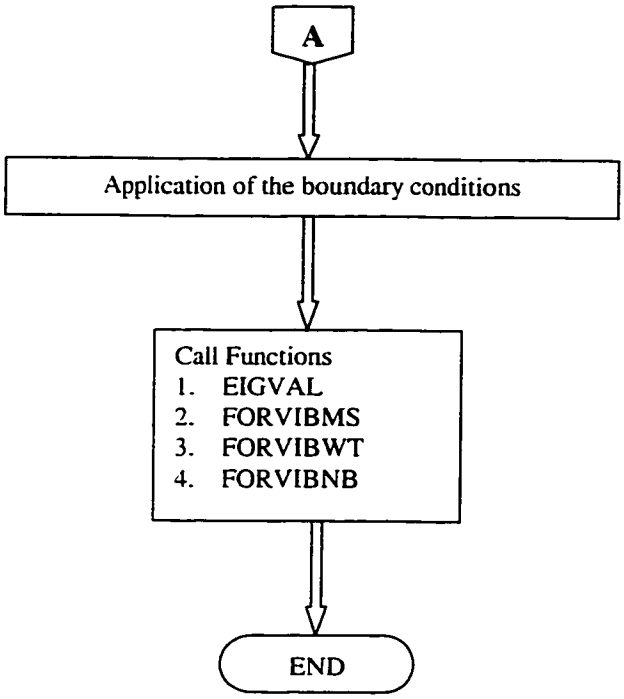

Figure 2.25 Flowchart used for the finite element vibration analysis

2.5 Conclusions and Discussion

In the previous sections the conventional and the hierarchical finite element methodologies have been described and example problems have been solved to illustrate their applications. The HFEM displays superior results as compared to the conventional FEM. We shall see how the results of the formulations compare with each other and within themselves in this section. The figures listed in this section plot the frequencies against the modes. It should be noted that this is done purely for visual convenience since modes and frequencies are not continuous quantities.

Figures 2.26 and 2.27 give us the comparison of the modal frequencies for the free vibration problem. The results have been obtained using the conventional FEM and the trigonometric and polynomial formulations of the HFEM. These results are then compared with the exact solution. The important thing to note is that apart from the less

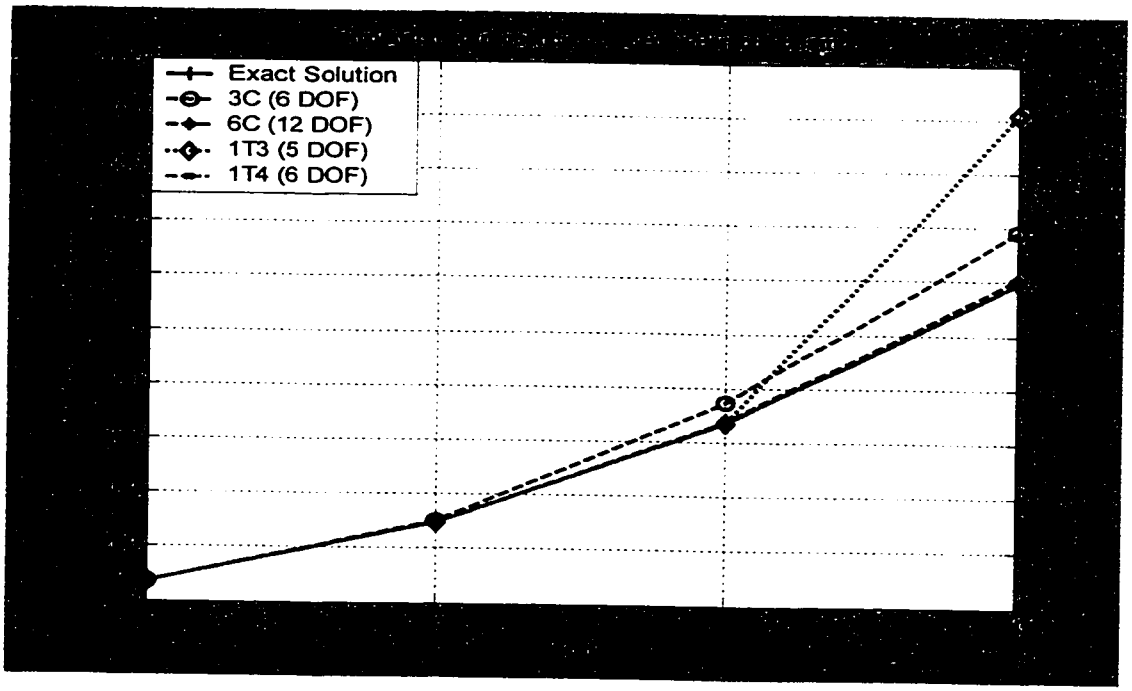

Figure 2.26 Comparison of frequencies of Euler-Bernoulli beam obtained using conventional FEM and trigonometric HFEM

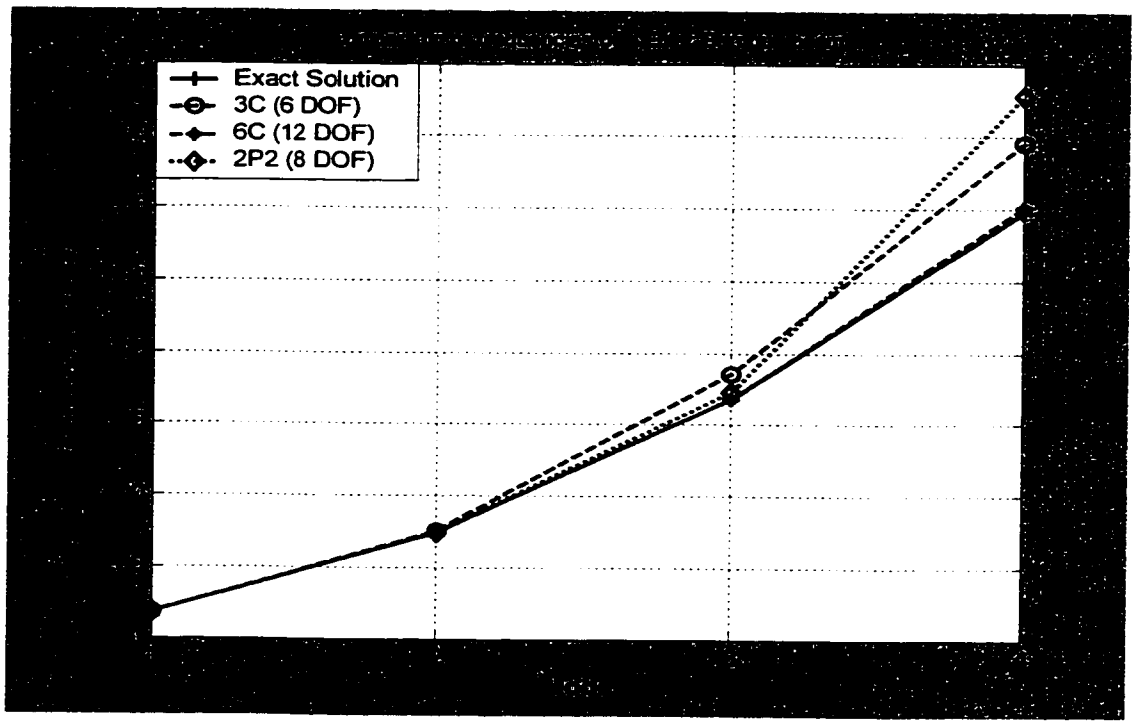

Figure 2.27 Comparison of frequencies of Euler-Bernoulli beam obtained using conventional FEM and polynomial HFEM

number of elements required for the modeling of the 1-D structure, there is a considerable decrease in the number of system degrees of freedom. These numbers have been specified in the legend of the Figure and they exclude the constrained DOF due to the boundary conditions. For the polynomial formulation, we had to resort to a minimum of two elements, as the results were lacking accuracy for 1 element. Figures 2.28 and 2.29 give us an idea of the manner of convergence of the 1-element and 2-element solutions for the trigonometric and polynomial formulation respectively. The frequency parameters, Ω_n ($\Omega_n = \omega_n \times \left(h \times (G/\rho)^{-1/2}\right)$), for different modes are plotted versus the number of trigonometric and polynomial terms for the simply-supported beam. These figures conform that the HFEM solutions converge from above to the exact solutions represented by dashed lines. As can be seen, convergence to the exact solutions in the

lowest two modes is much faster than in the third or fourth mode. This is due to the fact that the higher is the mode the more complex is the mode shape. Therefore, the higher the mode is, more number of hierarchical terms are needed to describe accurately this mode. It can also be seen that in the polynomial case, convergence is not obtained for the fourth mode frequency. This can again be explained by the fact that the combination of the polynomial terms that we make for the simply-supported beam, does not accurately describes the shape in which the beam deforms in the fourth mode. Also, addition of more terms in the polynomial case makes the solution numerically more expensive and sometimes inaccurate. Hence we see that the trigonometric formulation is more accurate than this set of chosen polynomials in describing the higher modes in the vibration of simply supported beams. Similar comparison for the results of forced vibration case shows that maximum response of the beam is obtained by using less number of elements

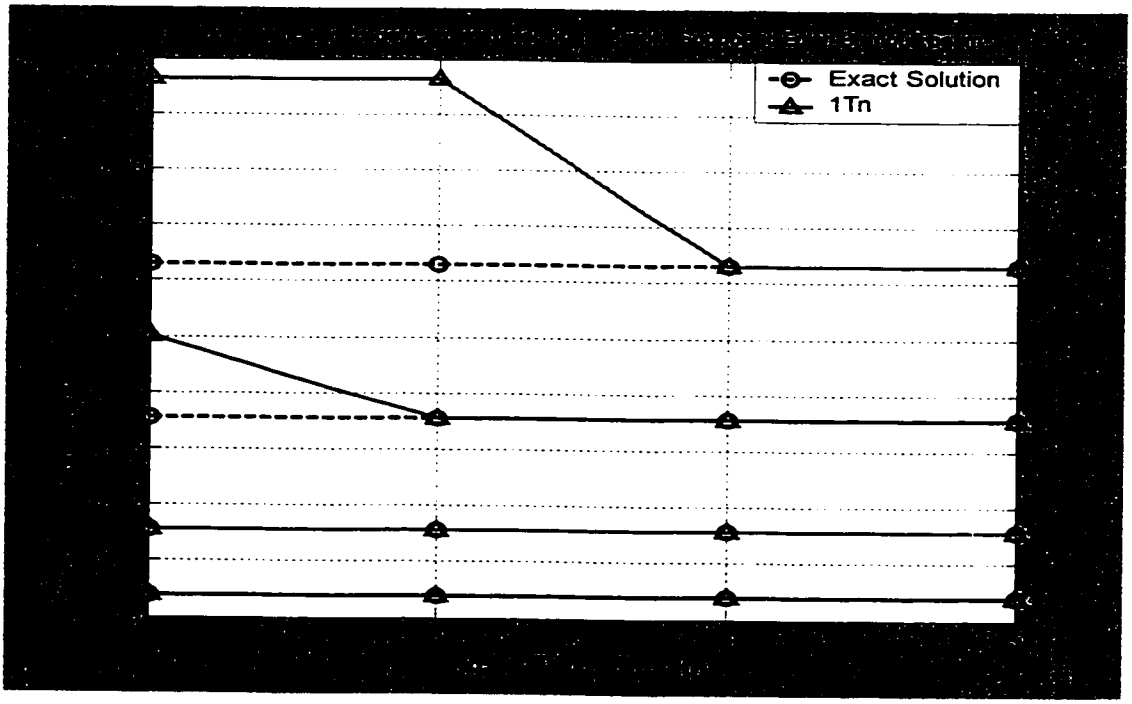

Figure 2.28 Convergence to $\Omega_1, \Omega_2, \Omega_3$ and Ω_4 of the Simply-Supported beam with increasing number of trigonometric terms in 1-element modeling

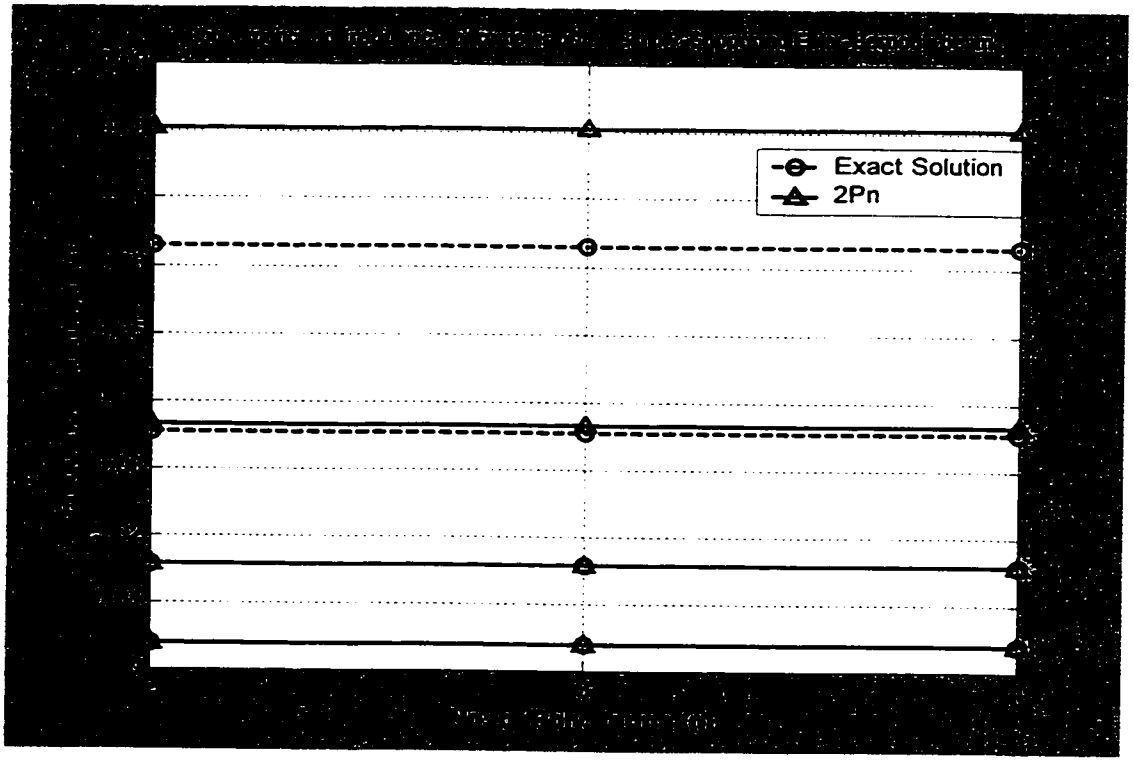

Figure 2.29 Convergence to $\Omega_1, \Omega_2, \Omega_3$ and Ω_4 of the Simply-Supported beam with increasing number of polynomial terms in 2-element modeling

and less number of system degrees of freedom in the modeling of beam. Figure 2.30 shows the frequencies obtained for the Timoshenko beam by the conventional and hierarchical formulations. As in the Euler-Bernoulli beam case, considerably less number of elements are required to obtain the exact solutions. Also, in Figures 2.31 and 2.32, a comparison between different cases of the same formulation is illustrated. Since the element is linear, a large number of elements are required to model the modes correctly.

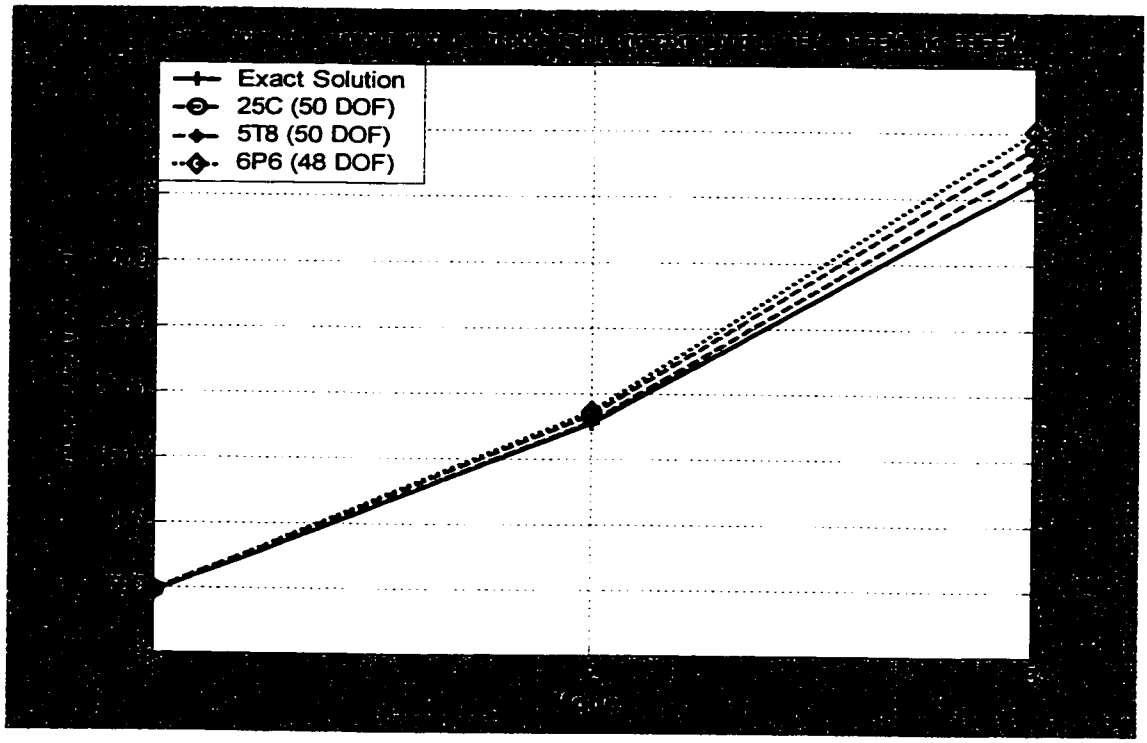

Figure 2.30 Comparison of frequencies of the Timoshenko beam obtained using conventional FEM, trigonometric HFEM and polynomial HFEM

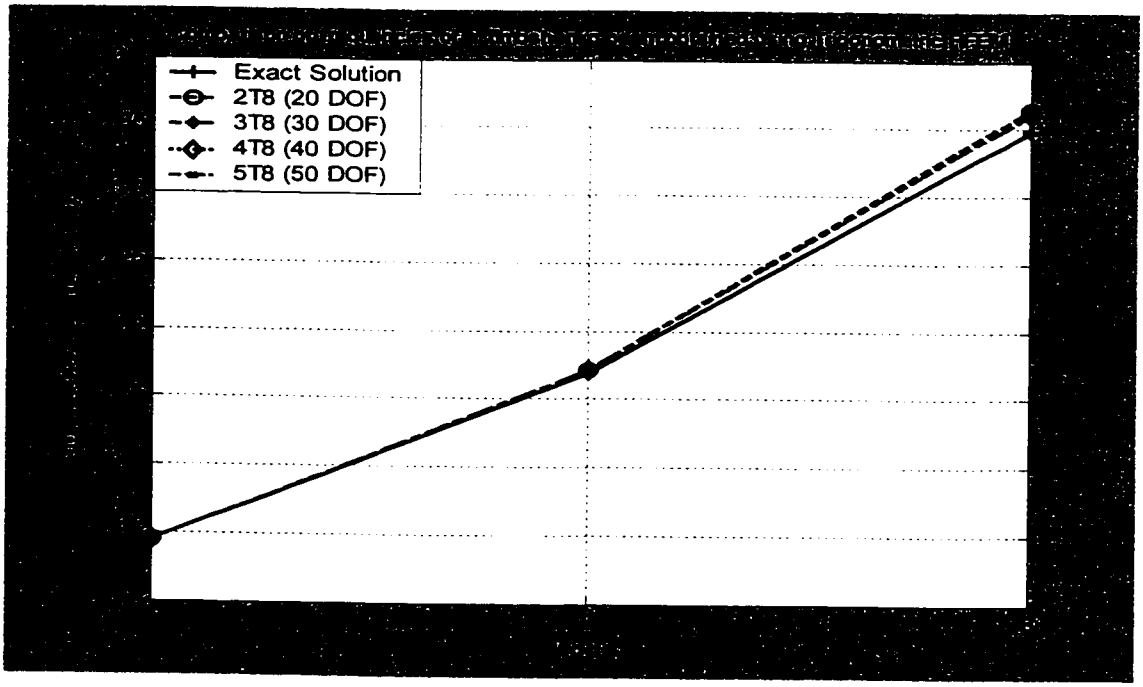

Figure 2.31 Comparison of frequencies of the Timoshenko beam obtained using trigonometric HFEM

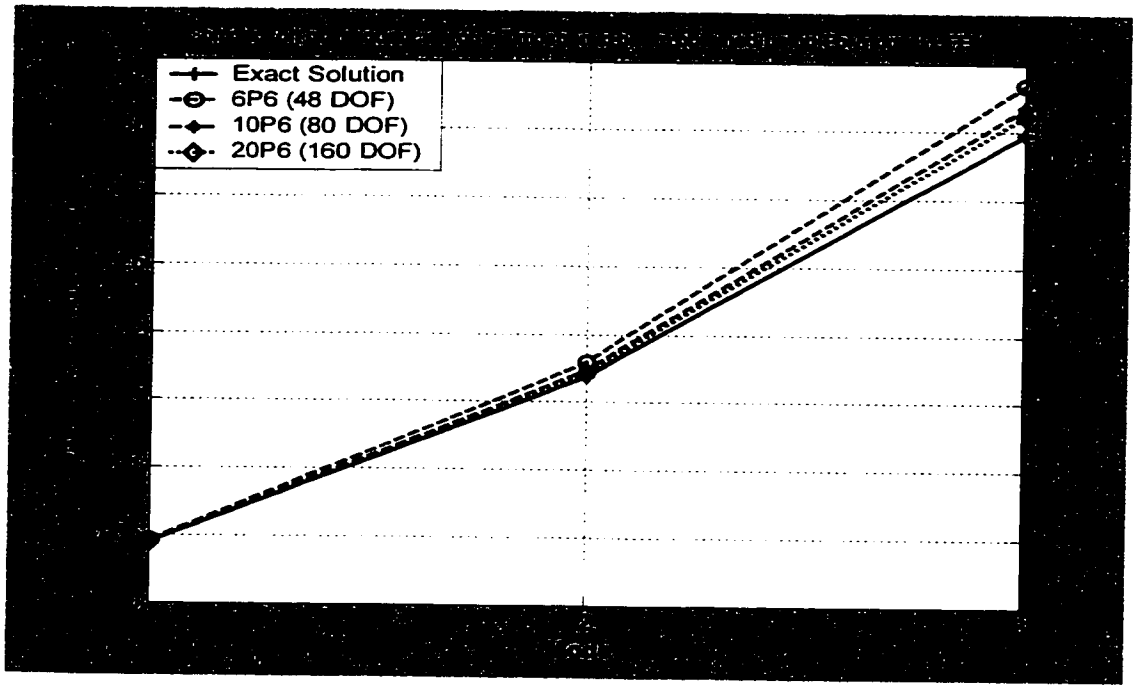

Figure 2.32 Comparison of frequencies of the Timoshenko beam obtained using polynomial HFEM

To sum up, in this chapter the Hierarchical Finite Element Method has been presented and its formulation has been applied to the free and forced vibration analysis of both the Euler- Bernoulli and Timoshenko beams made of isotropic materials. Two variations of the HFEM have been studied viz. Trigonometric and Polynomial HFEM. To start with, the conventional finite element formulation is presented and its derivation is detailed to stress the conceptual changes that are made in it for the HFEM. The problems of free and forced vibration are also solved using the conventional formulation so that a comparison can be made with regard to the HFEM results. The detailed formulation of the HFEM for both the trigonometric and the polynomial cases is also given to stress the major aspects of the method. Free and forced vibration problems are then solved using the developed HFEM techniques. Programs are developed both in MATLAB® and

MATHEMATICA® (for symbolic computing) software environment. The results obtained using the HFEM method are then compared with the results obtained using the conventional formulation and the exact solutions.

Both the forms of HFEM are found to give highly accurate results, viz. frequencies in free vibration and maximum responses in forced vibration, with substantially less number of elements and system degrees of freedom. The effect of adding internal degrees of freedom enhances the performance of the element and hence a single more efficient element can do the work of many conventional elements combined. Also, the number of system degrees of freedom can be varied without changing the mesh of elements. Results can be achieved to any desired degree of accuracy by simply increasing the numbers of hierarchical terms in each element. There is, however a limitation in the polynomial case; upon increasing the number of polynomial hierarchical terms as taken in this study beyond a limit, the resulting stiffness and mass matrices become ill-conditioned and hence, their solutions become inaccurate. In spite of this drawback, the polynomial formulation gives better results than the conventional formulation, although the trigonometric formulation yields the best results among the three. Example problems have been solved both for the Euler-Bernoulli and the Timoshenko models. The trigonometric HFEM formulation gives the best results followed by the polynomial HFEM and then the conventional formulation.

Now we have laid the foundation for the application of HFEM in the dynamic analysis of 1-D structures. The inspiring results for isotropic materials should lead us to

similar computational efficiency for structures made of composite materials. In the next chapter, we shall explore the applications to composite structures using the HFEM methodology.

Chapter 3

Dynamic Analysis of Composite Beams using Hierarchical Finite Element Method

3.1 Introduction

Composite materials, especially laminated composites are being increasingly used in the aerospace and automobile industries. This is mainly because these materials exhibit high strength-to-weight and stiffness-to-weight ratios. The in-service loadings on aerospace and automobile structures are dynamic in nature. There is therefore a need for accurate prediction of the dynamic response characteristics of composite structures in order that they can be designed against failure due to dynamic loads.

The application to isotropic beams in the preceding chapter showed us that the hierarchical finite element formulation performs much better than the conventional finite element method in terms of faster convergence and use of less number of elements. In composite structures, the in-plane strains and stresses in different plies of the laminate are functions of the curvature of the laminate, in accordance with the classical laminated plate theory [71]. As a result, the continuity of the in-plane stresses and strains in each ply of the laminate depends upon the continuity of curvature across adjacent elements.

This continuity is not enforced and guaranteed in the conventional finite element formulation, which requires the use of many elements to obtain reasonable accuracy. The use of many elements results in the presence of corresponding discontinuities. In the case of variable-thickness composite laminates, additional complexities arise due to the presence of drop-off plies. Hierarchical finite element method (HFEM) makes it possible to model a structure using very few elements; In some cases the use of just one hierarchical finite element provides accurate solutions. These features of the HFEM make it an attractive choice to overcome the limitations associated with the finite element formulation in the dynamic analysis of composite beams.

3.2 The Hierarchical Finite Element Formulation for Composite Beams

3.2.1 Weak Formulation for uniform composite beams based on the Euler – Bernoulli Theory

Consider a beam of composite material loaded in the x-z plane only (Figure 3.1). Also, for simplicity ignore the hygrothermal effects which add onto the strain terms in the constitutive equations. Because the beam considered is so narrow (b<<L), strains are ignored in the y-direction, implying that all Poisson effects can be ignored (classical beam assumption). Lastly, there is no y-direction dependence of any quantity involved in the set of governing equations. With these assumptions the force-displacement equations are reduced to [6]:

$$\begin{bmatrix} N_x \\ M_x \end{bmatrix} = \begin{bmatrix} A_{11} & B_{11} \\ B_{11} & D_{11} \end{bmatrix} \begin{bmatrix} \varepsilon_x^\circ \\ \kappa_x \end{bmatrix} \tag{3.1}$$

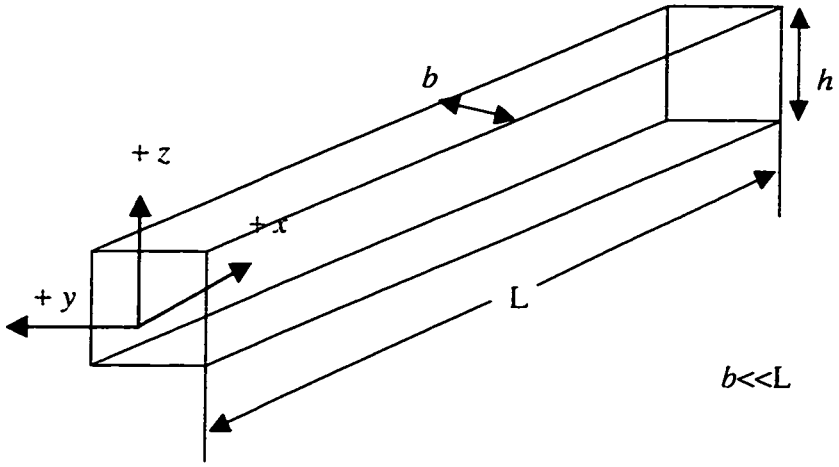

Figure 3.1 Typical beam in three dimensions

In the above equation, N_x denotes the normal force in the x direction per unit width, M_x denotes the bending moment in the x direction per unit width, ε_x° denotes the strain component in the x direction on the reference plane and κ_x denotes the curvature in the x direction.

If the beam has mid-plane symmetry, then there is no bending-stretching coupling so that $B_{11} = 0$ and the matrix Equation (3.1) becomes uncoupled, i.e.,

$$N_x = A_{11}\varepsilon_x^\circ \tag{3.2}$$

$$M_x = D_{11}\kappa_x = -D_{11}\frac{d^2w}{dx^2} \tag{3.3}$$

Then using Equations (3.1) – (3.3), Equation (2.1) can be rewritten for a composite beam as:

$$\frac{\partial^2}{\partial x^2}\left(bD_{11}\frac{\partial^2 w}{\partial x^2}\right)+\rho A\frac{\partial^2 w}{\partial t^2}-q'(x,t)=0 \qquad \text{for } 0<x<L \tag{3.4}$$

where b is the width of the beam and D_{11} is the bending stiffness of the composite beam. Rest of the terms have already been detailed in Equation (2.1). This is the governing equation for the forced undamped vibratory motion of a composite beam. The weak form for the above differential equation is obtained in the same way as done for beams of isotropic materials and is as follows:

$$\int_0^l\left(\frac{d^2v}{dx^2}bD_{11}\frac{d^2W}{dx^2}-\lambda\rho Avw-vq'\right)dx+\left[v\frac{d}{dx}\left(bD_{11}\frac{d^2W}{dx^2}\right)-\frac{dv}{dx}bD_{11}\frac{d^2W}{dx^2}\right]_0^l=0 \tag{3.5}$$

If however, the 1-D laminated beam theory is used instead of the cylindrical bending theory, then the coefficient D_{11} will change to $1/D_{11}^*$, where D_{11}^* is the first element in the inverse of the matrix [D].

3.2.2 HFEM formulation for uniform composite beams

3.2.2.1 Formulation based on Euler – Bernoulli Theory

The hierarchical finite element formulation for the composite beams proceeds in the same way as the procedure described in the previous chapter for isotropic beams. The difference being that now it is applied to the differential equation of the composite beam in Equation (3.4) instead of the isotropic beam in Equation (2.1) and that the term EI is replaced with bD_{11}. The salient steps in the HFEM formulation are mentioned below:

The transverse displacement of an element of length l is approximated as,

$$w(\xi) = c_1 + c_2\xi + c_3\xi^2 + c_4\xi^3 + c_{r+4}Sin[\delta_r\xi] \tag{3.6}$$

where $\delta_r = r\pi$, $r = 1,2,3....$

and $\xi = x/l$

The derivation that is similar to the one as described before in section 2.3.1.1, gives us the following expression for the displacement field, w

$$w = N_1 w_1 + N_2(l\theta_1) + N_3 w_2 + N_4(l\theta_2) + N_{r+4} w_{r+4} \tag{3.7}$$

where the shape functions N_i, i =1,2,3,4... are as follows,

$$\begin{aligned} N_1 &= 1 - 3\xi^2 + 2\xi^3 \\ N_2 &= \xi - 2\xi^2 + \xi^3 \\ N_3 &= 3\xi^2 - 2\xi^3 \\ N_4 &= -\xi^2 + \xi^3 \end{aligned} \tag{3.8}$$

and

$$N_{r+4} = -\delta_r\xi + \left(2\delta_r + (-1)^r\delta_r\right)\xi^2 + \left(-\delta_r - (-1)^r\delta_r\right)\xi^3 + Sin[\delta_r\xi] \tag{3.9}$$

where $\delta_r = r\pi$, $r = 1,2,3....$

The expressions for the shape functions and their properties are the same as detailed in the previous chapter. The finite element model for the composite beam is obtained by making use of the weak form equation (Equation (3.5)) and the shape functions given in Equations (3.8) and (3.9). Writing the resulting equation in the non-dimensional co-ordinate system the equation becomes,

$$\sum_{j=1}^{n}\left\{\frac{1}{l^3}\int_0^1\left(bD_{11}\frac{d^2N_i}{d\xi^2}\frac{d^2N_j}{d\xi^2}\right)d\xi-\int_0^1\lambda\rho AN_iN_jld\xi\right\}U_j-\int_0^1N_iq'ld\xi-Q_i=0 \tag{3.10}$$

Hence,

$$K_{ij}=\frac{1}{l^3}\int_0^1\left(bD_{11}\frac{d^2N_i}{d\xi^2}\frac{d^2N_j}{d\xi^2}\right)d\xi \tag{3.11}$$

$$M_{ij}=\int_0^1(\rho AN_iN_jl)d\xi \tag{3.12}$$

The element stiffness matrix and the mass matrix are then assembled into the system stiffness matrix and the mass matrix by the usual overlay procedure.

The polynomial hierarchical finite element formulation for the composite beams would differ from the above trigonometric formulation in the nature of the hierarchical shape functions chosen for the formulation. The shape functions for the polynomial formulation will be as described in the previous chapter and will be applied to the weak form for the composite beams given by Equation (3.5).

Hence, the displacement field for the beam element would be,

$$\text{w (x)} = N_1w_1+N_2\theta_1+N_3w_2+N_4\theta_2+N_{r+4}A_r \tag{3.13}$$

where the hierarchical shape functions are,

$$N_{r+4}=x^{r+1}(x-l)^{r+1}\qquad r=1,2,\ldots M \tag{3.14}$$

and A_r are the coefficients of the polynomial hierarchical terms.

The function is chosen such that,

$$N_{r+4}=0\qquad at\ \ x=0\ \ and\ \ x=l$$

$$N'_{r+4} = 0 \qquad at \quad x = 0 \quad and \quad x = l$$

The above equations illustrate that the hierarchical shape function provides zero displacement and zero slope at each end of the element. Again, it is important to mention that this property is highly significant, since these modes contribute only to the *internal* displacement field of the element, and do not therefore affect (i.e. over restrain) the displacement at the nodes.

3.2.2.2 Formulation based on Timoshenko Beam Theory

The application of the trigonometric hierarchical finite element to thick composite beams would require us to adopt the Timoshenko beam theory. In accordance with the Timoshenko theory for thick beams, the displacement and the rotation fields for an element of length l, will be approximated as follows:

$$w = q_1 + q_3\xi + q_{m1}Sin[\delta_m \xi] \tag{3.15}$$

$$\theta = q_2 + q_4\xi + q_{m2}Sin[\delta_m \xi] \tag{3.16}$$

where $\delta_m = m\pi$, $\quad m = 1,2,3.... M;$

and $\xi = x/l$

Further, m_1 and m_2 define the coefficients of the hierarchical terms added to the displacement and rotation expressions in Equations (3.15) and (3.16) and are defined as

$$m_1 = 2m + 3; \quad m_2 = m_1 + 1$$

The potential energy (PE) and the kinetic energy (KE) of the prismatic Timoshenko beam element in non-dimensional co-ordinate system will have the same form as that of

Equations (2.67) and (2.68) for isotropic beams. There will however, be suitable changes as we compute the expressions for composite beams.

In the case of composite beams the following changes in the expressions of potential and kinetic energies are required. As described in the previous section, in accordance with the cylindrical bending theory for composite beams [71], EI is replaced by bD_{11}. The consideration of transverse shear effects in composite beams leads to the addition of the following terms in the constitutive equation for laminates [72],

$$\begin{bmatrix} Q_y \\ Q_x \end{bmatrix} = \begin{bmatrix} H_{44} & H_{45} \\ H_{45} & H_{55} \end{bmatrix} \begin{bmatrix} \gamma^{\circ}_{yz} \\ \gamma^{\circ}_{xz} \end{bmatrix} \tag{3.17}$$

where, $H_{ij} = k_{ij} F_{ij} \qquad i, j = 4,5$

and is named as the transverse shear stiffness of the laminate. The parameters k_{ij} are the shear correction factors and the coefficients F_{ij} are defined as follows,

$$F_{ij} = \sum_{k=1}^{n} \left(C'_{ij}\right)_k t_p \tag{3.18}$$

where, C'_{ij} are the ply stiffness constants referred to the laminate's reference direction, t_p is the thickness of an individual layer and n is the total number of layers.

For a transversely-isotropic composite material $G_{12} = G_{13} = G$. We know that the constitutive equation of a laminate with transverse shear includes the coefficient, F_{ij},

where i, j = 4,5 [72]. The potential energy expression for a thick composite beam would include the coefficient F_{55}, where,

$$F_{55} = \sum_{p=1}^{n} (C'_{55})_p \, t_p = \sum_{p=1}^{n} (C_{44} \sin^2\theta + C_{55} \cos^2\theta) \, t_p \tag{3.18a}$$

Hence, the expression for the potential energy will become as given in Equation (3.19).

$$PE = \frac{1}{2}\left[bD_{11} \int_0^1 \left(\frac{1}{l}\frac{d\theta}{d\xi} \right)^2 l d\xi + kbF_{55} \int_0^1 \left(\theta - \frac{1}{l}\frac{dw}{d\xi} \right)^2 l d\xi \right] \tag{3.19}$$

$$KE = \frac{\rho\omega^2}{2}\left[A \int_0^1 w^2 l d\xi + I \int_0^1 \theta^2 l d\xi \right] \tag{3.20}$$

where ρ in Equation (3.20) is the mass density of the material.

The quantities needed to form the element stiffness and the mass matrices are obtained in the matrix form as explained in section 2.3.1.2 and are repeated here for continuity:

$$\{w\} = [C]\{q\}; \quad \{\theta\} = [D]\{q\}; \quad \left(\frac{1}{l}\right)\frac{d\theta}{d\xi} = [F]\{q\}; \quad \theta - \left(\frac{1}{l}\right)\frac{dw}{d\xi} = [H]\{q\} \tag{3.21-3.24}$$

where,

$$C = [1, 0, \xi, 0, Sin[\delta_m \xi], 0]; \qquad D = [0, 1, 0, \xi, 0, Sin[\delta_m \xi]]; \tag{3.25}$$

$$F = [0,\ 0,\ 0,\ 1/l,\ 0,\ \left(\frac{\delta_m}{l}\right)Cos[\delta_m\xi]]; \tag{3.26}$$

$$H = [0,\ 1,\ -1/l,\ \xi,\ -\left(\frac{\delta_m}{l}\right)Cos[\delta_m\xi],\ Sin[\delta_m\xi]]; \tag{3.27}$$

$$q^T = [q_1, q_2, q_3, q_4, q_{m1}, q_{m2}] \tag{3.28}$$

Substituting the above equations in the equations for PE and KE we get,

$$PE = \frac{1}{2}\{q\}^T[K_q]\{q\}; \qquad KE = \frac{1}{2}\omega^2\{q\}^T[M_q]\{q\} \tag{3.29}$$

where, $[K_q]$ and $[M_q]$ are, respectively, the element stiffness and mass matrices, expressed in the q co-ordinate system as

$$[K_q] = bD_{11}\int_0^1 [F]^T[F]ld\xi + kbF_{55}\int_0^1 [H]^T[H]ld\xi\ ;\ [M_q] = \rho A\int_0^1 [C]^T[C]ld\xi + \rho I\int_0^1 [D]^T[D]ld\xi \tag{3.30}$$

The element stiffness matrix, $[K_q]$ and the mass matrix, $[M_q]$ expressed in the q co-ordinate system will be obtained by integrating explicitly the expressions given above. A new set of generalized co-ordinates p is chosen in order to satisfy inter-element compatibility. The relation between the p co-ordinates and the q co-ordinates is obtained by applying the element "boundary conditions" and is given by

$$[q] = [T][p] \tag{3.31}$$

where, $p^T = [w_1, \theta_1, w_2, \theta_2, \ldots, w_m, \theta_m]$

The generalized co-ordinates $w_1, \theta_1, w_2, \theta_2$ are the transverse displacement w and the rotation of the beam cross-section θ at the two nodes of the element. The generalized co-

ordinates w_m *and* θ_m are the amplitudes of the trigonometric functions for the transverse displacement w and the rotation of the beam cross-section θ in the interior of the element. The transformation matrix T for M=1 is,

$$T = \begin{bmatrix} 1 & 0 & 0 & 0 & 0 & 0 \\ 0 & 1 & 0 & 0 & 0 & 0 \\ -1 & 0 & 1 & 0 & 0 & 0 \\ 0 & -1 & 0 & 1 & 0 & 0 \\ 0 & 0 & 0 & 0 & 1 & 0 \\ 0 & 0 & 0 & 0 & 0 & 1 \end{bmatrix} \tag{3.32}$$

As can be seen from the above matrix, the transformation matrix is composed of a fixed 4 x 4 block and a variable number of diagonal 2 x 2 blocks and zero coefficients outside these blocks. Hence, the above matrix is for M = 1. The order N of the matrix T depends on the number of trigonometric terms M chosen. The matrix T is simply found by expanding it along the diagonal with as many 2 x 2 blocks as the number of terms used. The order N of the element stiffness, mass and transformation matrices is,

$$N = 2M + 4 \tag{3.33}$$

The element stiffness and mass matrices are transformed to the p co-ordinate system by using the relations

$$[K_p] = [T]^T [K_q][T]; \; [M_p] = [T]^T [M_q][T] \tag{3.34}$$

The element stiffness matrix $[K_p]$, and the mass matrix $[M_p]$, are then assembled into the system stiffness and mass matrices by direct summation. We will use the subroutine developed for the assembly of the elements for this purpose, the details of which have

been provided in the program development section. After that any of the known techniques that solves a generalized eigenvalue problem can then be used to find the frequencies (eigenvalues) and mode shapes (eigenvectors). In the present study, the Generalized Jacobi method [66] has been used to solve the eigenvalue problem.

3.2.3 Free Vibration Analysis of uniform composite beams using HFEM

The free vibration response of uniform composite beams is sought by applying the hierarchical finite element methodology developed in the previous section. Two cases are considered for modeling the uniform composite beams, viz. cylindrical bending theory for mid-plane symmetric composite beams and 1-D Laminated Beam Theory. The results are obtained by the application of the hierarchical finite element method and they are consequently compared with the closed form solutions available in reference works.

The exact solutions corresponding to the **Euler-Bernoulli Theory,** for the transverse vibrations of uniform mid-plane symmetric composite beams, having different boundary conditions are listed below. Their respective references are also mentione. The following legend is common for all the cases;

ω_n - Natural frequency of the n^{th} mode; L – length of the beam;

A – area of cross-section of the beam; b - width of the beam; ρ - density

D_{11} - bending stiffness coefficient

(i) Cylindrical Bending Theory

(a) Simply Supported Beam [6]

$$\omega_n = \frac{n^2\pi^2}{L^2}\sqrt{\frac{bD_{11}}{\rho A}} \tag{3.35}$$

where, n = 1,2,3,...

(b) Fixed – Fixed Beam [67]

$$\omega_n = \left(\frac{K_n}{L}\right)^2\sqrt{\frac{bD_{11}}{\rho A}} \tag{3.36}$$

where n = 1,2,3,... and K_n denotes the values of constants given as follows,

$K_1 = 4.732$, $K_2 = 7.853$, $K_3 = 10.996$, $K_4 = 14.137$, and so on.

(ii) 1- D Laminated Beam Theory

(a) Simply Supported Beam

$$\omega_n = \frac{n^2\pi^2}{L^2}\sqrt{\frac{\left(b/D_{11}^*\right)}{\rho A}} \tag{3.37}$$

where n = 1,2,3,... and D_{11}^* is the first term of the inverse of [D] matrix.

(c) Fixed – Fixed Beam

$$\omega_n = \left(\frac{K_n}{L}\right)^2\sqrt{\frac{\left(b/D_{11}^*\right)}{\rho A}} \tag{3.38}$$

where n = 1,2,3,... ; D_{11}^{*} is the first term of the inverse of [D] matrix and K_n denotes the values of constants given as follows.

$$K_1 = 4.732,\ K_2 = 7.853,\ K_3 = 10.996,\ K_4 = 14.137 \text{ and so on.}$$

The exact solution according to the **Timoshenko Beam Theory** for the transverse vibrations of uniform composite beams is given as follows [73]:

Simply – Supported Beam

$$\omega_n = \left(\frac{n\pi}{L}\right)^2 \left(\sqrt{\frac{bD_{11}}{\rho A}}\right) \left(\sqrt{\frac{kbF_{55}}{kbF_{55} + \left(\frac{n\pi}{L}\right)^2 bD_{11}}}\right) \tag{3.39}$$

where n = 1,2,3,...; D_{11} - bending stiffness coefficient ; k - shear correction factor; G – shear modulus; L – length of the beam; A- area of cross-section of the beam.

The closed form solutions for the natural frequencies for different cases as listed above highlight the important feature, that all the above cases are applicable for unit width. The width, b, in all the above cases, cancels and hence is not a determining factor in the natural frequencies of the beams.

3.2.4 Example Applications

In this section a complete set of example problems will be solved using the formulations developed in the preceding sections. Examples are solved considering both the Euler- Bernoulli and Timoshenko Beam Theories. The cylindrical bending theory and the 1-D laminated beam theory are also considered. Solutions are validated by comparing

them with results obtained using the available exact solutions or other approximate methods.

3.2.4.1 Examples Based on Euler – Bernoulli Theory

Ex. 1 Problem Description

Uniform composite beams with different boundary conditions as shown in the Figures 3.2 (a) and (b), are made up of T300/5208 graphite-epoxy having the following mechanical properties at 70-degree farenhite.

$E_1 = 144$ GPa; $E_2 = 12.14$ GPa; $G_{12} = 4.48$ GPa; $\rho = 1660.80\ Kg/m^3$; $\nu_{12} = 0.21$.

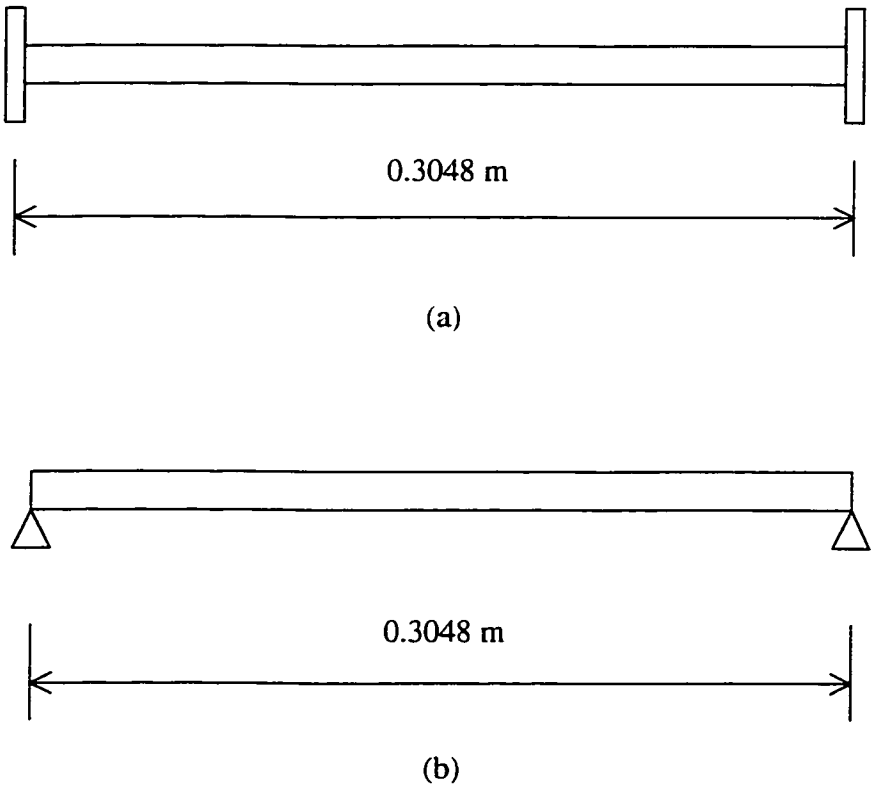

Figure 3.2 Uniform composite beam of Ex. 1. (a) Fixed- fixed (b) Simply-Supported

The geometric properties of the beams are: length (L) = 0.3048 m; individual ply thickness (t_p) = 0.1524 mm. There are 32 plies in the laminate and the configuration of the laminate is $[0^\circ/90^\circ]_{8s}$. The laminate thickness of 4.8768 mm is obtained by multiplying the number of plies, 32 in this case with the ply thickness, i.e.0.0001524 m.

The given problem is solved using both the hierarchical formulation and the conventional finite element formulation. For the HFEM, both the sub-formulations, viz. trigonometric and polynomial formulations are used to obtain the results. While solving the problem with either formulation, the beams are discretized such that the number of degrees of freedom used in the analysis by HFEM and by conventional FEM are comparable. This is done to make a comparison between the two formulations vis-à-vis the number of elements required, the number of nodal degrees of freedom to obtain the desired accuracy.

The analysis is done based on both the cylindrical bending theory and the 1-D laminated beam theory. Tables 3.1 and 3.2 give the results for the fixed-fixed and simply-supported beams based on the cylindrical bending theory for mid-plane symmetric composite laminate having the configuration $[0^\circ/90^\circ]_{8s}$. Comparison is made between the trigonometric HFEM and the conventional formulation and the results are then compared with the exact solutions. In the tables, nTm refers to the solution using n elements in the complete beam with m trigonometric terms in each element. Similarly, nC refers to n conventional elements used to model the beam. The numbers in the brackets refer to the system degrees of freedom excluding the constrained ones.

(a) Cylindrical bending of mid-plane symmetric composite beams

(i) TRIGONOMETRIC FORMULATION

Table 3.1 Natural frequencies of the Fixed-Fixed composite beam of Ex. 1

Mode	Exact Solution	2T1 (4 DOF)	2T2 (6 DOF)	3C (4 DOF)	4C(6 DOF)
1	2420.62	2420.82	2420.62	2428.51	2421.82
2	6666.67	6674.85	6667.15	6800.12	6728.67
3	13070.94	13459.22	13131.71	15815.97	13349.15
4	21604.89	32190.75	21694.10	31431.34	25255.41

Table 3.2 Natural Frequencies of the Simply-Supported composite beam of Ex. 1

Mode	Exact Solution	2T1 (6 DOF)	2T2 (8 DOF)	3C (6 DOF)	4C(8 DOF)
1	1066.93	1067.01	1066.93	1067.78	1067.20
2	4267.73	4267.83	4267.73	4318.17	4284.56
3	9602.40	9885.59	9613.31	10657.88	9777.84
4	17070.93	21706.89	17070.92	19817.55	18947.29

Two hierarchical trigonometric elements have been used to model the beams in Ex. 1. The numbers of hierarchical trigonometric terms per element are taken to be one (2T1) and two (2T2), thereby keeping the discretization of the beam same and increasing the internal degrees of freedom per element. In both the cases of fixed-fixed and simply – supported boundary conditions, it is observed that the accuracy associated with the natural frequencies increase with the increase in internal degrees of freedom. This is achieved by adding more hierarchical trigonometric terms per element. It is also noticed that for the same number of system degrees of freedom (DOF) in the trigonometric HFEM and the conventional FEM, the trigonometric HFEM gives more accurate results for the natural frequencies. This is significant as it establishes greater efficiency that the trigonometric HFEM possesses. The trigonometric HFEM uses less number of elements than the conventional formulation and increases the accuracy by adding internal degrees

of freedom rather than the nodal degrees of freedom as the conventional FEM does. The addition of the internal DOF better simulates the mode shapes of the vibration of beams than the nodal DOF and hence gives more accurate results. In the trigonometric HFEM, the accuracy of higher modes can be increased by increasing the number of internal degrees of freedom.

Tables 3.3 and 3.4 give the results for the two beams using the polynomial HFEM. The conventional formulation results are also given for comparison. nPm refers to the solution using n elements in the complete beam with m polynomial terms in each element.

(ii) POLYNOMIAL FORMULATION

Table 3.3 Natural frequencies of the Fixed-Fixed composite beam of Ex. 1

Mode	Exact Solution	2P1 (4 DOF)	2P2 (6 DOF)	3P2 (10 DOF)	3C (4 DOF)	4C (6 DOF)
1	2420.62	2420.82	2420.82	2420.72	2428.51	2421.82
2	6666.67	6681.12	6674.73	6677.92	6800.12	6728.67
3	13070.94	13555.81	13385.68	13085.62	15815.97	13349.15
4	21604.89	32574.33	30757.10	22016.52	31431.34	25255.41

Table 3.4 Natural frequencies of the Simply-Supported composite beam of Ex. 1

Mode	Exact Solution	2P1 (6 DOF)	2P2 (8 DOF)	3P2 (12 DOF*)	3C (6 DOF)	4C (8 DOF)
1	1066.93	1067.01	1067.01	1066.93	1067.78	1067.20
2	4267.73	4268.99	4267.73	4269.31	4318.17	4284.56
3	9602.40	9906.20	9873.40	9602.40	10657.88	9777.84
4	17070.93	21706.90	21706.90	17346.30	19817.55	18947.29

(*Further increasing the DOF in the Polynomial Formulation does not improve the accuracy.)

The polynomial HFEM works in a similar way as the trigonometric HFEM albeit with a difference. It uses polynomials as internal degrees of freedom. Tables 3.3 and 3.4 detail the results obtained for Ex. 1 and compare them with the conventional FEM results. It can be noticed from the tables that the polynomial HFEM is more accurate than the conventional FEM for the lower modes. For higher modes though, for the same number of system degrees of freedom, the conventional FEM gives better results than the polynomial HFEM although the polynomial HFEM uses less number of elements than the conventional FEM. The polynomial HFEM also has another limitation in terms of adding polynomials as internal degrees of freedom. As the degree of the polynomials to be added gets higher, the matrices become positive indefinite and hence the solution for the natural frequencies are unachievable. Inspite of these limitations, the polynomial HFEM gives better results for the lower modes than the conventional FEM.

Results obtained for Ex. 1 in the preceding tables were based on the cylindrical bending theory. Tables 3.5 through 3.8 list the results obtained for the same problem by considering the 1-D laminated beam theory. As done in the previous case, both the trigonometric and the polynomial formulations are presented and are compared with the conventional and the exact solutions.

(b) 1- D Laminated Beam Theory

(i) TRIGONOMETRIC FORMULATION

Table 3.5 Natural frequencies of the Fixed-Fixed composite beam of Ex. 1

Mode	Exact Solution	2T1 (4 DOF)	2T2 (6 DOF)	3C (4 DOF)	4C(6 DOF)
1	2419.73	2419.95	2419.73	2427.62	2420.93
2	6664.20	6672.32	6664.68	6797.65	6726.20
3	13066.12	13454.40	13126.89	15811.15	13344.33
4	21596.91	32182.77	21686.12	31423.36	25247.43

Table 3.6 Natural frequencies of the Simply-Supported composite beam of Ex. 1

Mode	Exact Solution	2T1 (6 DOF)	2T2 (8 DOF)	3C (6 DOF)	4C(8 DOF)
1	1066.54	1066.62	1066.54	1067.39	1066.81
2	4266.16	4266.26	4266.16	4316.60	4282.99
3	9598.85	9882.04	9609.76	10654.33	9774.29
4	17064.62	21700.58	17064.60	19811.24	18940.98

(ii) POLYNOMIAL FORMULATION

Table 3.7 Natural frequencies of the Fixed-Fixed composite beam of Ex. 1

Mode	Exact Solution	2P1 (4 DOF)	2P2 (6 DOF)	3C (4 DOF)	4C(6 DOF)
1	2419.73	2419.93	2419.93	2427.62	2420.93
2	6664.20	6678.65	6672.26	6797.65	6726.20
3	13066.12	13550.99	13380.86	15811.15	13344.33
4	21596.91	32566.35	30749.12	31423.36	25247.43

Table 3.8 Natural frequencies of the Simply-Supported composite beam of Ex. 1

Mode	Exact Solution	2P1 (6 DOF)	2P2 (8 DOF)	3C (6 DOF)	4C(8 DOF)
1	1066.54	1066.62	1066.62	1067.39	1066.81
2	4266.16	4267.36	4266.16	4316.60	4282.99
3	9598.85	9602.65	9869.85	10654.33	9774.29
4	17064.62	21700.59	21700.59	19811.24	18940.98

The results obtained for 1-D laminated beam theory essay the same conclusions, in terms of finite element method efficiency, as those obtained for the cylindrical bending theory.

3.2.4.2. Based on Timoshenko Beam Theory

Ex. 2 Problem Description

A beam as the one shown in the Figure 3.2 (b), is made up of T300/5208 graphite-epoxy with the following mechanical properties at 70-degree farenhite.

E_1 = 144 GPa; E_2 = 12.14 GPa; G_{13} = 4.48 GPa; G_{23} = 4.90 GPa; ρ = 1660.80 Kg/m^3;

$\nu_{12} = 0.21$ D_{11} = 817.1272 N.m.

The geometric properties of the beam are: L = 0.0243 m; individual ply thickness (t_p) = 0.1524 mm; Laminate thickness (h) = 4.8768 mm; area of cross-section (A) = 9.8755 mm^2; moment of inertia (I) = 1.9573×10^{-11} m^4. There are 32 plies in the laminate and the configuration of the laminate is $[0^\circ/90^\circ]_{8s}$. The boundary conditions for the beam are Simply- Supported. The laminate thickness of 4.8768 mm is obtained by multiplying the number of plies, 32 in this case, with the ply thickness, i.e. 0.0001524 m.

The problem in Ex. 2 ($L/h \approx 5$) is solved by the HFEM based on the Timoshenko beam theory. Results are presented for both the hierarchical formulations, viz. trigonometric and polynomial formulations and the conventional finite element formulation based on the Timoshenko beam theory. All the results are also compared with the exact solution available in the reference [73].

The conventional Timoshenko beam element chosen for this analysis is a linear element. In the hierarchical finite element analysis, the internal degrees of freedom are added to a linear element and hence a large number of hierarchical terms are required to obtain the desired accuracy. As can be seen, 2T8 formulation gives exact results until the fourth mode. In the polynomial formulation though, the resulting stiffness and mass matrices become ill-conditioned and hence the accuracy of the solutions is limited.

Table 3.9 Natural frequencies ($\times 10^5$) of the Simply-Supported composite Timoshenko beam of Ex. 2 obtained using the trigonometric HFEM

Mode	Exact Solution	1T2 (4)	2T4 (12)	2T8 (20)	1C (2)	4C (8)	8C (16)
1	**1.27**	1.34	1.27	1.27	10.65	2.03	1.58
2	**3.36**	10.65	3.35	3.34	14.73	3.02	4.12
3	**5.43**	14.79	5.50	5.43	-*	5.87	6.38
4	**7.45**	23.72	7.53	7.45	-*	10.87	6.92

(*Only 2 DOF after application of the boundary conditions, hence just 2 values are obtained)

Table 3.10 Natural frequencies ($\times 10^5$) of the Simply-Supported composite Timoshenko beam of Ex. 2 obtained using the polynomial HFEM

Mode	Exact Solution	1P2 (4)	2P4** (12)	1C (2)	4C (8)	8C (16)
1	**1.27**	1.69	1.44	10.65	2.03	1.58
2	**3.36**	10.65	4.22	14.73	3.02	4.12
3	**5.43**	14.78	4.87	-*	5.87	6.38
4	**7.45**	21.41	6.57	-*	10.87	6.92

(*Only 2 DOF after application of the boundary conditions, hence just 2 values are obtained)
(**Increasing the order further makes the matrices positive indefinite and ill-conditioned.)

3.2.5 Static analysis of uniform-thickness composite beam using HFEM

In the application of the hierarchical FEM to isotropic beams in the previous chapter, we saw that substantial computational efficiency is achieved. We now intend to apply the hierarchical formulations for the static analysis of Euler-Bernoulli composite beams in order to systematically bring out certain key aspects of the HFEM. In engineering analysis, from a designer's point of view, the quantities of paramount importance are the bending moment and shearing force distributions, which are found, respectively, from the second and third derivatives of the displacement. The conventional FEM will give a sufficiently accurate answer for the displacement distribution, however, the bending moment and shear force distribution, will at best be crude, and at worst misleading, in a coarsely meshed problem. The HFEM offers us an efficient way to increase the accuracy of the second and third derivatives of displacement by the addition of hierarchical terms to each element.

In addition to obtaining the stiffness matrix as done in the vibration analysis, for the static analysis we will have to obtain the force matrix as well. In Equation (3.10), the last two terms on the left-hand side give us the force matrix. Hence the force matrix for an element will be,

$$F_i = \int_0^1 N_i f l \, d\xi \; - Q_i \tag{3.40}$$

where f (f = q'(x) as per Equation (3.10)) is the distributed loading over the element and Q_i represents the natural (or internal force) boundary conditions of the element (Q_1 and Q_3 denote the resultant shear forces, and Q_2 and Q_4 denote the resultant bending moments at the nodes).

Hence, the statement for the static problem can be written as,

$$[K]\{q\} = \{F_i\} \tag{3.41}$$

where [K] is the stiffness matrix of the beam, {q} is the matrix having generalized co-ordinates associated with the DOF and $\{F_i\}$ is the force matrix.

To illustrate the application of the HFEM to the static analysis of a composite Euler-Bernoulli beam, we consider the following example. A uniform-thickness composite beam is made up of T300/5208 graphite-epoxy and is subjected to a linearly varying distributed load as shown in Figure 3.3 and has the following mechanical properties at 70-degree ferenhite.

E_1 = 144 GPa; E_2 = 12.14 GPa; G_{12} = 4.48 GPa; ρ = 1660.80 Kg/m^3; ν_{12} = 0.21; $D_{11} = 817.13\ N.m$.

The geometric properties of the beam are: width (b) = 0.0254 m; length (L) = 0.3048 m; individual ply thickness (t_p) = 0.1524 mm. There are 32 plies in the laminate and the configuration of the laminate is $[0^\circ/90^\circ]_{8s}$.

Solution of the above problem is obtained using the trigonometric and the polynomial Hierarchical FEM formulations. The beam is modeled using the cylindrical bending theory.

Exact Solution

The exact solutions for the deflection, slope, bending moment and the shearing force are given as follows [74] and they will be compared with those obtained with the conventional and the hierarchical finite element methods.

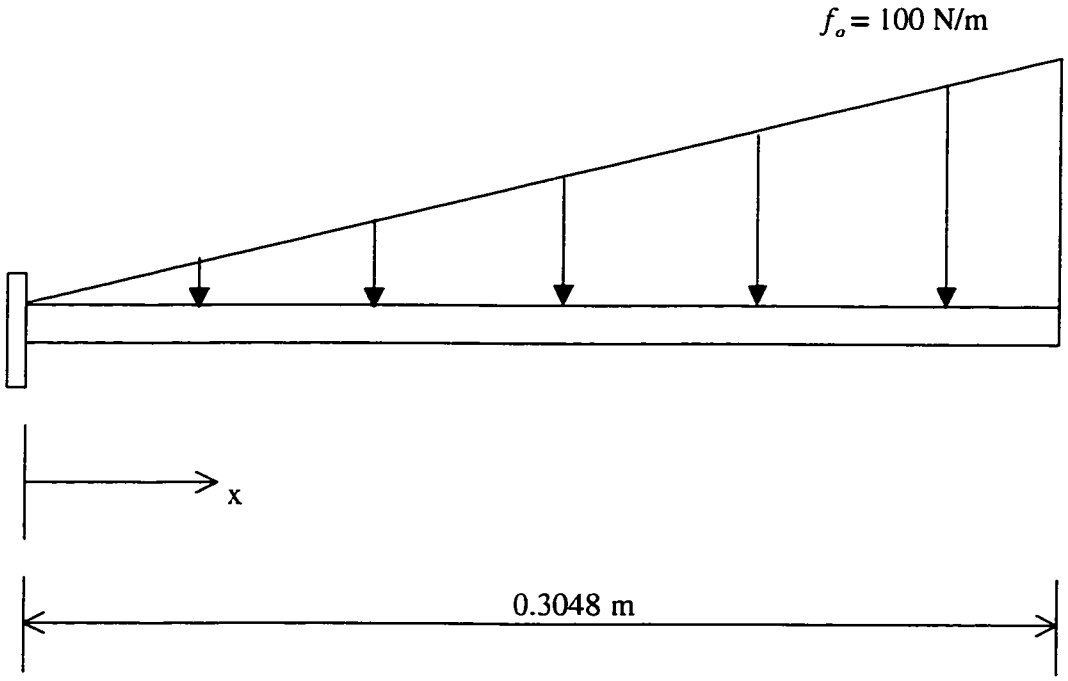

Figure 3.3 Fixed - Free beam for the static analysis using HFEM

Deflection:

$$w = \frac{f_o x^2}{120 L b D_{11}} \left(20L^3 - 10L^2 x + x^3\right) \tag{3.42}$$

Slope:

$$\theta = \frac{f_o x}{24 L b D_{11}} \left(8L^3 - 6L^2 x + x^3\right) \tag{3.43}$$

Bending Moment:

$$M = -bD_{11} \frac{d^2 w}{dx^2} = -\frac{f_o}{120L} \left(40L^3 - 60L^2 x + 20x^3\right) \tag{3.44}$$

Shear Force:

$$SF = -bD_{11}\frac{d^3w}{dx^3} = -\frac{f_o}{120L}\left(-60L^2 + 60x^2\right) \tag{3.45}$$

where, L – length of the beam; f_o - distributed loading on the beam;

b - width of the beam; ρ - density; D_{11} - bending stiffness coefficient

Solution using Trigonometric HFEM

In the non-dimensional co-ordinate system, the load equation for the given loading will become as,

$$f = 100\xi \quad (N) \qquad\qquad 0 \le \xi \le 1 \tag{3.46}$$

The solution of the given static problem by trigonometric HFEM is obtained by modeling the beam with trigonometric hierarchical elements and obtaining the stiffness matrix. For the static case, we will also obtain the force matrix as given in Equation (3.40). We model the beam with one hierarchical element that has two trigonometric terms as internal degrees of freedom. The stiffness and force matrices are obtained according to Equations (3.11) and (3.40). They are then plugged in Equation (3.41) and the resulting equation is given as follows:

$$\left[\begin{array}{cccc:cc} 8795.51 & 1340.44 & -8795.51 & 1340.44 & 0 & 0 \\ 1340.44 & 272.377 & -1340.44 & 136.188 & 0 & 0 \\ -8795.51 & -1340.44 & 8795.51 & -1340.44 & 0 & 0 \\ 1340.44 & 136.188 & -1340.44 & 272.377 & 0 & 0 \\ \hdashline 0 & 0 & 0 & 0 & 6762.38 & 0 \\ 0 & 0 & 0 & 0 & 0 & 223942 \end{array}\right]\left[\begin{array}{c} q_1 \\ q_2 \\ q_3 \\ q_4 \\ \hdashline q_5 \\ q_6 \end{array}\right] = \left[\begin{array}{c} 4.5720 \\ 0.3097 \\ 10.6680 \\ -0.4645 \\ \hdashline 1.7224 \\ -1.6592 \end{array}\right] + \left[\begin{array}{c} R \\ M \\ 0 \\ 0 \\ \hdashline 0 \\ 0 \end{array}\right] \tag{3.47}$$

$$\left[\begin{array}{c|c} K_c & 0 \\ \hline 0 & K_h \end{array}\right]\left[\begin{array}{c} q_c \\ \hline \overline{\overline{q_h}} \end{array}\right]=\left[\begin{array}{c} F_c \\ \hline \overline{\overline{F_h}} \end{array}\right] \tag{3.48}$$

Equation (3.47) gives the complete equation for the static analysis of the given problem, done by modeling the beam with one trigonometric hierarchical finite element. It should be noted that the top left part of the [K] matrix in Equation (3.47), is the 4x4 matrix that we would obtain if we model the beam with one conventional finite element. The bottom right hand part is a diagonal matrix and the remaining two parts are null matrices. The trigonometric hierarchical shape functions that we obtain are second derivative orthogonal, both with respect to themselves and the original four Hermite cubic functions. It is this property that makes the mentioned sub-matrices null and diagonal. In Equation (3.48) the deformation equation has been presented in the symbolic form with the subscripts "c" for conventional and "h" for hierarchical contributions. Since the problem considered here is a fixed-free beam, upon application of the boundary conditions and suitable matrix manipulation, we get the following:

$$\{q_c\}=[K_c]^{-1}\{F_c\} \tag{3.49}$$

$$\{q_h\}=[K_h]^{-1}\{F_h\} \tag{3.50}$$

Hence for the above case, we will get the following,

$$\begin{Bmatrix} q_3 \\ q_4 \end{Bmatrix}=\begin{Bmatrix} 3.8112\times10^{-3} \\ 1.7050\times10^{-2} \end{Bmatrix} \tag{3.51}$$

and,

$$\begin{Bmatrix} q_5 \\ q_6 \end{Bmatrix} = \begin{Bmatrix} 2.5471\times10^{-4} \\ -7.4090\times10^{-6} \end{Bmatrix} \tag{3.52}$$

Now w can be expressed as follows,

$$w(\xi) = \sum_{c=1}^{4} q_c N_c(\xi) + \sum_{h=1}^{2} q_h N_h(\xi) \tag{3.53}$$

where, $N_c(\xi)$ and $N_h(\xi)$ are the shape functions given in Equations (3.8) and (3.9) respectively. They have been mentioned differently as conventional and hierarchical shape functions to bring into focus the details of the hierarchical method and the nature of the resulting stiffness matrix. Consequently, the slope, bending moment and shear force can also be found once the expression for the displacement is obtained. Figures 3.4 – 3.7 give the distribution of these quantities along the beam, obtained by trigonometric HFEM and also compares them with the exact and conventional FEM solutions.

Solution using Polynomial HFEM

The solution to the static analysis problem for the composite Euler-Bernoulli beam is now sought by the polynomial HFEM. The procedure outlined in the trigonometric HFEM case is applicable here although the element considered will be the polynomial hierarchical finite element. The equation obtained upon substitution of suitable quantities in Equation (3.41) are as follows:

$$\left[\begin{array}{cccc:cc} 8795.51 & 1340.44 & -8795.51 & 1340.44 & 0 & 0 \\ 1340.44 & 272.377 & -1340.44 & 136.188 & 0 & 0 \\ -8795.51 & -1340.44 & 8795.51 & -1340.44 & 0 & 0 \\ 1340.44 & 136.188 & -1340.44 & 272.377 & 0 & 0 \\ \hdashline 0 & 0 & 0 & 0 & 0.0436807 & -0.0008695 \\ 0 & 0 & 0 & 0 & -0.0008695 & 0.00002693 \end{array}\right]\left[\begin{array}{c} q_1 \\ q_2 \\ q_3 \\ q_4 \\ \hdashline q_5 \\ q_6 \end{array}\right]=\left[\begin{array}{c} 4.5720 \\ 0.3097 \\ 10.6680 \\ -0.4645 \\ \hdashline 0.004385 \\ -0.00008729 \end{array}\right]+\left[\begin{array}{c} R \\ M \\ 0 \\ 0 \\ \hdashline 0 \\ 0 \end{array}\right]$$

(3.54)

$$\left[\begin{array}{c:c} K_c & 0 \\ \hdashline 0 & K_h \end{array}\right]\left[\begin{array}{c} q_c \\ \hdashline q_h \end{array}\right]=\left[\begin{array}{c} F_c \\ \hdashline F_h \end{array}\right] \tag{3.55}$$

Hence, upon application of the boundary conditions for the fixed-free beam and suitable matrix manipulation we get the following results:

$$\{q_c\}=[K_c]^{-1}\{F_c\} \tag{3.56}$$

$$\{q_h\}=[K_h]^{-1}\{F_h\} \tag{3.57}$$

$$\begin{Bmatrix} q_3 \\ q_4 \end{Bmatrix}=\begin{Bmatrix} 3.8112\times10^{-3} \\ 1.7050\times10^{-2} \end{Bmatrix} \tag{3.58}$$

$$\begin{Bmatrix} q_5 \\ q_6 \end{Bmatrix}=\begin{Bmatrix} 0.10038 \\ 1.8882\times10^{-5} \end{Bmatrix} \tag{3.59}$$

Now w can be expressed as follows,

$$w(x)=\sum_{c=1}^{4} q_c N_c(x)+\sum_{h=1}^{2} q_h N_h(x) \tag{3.60}$$

where, $N_c(x)$ and $N_h(x)$ are respectively the Hermite shape functions and the polynomial hierarchical shape functions given in Equation (3.14). Consequently, the slope, bending moment and shear force can also be found once the expression for the displacement is obtained. Figures 3.4 through 3.11 in the following pages show the distribution of the displacement, rotation, bending moment and shear force along the length of the beam.

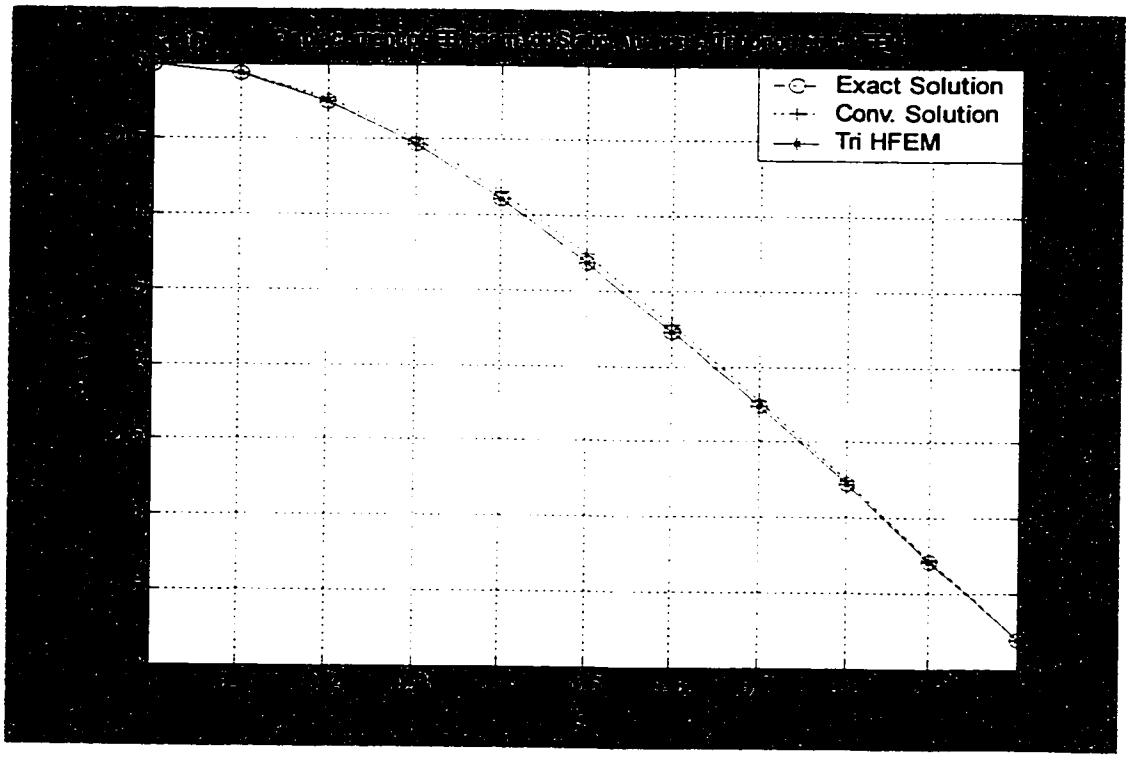

Figure 3.4 Displacement distribution obtained using trigonometric HFEM

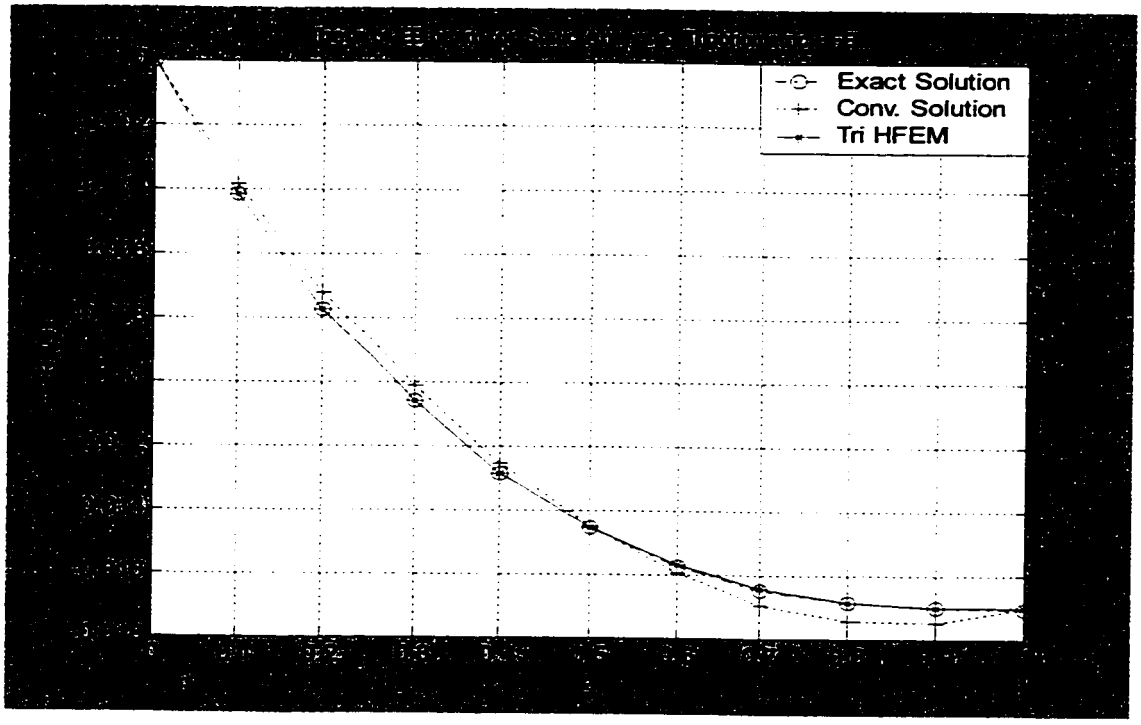

Figure 3.5 Rotation distribution obtained using trigonometric HFEM

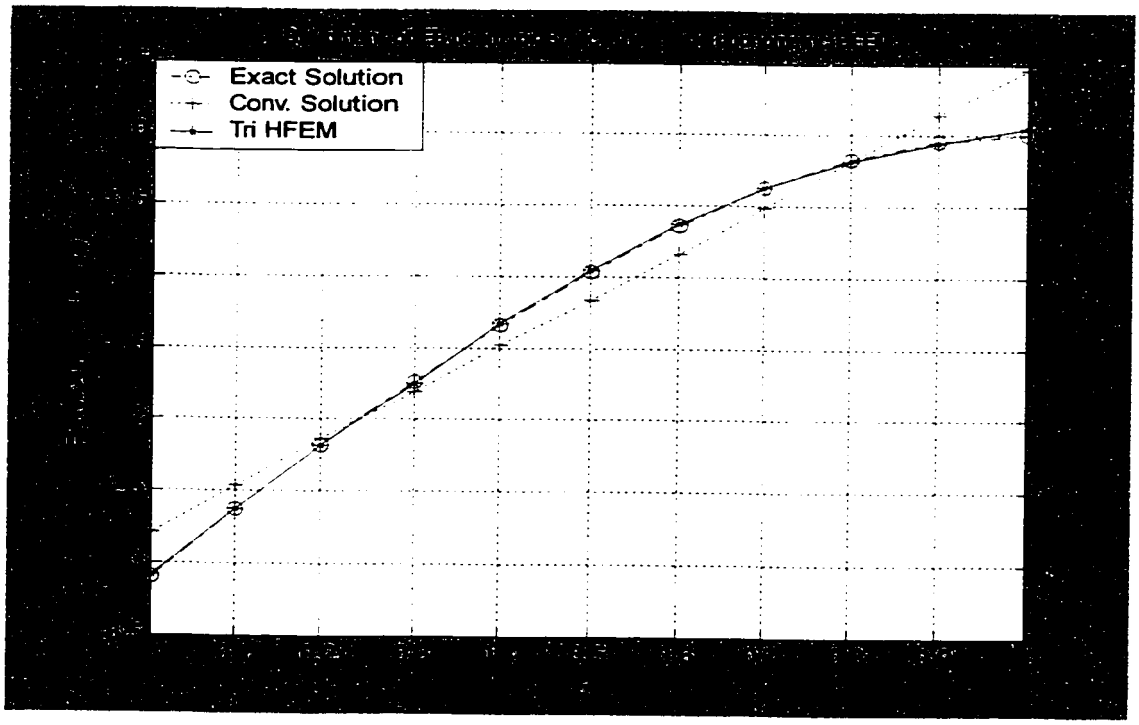

Figure 3.6 Bending moment distribution obtained using trigonometric HFEM

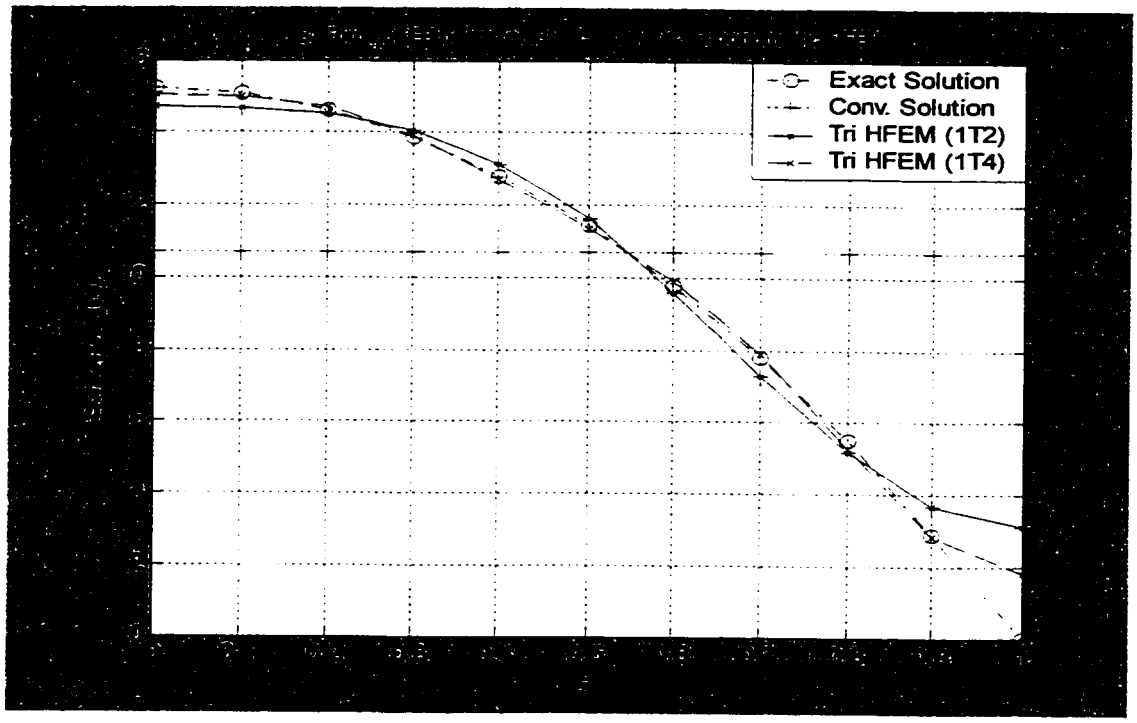

Figure 3.7 Shear force distribution obtained using trigonometric HFEM

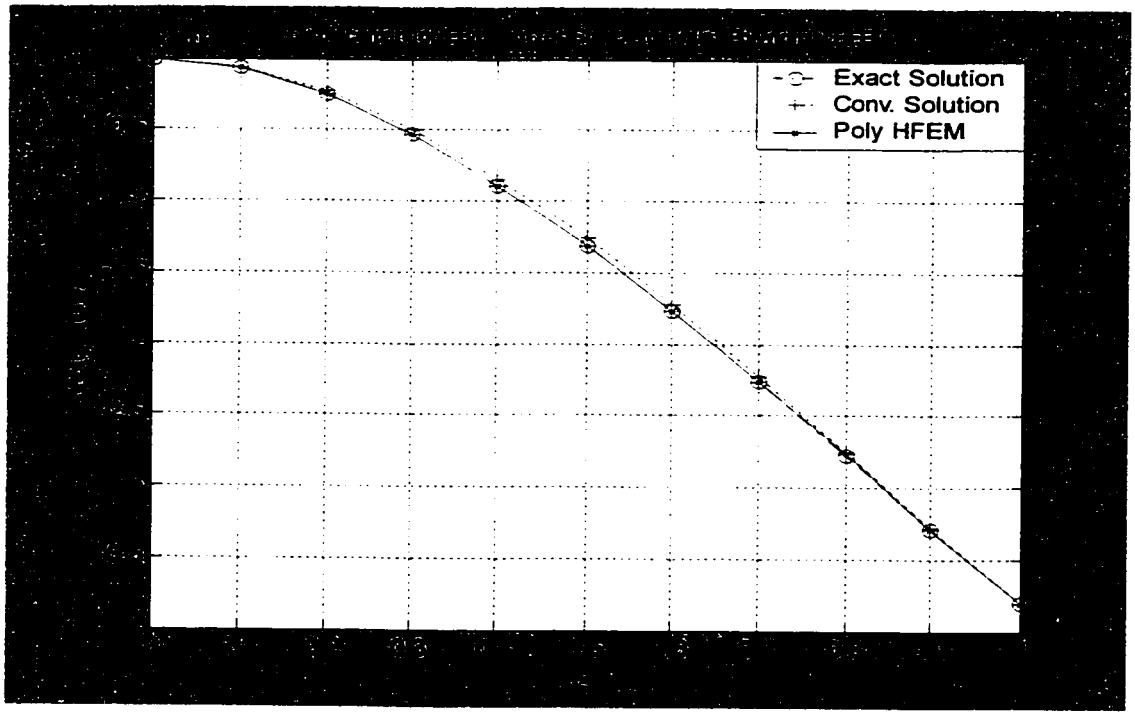

Figure 3.8 Displacement distribution obtained using polynomial HFEM

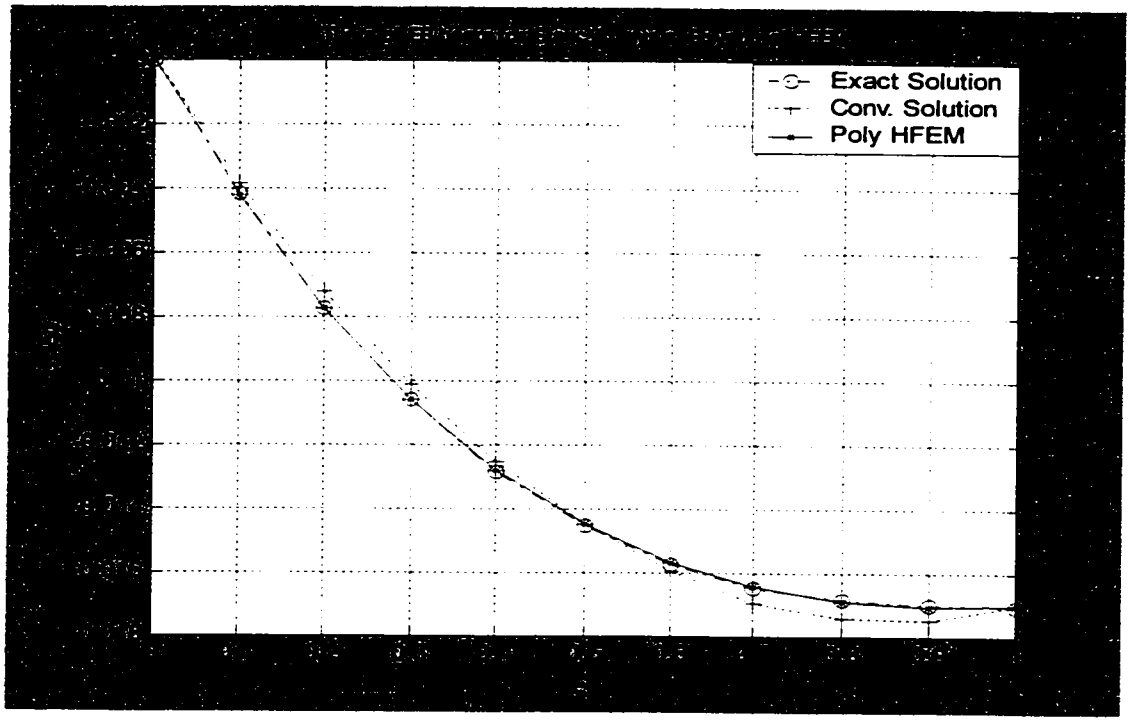

Figure 3.9 Rotation distribution obtained using polynomial HFEM

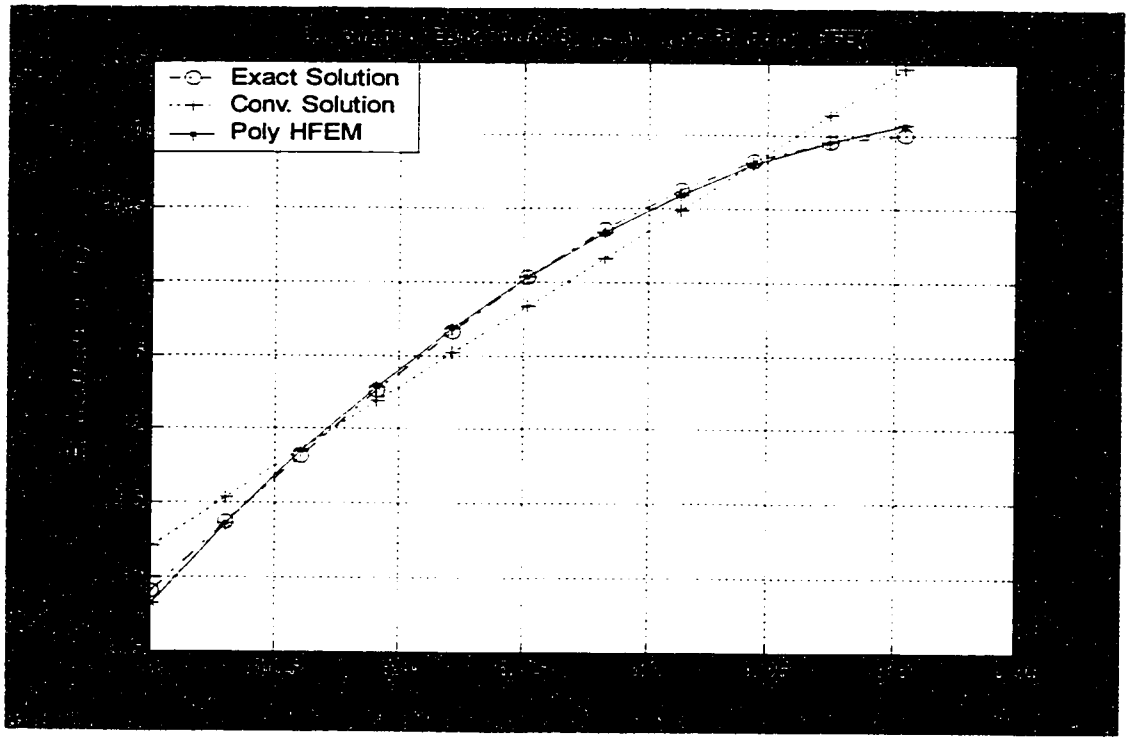

Figure 3.10 Bending moment distribution obtained using polynomial HFEM

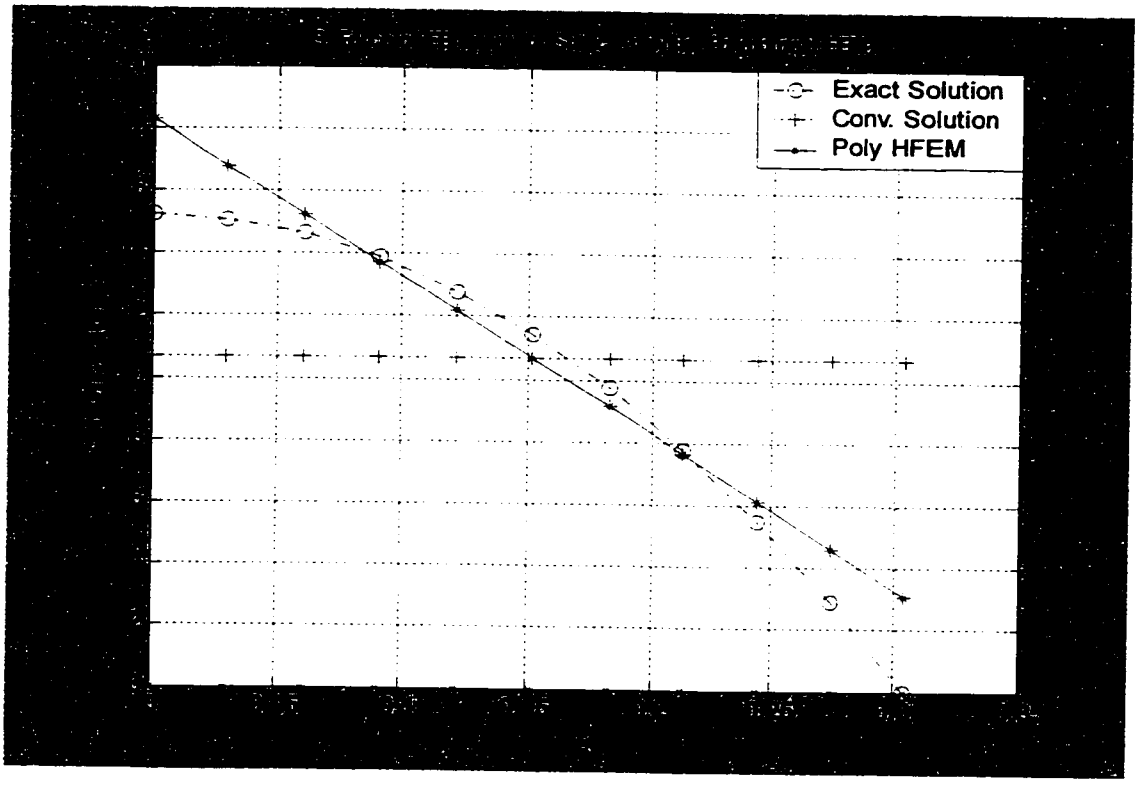

Figure 3.11 Shear force distribution obtained using polynomial HFEM

The results obtained by both the trigonometric and the polynomial formulations have been illustrated. Significant improvements can be observed in the bending moment and shear force distributions as compared to that obtained by the conventional finite element formulation. The rotation, bending moment and shear force distributions are all obtained by the consecutive differentiation of the displacement distribution. Differentiation, as an operator increases the error. Hence, we see that although the conventional formulation gives satisfactory results for the displacement and rotation distributions, the error continuously increases with each differentiation and the errors associated with the bending moment and shear force are significant. In comparison, the expressions obtained by applying the hierarchical formulations, depicts more accurately the manner in which the beam deforms. This is because the hierarchical formulations

consider the internal degrees of freedom. Hence, the resulting expressions involving higher derivatives of the displacement field are accurate. It should be mentioned here that the polynomial formulation does not fare as well as the trigonometric formulation, but is significantly better than the conventional formulation.

3.2.6 Analysis of Variable-Thickness Composite Beams

In the analysis done till now, we have analyzed uniform- thickness isotropic and composite beams. The hierarchical finite element formulation has been very effective in giving us computational efficiency and faster convergence. The application to both the static and dynamic analyses has been carried out and excellent results have been obtained. We now intend to apply the hierarchical FEM to the dynamic analyses of tapered composite beams and evaluate the efficiency of the method.

Variable-thickness composite beams have significant structural applications. Their high stiffness-to-weight and strength-to-weight ratios, superb fatigue characteristics, excellent damage tolerance and structural tailoring capabilities lend it a tremendous advantage. It therefore becomes essential to have a clear idea about their structural behavior. Much of the research works done on tapered composite beams have centered on understanding failure mechanisms and efforts to increase the structural integrity of the tapered sections.

The dynamic response of tapered composite beams needs to be understood clearly for their optimum use. Exact analytical solutions are hard to obtain since the mathematical modeling involved is too complex. Hence, it is essential to have a very

efficient approximate method to study the dynamic behavior of these beams. Hierarchical FEM has shown great promise in the case of uniform- thickness beams, and hence gives us the hope that it will work for tapered beams as well. In this study, we consider the mid-plane tapered composite beams (Figure 3.12) and apply the hierarchical finite element method.

The weak form for composite beams is as given in Equation (3.5) and is given below,

$$\int_0^l \left(\frac{d^2 v}{dx^2} bD_{11} \frac{d^2 W}{dx^2} - \lambda \rho A v W - v q' \right) dx + \left[v \frac{d}{dx} \left(bD_{11} \frac{d^2 W}{dx^2} \right) - \frac{dv}{dx} bD_{11} \frac{d^2 W}{dx^2} \right]_0^l = 0 \qquad (3.61)$$

The classical lamination theory [75] states that,

$$D_{11} = \sum_{p=1}^{m1} \left[t_p \overline{Z}_p^2 + \frac{t_p^3}{12} \right] \left(\overline{Q}_{11} \right)_p \qquad (3.62)$$

where $\left(\overline{Q}_{11}\right)_p$ is the transformed stiffness coefficient of a ply, t_p is the ply thickness, $\overline{Z}_p$ is the distance between the centerline of the ply and the centerline of the laminate, and m is the total number of plies. For a mid-plane tapered composite beam, shown in Figure 3.12, the height of the centerline of each ply ($\overline{Z}_p$) is a function of x (see Figure 3.13) and is expressed as:

$$\overline{Z}_p = mx + g \qquad (3.63)$$

The element stiffness and mass matrices (Equations (3.11) and (3.12)) for the mid-plane tapered composite beam are obtained using the Equation (3.62) for the bending stiffness coefficient, D_{11}. By performing the symbolic computation using the software MATHEMATICA®, the stiffness and mass matrices for the mid-plane tapered composite beam are obtained. The mass matrix for a mid-plane tapered composite beam will have the area of cross-section as a variable quantity and hence will have to be included in the integral in Equation (3.65).

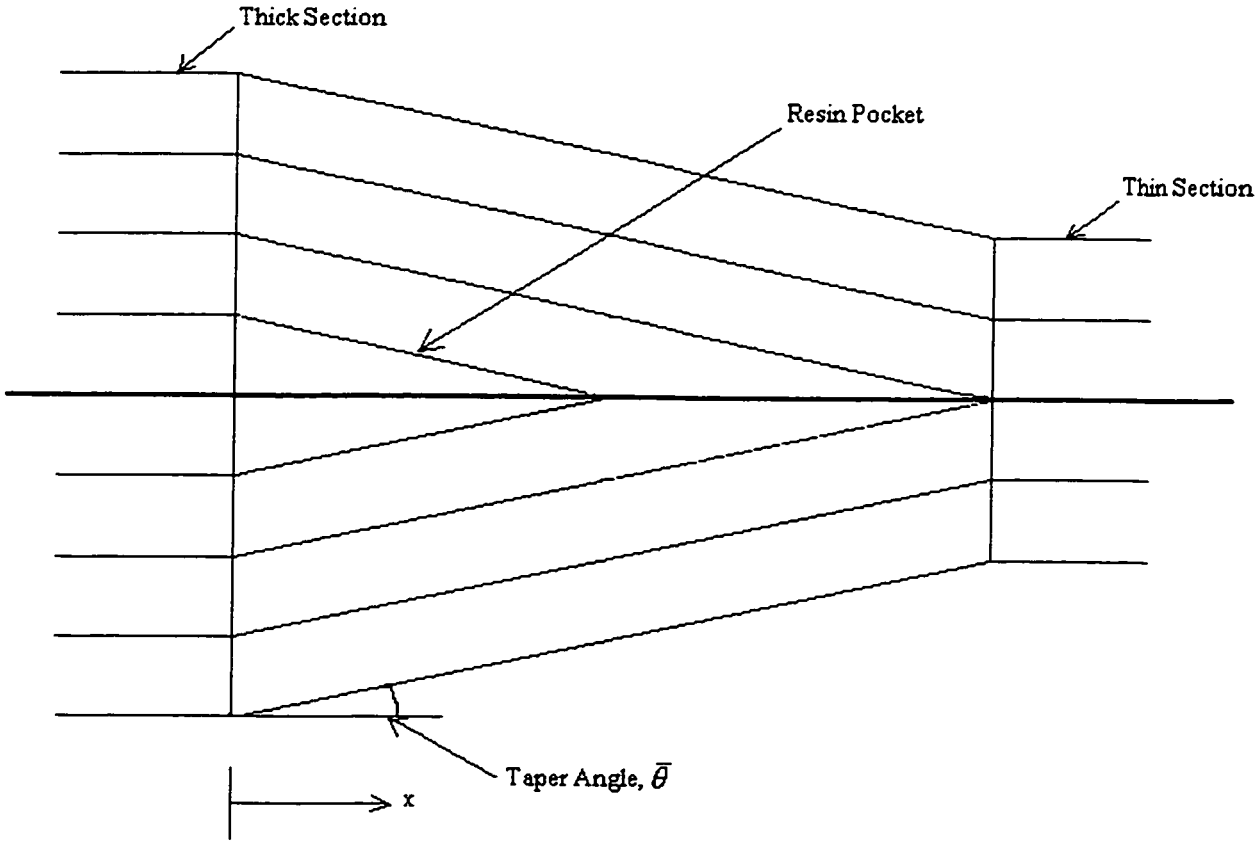

Figure 3.12 Schematic of a composite mid-plane tapered beam

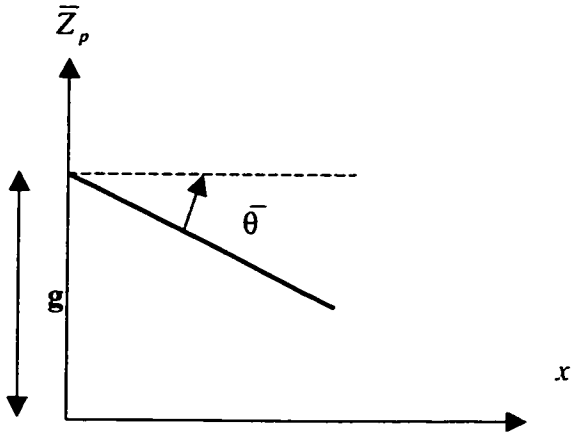

Figure 3.13 Variation of $\bar{Z}_p$ along the x-axis

Hence, according to the Euler-Bernoulli formulation, the expressions for the stiffness and mass matrices for a mid-plane tapered composite beam element will be as follows:

$$K_{ij} = \frac{1}{l^3}\int_0^1 \left(bD_{11}(\xi)\frac{d^2N_i}{d\xi^2}\frac{d^2N_j}{d\xi^2} \right) d\xi \tag{3.64}$$

$$= \frac{1}{l^3}\int_0^1 \left(b\left(\sum_{p=1}^{m1}\left[t_p(m\,\xi\, l + g)_p^2 + \frac{t_p^3}{12} \right] (\bar{Q}_{11})_p \right) \frac{d^2N_i}{d\xi^2}\frac{d^2N_j}{d\xi^2} \right) d\xi \tag{3.64 a}$$

$$M_{ij} = \int_0^1 (\rho\, A(\xi)\, N_i\, N_j\, l)\, d\xi = \int (\rho\, (((nthin - nthick)A_o)\xi + (nthick)A_o)N_i N_j l)\, d\xi \tag{3.65}$$

where nthick and nthin are respectively the number of plies in the thick and thin sections of the tapered beam and A_o is the area of cross section of a single ply, all other quantities hold the same meaning as explained in Equations (3.11) and (3.12). In analyzing the variable-thickness composite beams for their dynamic characteristics by using trigonometric HFEM, we model the beam using one hierarchical element only and

variable number of trigonometric terms. Since there is a variation in the number of plies across the length of the beam, the expression of the bending coefficient, D_{11}, will be different for different sections having different number of plies. Hence the integration in Equation (3.64) has to be broken into as many parts as the number of sections. The calculation of the bending coefficient, D_{11}, for the section having the resin pocket also needs special mention. To consider the resin pocket in calculating the D_{11}, the resin pocket is divided into a suitable number of isotropic plies and their contribution to the expression of D_{11} is considered as given in Equation (3.62), i.e. in the same way as we consider the remaining plies of composite material (see Figure AI.1 in Appendix-I). There is a difference though, the resin material is isotropic in nature and hence the expression for the transformed reduced stiffness coefficient, $\overline{Q}_{11}$, would be as given in Appendix-I. Hence, in this way the expression for D_{11} is calculated for the section that contains the resin pocket (For more details see Appendix-II). Similar methodology is adopted for the calculation of D_{11} wherever the resin pocket appears. After obtaining the expressions for D_{11} for the different sections across the length of the beam, the stiffness is calculated by using Equation (3.64).

3.2.7 Example applications for variable-thickness composite beams

As the analyses results for uniform composite beams in section 3.2.4 have shown, the trigonometric HFEM seems to be the best amongst the formulations that we have seen. Hence, we will apply it for the calculation of the natural frequencies of tapered composite beams. Since no closed form solution is available for the vibration of tapered composite beams, the validity of the program and the formulation is checked by obtaining

the results for a tapered beam with a very small taper angle ($\theta = 0.1061^{\circ}$) and comparing them with the closed form solution for an equivalent uniform-thickness composite beam. The results were in very good agreement and are given in Example 1. Henceforth, we will apply the formulation to actual tapered composite beams. We will apply both the Euler-Bernoulli and the Timoshenko formulations to solve the examples on variable-thickness composite beams.

3.2.7.1 Examples based on the Euler-Bernoulli Formulation

Ex.1 Problem Description

This example is being solved to establish the validity of the program as described before. A mid-plane tapered laminate having 36 plies in the thick section and 34 in the thin section has the following mechanical properties:

$E_1 = 144$ GPa; $E_2 = 12.14$ GPa; $G_{12} = 4.48$ GPa; $\rho = 1660.80\ Kg/m^3$. The value of the bending stiffness for the uniform composite beam having 36 plies is, $D_{11} = 1.3435 \times 10^3\ N.m$

The mechanical properties of the Resin are: $E_1 = 3.93$ GPa; $\nu = 0.37$; $G_{12} = 1.034$ GPa.

The geometric properties of the tapered laminate are: height (H) = 5.49 mm; length (L) = 82.29 mm (L/H=15). The laminate has the following configuration: Thick section: $[0_4/\pm 45_4/\pm 45_3]_s$ and thin section: $[0_4/\pm 45_4/\pm 45_2/45]_s$ and the boundary conditions are simply-supported.

The validation problem is solved by applying the Euler-Bernoulli formulation for beams. The present problem is first solved as a uniform-thickness laminate problem. This is done by considering that the laminate is composed of 36 plies and that no plies are

dropped over its length. It is then solved for the natural frequencies by making use of the closed form solution available for uniform-thickness composite beams.

The solution for, the first three natural frequencies of the uniform laminate considered are,

$\omega_1 = 1.77 \times 10^4 \quad Hz$
$\omega_2 = 7.08 \times 10^4 \quad Hz$
$\omega_3 = 15.93 \times 10^4 \quad Hz$

Now the same laminate is considered as a tapered beam problem by dropping 2 plies over a length of **0.0823 m** and making an angle of **0.1061** degrees. This is as close as we can get to the uniform-thickness beam. The natural frequencies obtained for this tapered laminate should be very close to that of the uniform beam if our formulation and program are correct. This will serve as our comparison meter and hence the results that we obtain by our program for this tapered laminate will be compared to the exact solutions for the uniform beam described above.

Also, the tapered beam problem will be solved first by the conventional method i.e. using elements having 4 DOF ($w_1, \theta_1, w_2, \theta_2$) and then the trigonometric HFEM will be applied to it wherein we will make use of 1 and 2 trigonometric terms.

Table 3.11 Natural frequencies ($\times 10^5$) for the slightly tapered beam

Mode	Exact Sol. (Uniform Beam)	Conventional* (2DOF)	1T1* (3 DOF)	1T2* (4 DOF)
1	0.1769	0.192	0.173	0.173
2	0.708	0.881	0.879	0.692
3	1.593	-	2.2	2.19

* Results are for Tapered Beam described above.

Table 3.11 gives a comparison of the results obtained by the formulation and the program for the mid-plane tapered composite beam with the exact solution obtained for the uniform-thickness composite beam. Results for the mid-plane tapered laminate are obtained using both the conventional formulation and the trigonometric HFEM. As is evident from the Table 3.11, the values obtained using the program for the mid-plane tapered laminate are very close to those of the exact solution for the uniform beam. This should be the case, since the taper angle that we have considered, is very small and makes the beam nearly very similar to the uniform- thickness beam. After validating the formulation and the program as in the previous example, we can now apply the trigonometric HFEM to actual tapered beams. Examples 2 and 3 that follow will take into consideration different taper angles.

Ex. 2 Problem Description

The mid-plane tapered composite beam considered in this example has the following mechanical properties:

$E_1 = 144$ GPa; $E_2 = 12.14$ GPa; $G_{12} = 4.48$ GPa; $\rho = 1660.80\ Kg/m^3$.

The mechanical properties of the resin are: $E_1 = 3.93$ GPa; $\nu = 0.37$; $G_{12} = 1.034$ GPa.

The geometrical properties of the mid-plane tapered beam are: height (H) = 1.2192 mm; length (L) = 12.2 mm (L/H=10). There are 8 plies in the thick section and 4 in the thin section. The laminate configuration of the thick section is $[\pm 45_2]_s$ and that of the thin section is $[\pm 45]_s$. The taper angle will be equal to **1.43 degrees.** The boundary conditions of the beam are fixed-free.

The problem at hand is solved, first by the conventional method i.e. with 4 DOF per element. In the conventional case, it is solved by using 1 and 2 elements. Then the

problem is tackled by making use of the Trigonometric HFEM. The results for various cases are listed below:

Table 3.12 Natural frequencies ($\times 10^5$) of the tapered composite beam of Ex. 2

Mode	1C (2 DOF)*	2C (4 DOF)*	1T1 (3 DOF)*	1T2 (4 DOF)*	1T4 (6 DOF)*	1T2 **(No Resin)**
1	0.474	0.453	0.471	0.470	0.470	0.468
2	2.69	2.29	2.32	2.26	2.26	2.24
3	-	6.69	8.06	6.10	5.84	6.06

*DOF excluding the restrained ones

Ex. 3 Problem Description

The mid-plane tapered beam problem considered in this example has the following mechanical properties,

$E_1 = 144$ GPa; $E_2 = 12.14$ GPa; $G_{12} = 4.48$ GPa; $\rho = 1660.80\ Kg/m^3$;

The mechanical properties of the resin are, $E_1 = 3.93$ GPa; $\nu = 0.37$; $G_{12} = 1.034$ GPa;

The geometric properties of the tapered beam are height (H) = 7.3152 mm; length of the taper (L) = 36.6 mm (L/H = 5). The number of plies in the thick section is 48 and in the thin section is 24. The configuration of the thick section is $[0_4/\pm 45_4/\pm 45_4/-45_4]_s$ and that of the thin section is $[0_4/\pm 45_4]_s$. The angle of taper is equal to **2.86 degrees.** The boundary conditions of the beam are fixed-free.

Table 3.13 Natural frequencies ($\times 10^5$) of the tapered composite beam of Ex. 3

Mode	1C (2 DOF)*	1T1 (3 DOF)	1T2 (4 DOF)	1T3 (5 DOF)	1T4 (6 DOF)	1T4 **(No Resin)**
1	0.449	0.447	0.447	0.447	0.447	0.447
2	2.68	2.24	2.20	2.20	2.20	2.20
3	-	8.11	5.91	5.73	5.73	5.73

*DOF excluding the restrained ones

In both the Examples 2 and 3, the mid-plane tapered composite beam problem is solved using both the conventional and the trigonometric HFEM. In the HFEM, the beams are modeled using only 1 element and variable number of trigonometric hierarchical terms. It is observed that upon increasing the number of hierarchical trigonometric terms, the values of frequencies of higher modes of the tapered composite beam change, untill they converge to a definite value. This can be taken as the value of the frequency for that mode. To determine the effect of the presence of resin pocket on the natural frequencies of the tapered composite beam, the program was modified to obtain the natural frequencies without considering resin pockets and considering the relevant part as composed of composite plies. As evident from the values, no appreciable changes were recorded in the natural frequencies. Hence, the results obtained using the 1T4 formulation for the natural frequencies for the first three modes of the tapered composite beams of Examples 2 and 3 can be taken as the most accurate solutions achievable by the HFEM.

Ex. 4 Problem Description

In the previous two examples, the free vibration analysis of the mid-plane tapered composite beams was undertaken. Now we intend to conduct the forced vibration

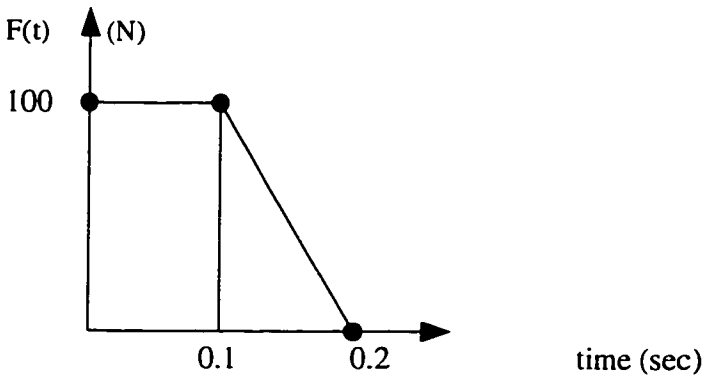

Figure 3.14 Force applied at the free end of the tapered composite beam

analysis of the mid-plane tapered composite beam of Example 3. The loading at the free end of the beam is shown in the Figure 3.14.

The solution to the forced vibration problem is obtained using both the Newmark-β direct integration method and the mode superposition method. Both the methods give answers that are in excellent agreement. The beam is modeled using one element and varying number of hierarchical trigonometric terms. Since the boundary conditions of the beam are fixed-free, the maximum values of the two degrees of freedom viz. displacement and rotation that are associated with the free end have been evaluated. They are numbered as degrees of freedom (D. O. F.) 3 and 4 respectively, and their values are listed in Table 3.14.

Table 3.14 Maximum values of the free end displacement (m) and rotation (degrees) of the beam of Ex. 4

D.O.F	1C (2 DOF)	1T1 (3 DOF)	1T2 (4 DOF)	1T3 (5 DOF)	1T4 (6 DOF)	1T4 **(No Resin)**
3	0.0027	0.0028	0.0028	0.0028	0.0028	0.0028
4	0.1395	0.1364	0.1360	0.1360	0.1327	0.1327

3.2.7.2 Examples based on the Timoshenko Formulation

The mid-plane tapered beam problems of examples 2 and 3 of the previous section are solved here using the Timoshenko formulation. The L/H ratio for these problems are 10 and 5 respectively, so it would be of interest to see the results for beams having such ratios. Secondly, it would serve to compare the answers obtained using the Euler-Bernoulli formulation and the Timoshenko formulation for the same problems.

Ex. 1 Problem Description

The mid-plane tapered composite beam considered in this example has the following mechanical properties:

$E_1 = 144$ GPa; $E_2 = 12.14$ GPa; $G_{12} = 4.48$ GPa; $G_{23} = 4.90$ GPa; $\rho = 1660.80\ Kg/m^3$.

The mechanical properties of the resin are: $E_1 = 3.93$ GPa; $\nu = 0.37$; $G_{12} = 1.034$ GPa.

The geometric properties of the mid-plane tapered beam are: height (H) = 1.2192 mm; length (L) = 12.2 mm (L/H=10). There are 8 plies in the thick section and 4 in the thin section. The laminate configuration of the thick section is $[\pm 45_2]_s$ and that of the thin section is $[\pm 45]_s$. The taper angle will be equal to **1.43 degrees.** The boundary conditions of the beam are fixed-free.

The problem is solved using the trigonometric hierarchical formulation based on the Timoshenko theory. Results are obtained by modeling the beam by a single Timoshenko beam element and adding 2 and 4 trigonometric terms to the element. Table 3.15 gives the natural frequencies of the first three modes of the mid-plane tapered beam analyzed using the Timoshenko formulation. Comparison of the values in Tables 3.12 and 3.15 clearly indicate that the results obtained for this mid-plane tapered beam are the

Table 3.15 Natural frequencies ($\times 10^5$) of the tapered composite beam of Ex. 1

Mode	1T2 (4 DOF)*	1T4 (6 DOF)*	1T4 **(No Resin)**
1	0.5246	0.4733	0.4623
2	3.5462	2.2281	2.2023
3	61.2270	6.7508	6.6235

*DOF excluding the restrained ones

same with both the Euler-Bernoulli and the Timoshenko formulations. This can be attributed to the fact that the length to height (L/H) ratio for this beam is 10 and hence ignoring the transverse shear effects on the beam does not have a profound effect on the results.

Ex. 2 Problem Description

The mid-plane tapered beam problem considered in this example has the following mechanical properties:

$E_1 = 144$ GPa; $E_2 = 12.14$ GPa; $G_{12} = 4.48$ GPa; $G_{23} = 4.90$ GPa; $\rho = 1660.80\ Kg/m^3$.

The mechanical properties of the resin are: $E_1 = 3.93$ GPa; $\nu = 0.37$; $G_{12} = 1.034$ GPa.

The geometric properties of the tapered beam are: height (H) = 7.3152 mm; length of the taper (L) = 36.6 mm (L/H = 5). The number of plies in the thick section is 48 and in the thin section is 24. The configuration of the thick section is $[0_4/\pm 45_4/\pm 45_4/-45_4]_s$ and that of the thin section is $[0_4/\pm 45_4]_s$. The angle of taper is equal to **2.86 degrees.** The boundary conditions of the beam are fixed-free.

Table 3.16 Natural frequencies ($\times 10^5$) of the tapered composite beam of Ex. 2

Mode	1T4 (6 DOF)*	1T8 (10 DOF)	1T8 **(No Resin)**
1	0.3874	0.3861	0.3798
2	1.3590	1.3350	1.3256
3	2.8920	2.6752	2.6689

*DOF excluding the restrained ones

The problem is solved using trigonometric hierarchical formulation for thick tapered composite beams and the natural frequencies for the first three modes are given in Table 3.16. The beam is modeled using one trigonometric hierarchical element having

four and eight trigonometric terms respectively. The results obtained in this case are different from those obtained for the same example in the previous section, where the example was solved using the Euler-Bernoulli formulation. It is imperative to note that since the length to height (L/H) ratio is 5, it implies that the beam under consideration is a thick beam, hence the results obtained using the Timoshenko formulation will be more accurate than those obtained using the Euler-Bernoulli formulation.

3.3 Conclusions and Discussion

The Hierarchical Finite Element Method developed and applied to isotropic beams in the previous chapter has been applied in this chapter to uniform-thickness and variable-thickness composite beams. The uniform-thickness composite beams have been modeled using the cylindrical bending theory and the 1-D laminated beam theory. Both the forms of HFEM are applied, and as with the case of isotropic beams, the trigonometric HFEM gives better results than the polynomial form. Results for both the Euler-Bernoulli and Timoshenko beams have been presented. The static analysis of uniform-thickness composite beams is also performed and detailed results for the bending moment and shear force are presented and compared with the conventional formulation and the exact solution. The application of the HFEM is further extended to the thickness-tapered composite beams. The dynamic analysis of tapered composite beams is performed.

Application of the hierarchical finite element method to composite beams, as in the case of isotropic beams, yields the same advantages of numerical efficiency and faster convergence. Less number of elements are required to model and obtain precise answers for the static and dynamic analysis of composite beams. The system degrees of freedom

are also substantially less. The graphs in Figures 3.15 and 3.16 give us a comparison of the convergence of natural frequencies obtained using the trigonometric HFEM, polynomial HFEM and the conventional formulation to their exact solutions. There is a substantial reduction in the number of elements required to obtain results that are almost the same as exact answers. Also, much less number of system degrees of freedom are required. Figure 3.17 gives us the convergence to the exact solution with increase in the number of trigonometric terms (Ω, the non-dimensional frequency $=\omega\times(h/(E/\rho)^{1/2})$. The non-dimensional frequencies for different modes are plotted versus the number of trigonometric and polynomial terms for the simply- supported beam. For the Timoshenko beam, Figure 3.18 illustrates the convergence of the three methods and shows that the trigonometric method gives the best results.

The results stated for the static analysis done for uniform composite beams also reaffirm that the hierarchical formulation with less number of elements and system degrees of freedom yields much better results than the conventional formulation. It should be noted that significant improvements in the bending moment and shear force diagrams are achieved. These quantities are critical parameters in the design of any structure and accurate prediction of these with minimal computational efforts is achieved by the hierarchical method.

Analysis of the mid-plane tapered composite beams is done using the trigonometric HFEM. The thickness-tapered beams are modeled by using just one element and varying number of trigonometric terms. As mentioned before, due to the linear nature of the bending stiffness, D_{11}, the nature of the stiffness matrix is different from that of the uniform-thickness beam.

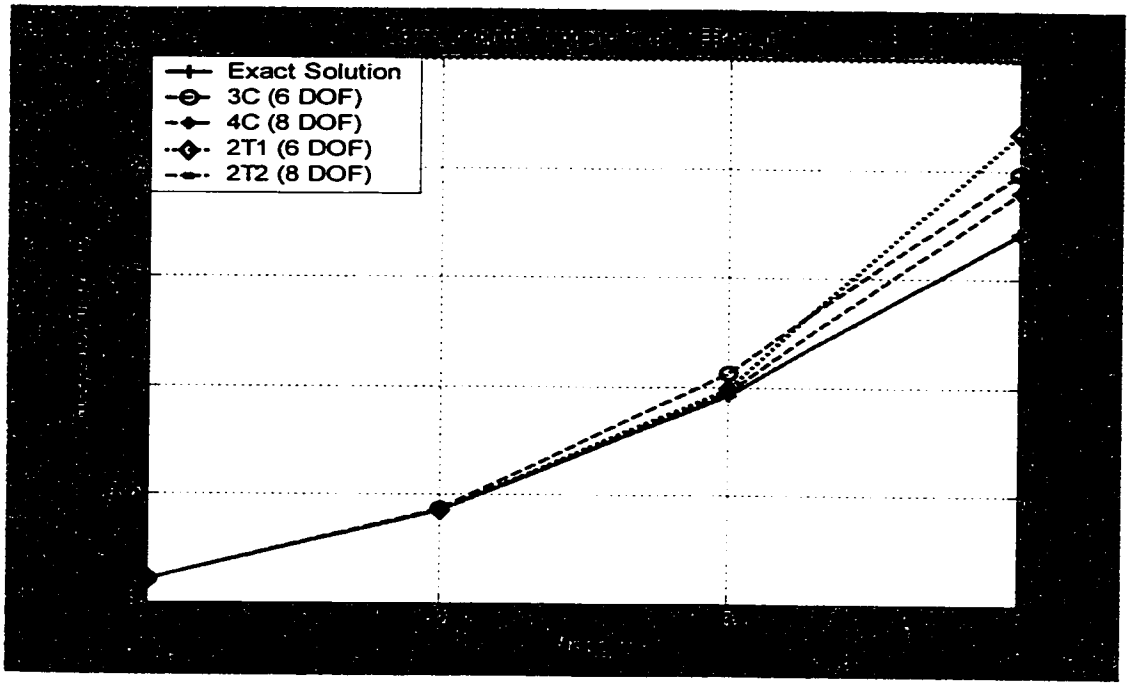

Figure 3.15 Comparison of frequencies of composite Euler-Bernoulli beam by conventional FEM and trigonometric HFEM

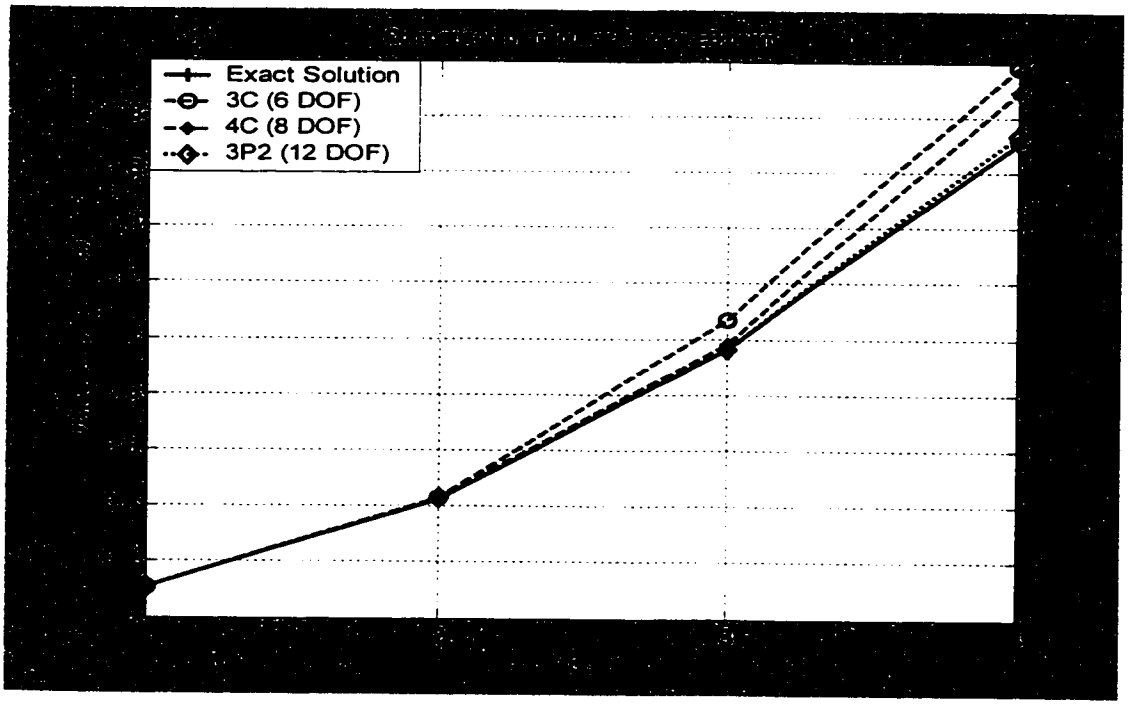

Figure 3.16 Comparison of frequencies of composite Euler-Bernoulli beam by conventional FEM and polynomial HFEM

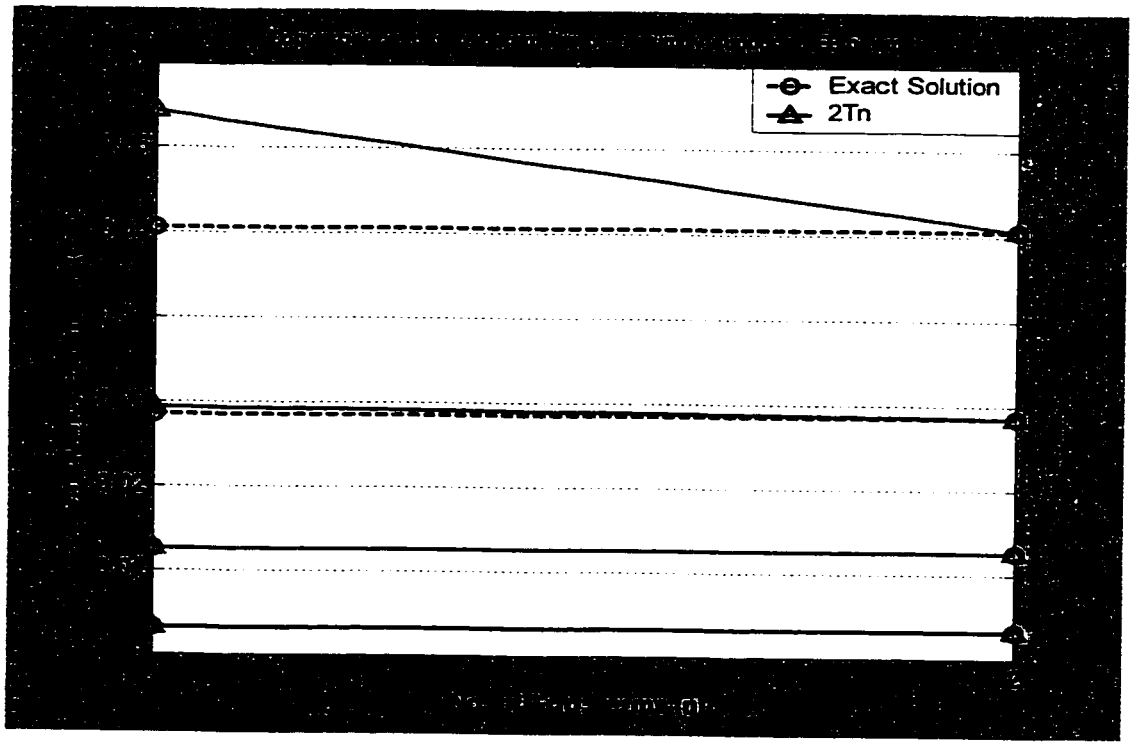

Figure 3.17 Convergence to $\Omega_1, \Omega_2, \Omega_3$ and Ω_4 of the Simply-Supported composite beam in 2-element modeling

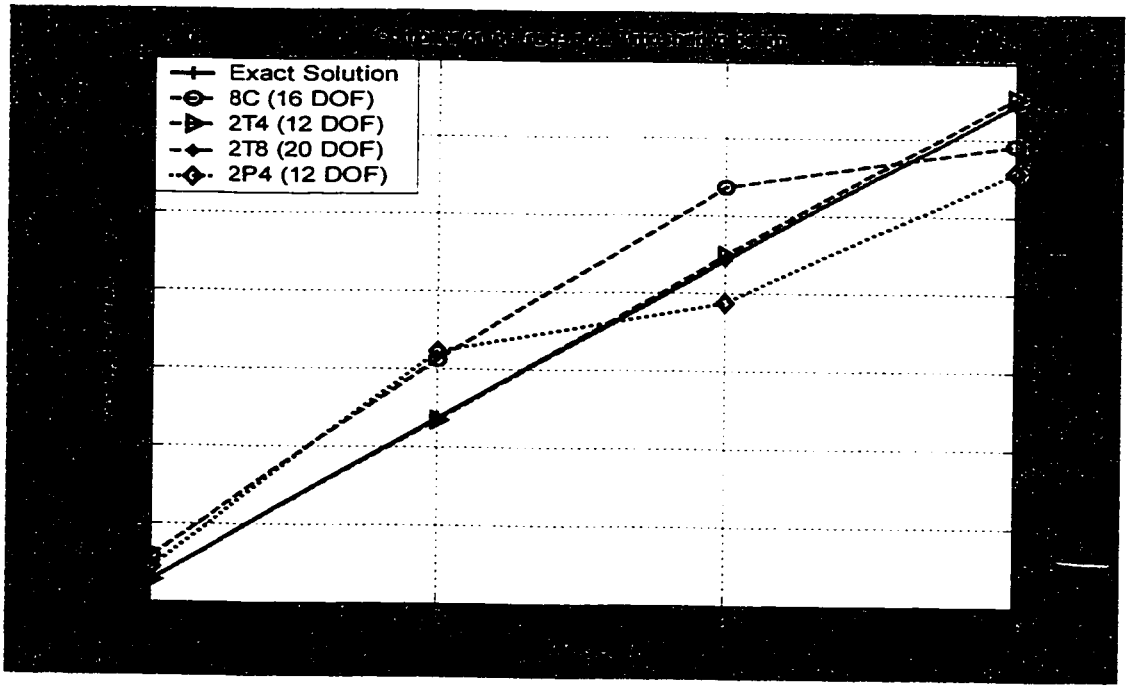

Figure 3.18 Comparison of frequencies of the composite Timoshenko beam obtained using conventional FEM, trigonometric HFEM and polynomial HFEM

The stiffness and mass matrices for the formulation having one element and four hierarchical trigonometric terms (1T4), without applying the boundary conditions, are given in Tables 3.17 and 3.18 to point out certain important aspects of the procedure.

Table 3.17 Stiffness matrix for the tapered beam in Ex. 2 for the case 1T4

2.3177e4	1.8101e2	-2.3177e4	1.0198e2	-8.7759e3	-8.6919e3	1.0491e5	1.9870e4
1.8101e2	1.6128	-1.8101e2	5.9723e-1	-5.9499e1	-5.2909e1	7.0830e2	1.1450e2
-2.3177e4	-1.8101e2	2.3177e4	-1.0198e2	8.7759e3	8.6919e3	-1.0491e5	-1.9870e4
1.0198e2	5.9723e1	-1.0198e2	6.4790e-1	-4.7654e1	-5.3219e1	5.7264e2	1.2810e2
-8.7759e3	-5.9499e1	8.7759e3	-4.7654e1	1.7342e4	4.1176e4	-2.0406e5	-1.1012e5
-8.6919e3	-5.2909e1	8.6919e3	-5.3219e1	4.1176e4	5.6312e5	5.3338e4	-1.5469e6
1.0491e5	7.0830e2	-1.0491e5	5.7264e2	-2.0406e5	5.3338e4	6.1620e6	2.4453e6
1.9870e4	1.1450e2	-1.9870e4	1.2810e2	-1.1012e5	-1.5469e6	2.4453e6	1.8037e7

Table 3.18 Mass matrix for the tapered beam in Ex. 2 for the case 1T4

8.2533e-6	1.3509e-8	2.4222e-6	-7.3023e-9	1.1312e-6	1.7151e-6	-1.3325e-5	-4.2754e-6
1.3509e-8	2.8977e-11	6.9372e-9	-2.0061e-11	2.8952e-9	2.8304e-9	-3.6486e-8	-8.2490e-9
2.4222e-6	6.9372e-9	5.7414e-6	-1.0588e-8	9.9805e-7	-1.0314e-6	-1.2269e-5	2.6444e-6
-7.3023e-9	-2.0061e-11	-1.0588e-8	2.4519e-11	-2.6912e-9	1.4152e-9	3.4679e-8	-4.1245e-9
1.1312e-6	2.8952e-9	9.9805e-7	-2.6912e-9	3.4696e-7	7.1782e-8	-4.5949e-6	-2.3872e-7
1.7151e-6	2.8304e-9	-1.0314e-6	1.4152e-9	7.1782e-8	1.5084e-6	-7.1150e-7	-5.0854e-6
-1.3325e-5	-3.6486e-8	-1.2269e-5	3.4679e-8	-4.5949e-6	-7.1150e-7	6.3503e-5	2.7488e-6
-4.2754e-6	-8.2490e-9	2.6444e-6	-4.1245e-9	-2.3872e-7	-5.0854e-6	2.7488e-6	2.0723e-5

Table 3.17 gives the stiffness matrix for the tapered beam in Ex. 2 for the 1T4 case. The shaded part is the usual 4x4 sub-matrix that we will obtain if we follow the conventional formulation. The sub-matrices in the unshaded parts are generally null matrices in the case of the application of the HFEM method to uniform beam problems, as we have seen in the analysis done in previous sections (see for example the stiffness matrix in Equation

(3.47) in section 3.2.5). In the tapered case, as we can see in Tables 3.17 and 3.18, these sub-matrices are not null matrices. In the case of a tapered beam, the coefficient D_{11} is not a constant but it varies in a linear manner. Hence, the products of $D_{11}(\xi)$ (see Equations (3.62) and (3.63)), the second order derivatives of the trigonometric hierarchical shape functions and the hermite shape functions of the conventional finite element method are not orthogonal. Hence the sub-matrices mentioned here in the [K] and [M] matrices are not null matrices. The diagonally shaded part in this case, shows a sub-matrix, which as opposed to the case of the uniform-thickness composite beam, is not a diagonal matrix. This is because of the fact that due to the linearly varying nature of the coefficient D_{11}, the coefficients involving trigonometric hierarchical shape functions also become non-orthogonal among themselves and hence, we have a fully populated matrix for this sub-matrix.

In spite of the fact that the nature of these matrices is different from what we have seen in the uniform-thickness beam examples until now, they still add to the internal degrees of freedom of the element. Hence, the performance of the element is improved in the way that we have so far seen in many examples although its application does invoke certain computational inefficiencies and we loose some of the advantages that are inherent in and characteristic of the hierarchical FEM.

The stiffness matrix corresponding to the $(r+1)^{th}$ order approximation is formed by adding one row and one column to the r^{th} order matrix (for all r > 4), while leaving the entries of the r^{th} order matrix unaffected, i.e. the matrix K^r is embedded in the

matrix K^{r+1} [76]. Hence, we see that this property of the HFEM is intact, but the second feature wherein the hierarchical shape functions are chosen such that they exert no influence on the nodal degrees of freedom is compromised. Hence, there results a coupling due to the population of the two unshaded sub-matrices (see Table 3.17). This indirectly influences the nodal degrees of freedom and is a situation that would prove computationally expensive in vibration or static analysis. Also, such a "design" would restrict us to add any number of hierarchical shape functions to an individual element without them having any influence whatsoever on neighboring elements. This limits our capability to manipulate at will, the mesh size and the hierarchical degree of approximation in individual elements within the mesh. Since the internal hierarchical degrees of freedom influence the nodal degrees of freedom of an element, hence, in the assembly of elements in such a case, an overlay procedure similar to the one adopted in the conventional FEM will have to be adopted in this case as well.

The results obtained for the dynamic analyses of uniform composite beams show that the accuracy obtained is the same as that for isotropic beams. The inherent features and advantages of the HFEM as pointed out for the case of isotropic beams hold good for uniform composite beams too. In addition, the static analysis performed for the uniform composite beams gives accurate results for the bending moment and shear force using minimum number of elements. Finally, the free and forced vibration analyses of the thickness-tapered composite beams is done. The trigonometric HFEM is applied to it since it has been the best method for uniform beams. Due to the varying thickness of the beams, the bending stiffness becomes a linear function and hence renders the orthogonality property of the hierarchical shape functions ineffective in the calculation of

the stiffness and mass matrices. This results in a fully populated stiffness and mass matrices and increases the computational effort required to obtain a solution. Nonetheless, the efficiency and accuracy of the solution for the tapered beams are forthcoming.

Chapter 4

Parametric Study on Variable-Thickness Composite Beams

4.1 Introduction

In the previous chapter, the hierarchical finite element analysis methodology for both the uniform and the thickness-tapered composite beams has been developed. Both the forms of HFEM viz. polynomial and trigonometric forms were developed. The HFEM was applied first to uniform composite beams and subsequently to thickness-tapered composite beams. The HFEM was applied to the static and dynamic analyses of uniform-thickness composite beams and to the dynamic analysis of thickness-tapered composite beams.

The design of a tapered structure involves considerations of stiffness, static strength, dynamic stability and damage tolerance. Major considerations in designing a thickness-tapered composite beam are laminate configuration, ply orientation and taper angle of the laminate. We now intend to conduct a comprehensive parametric study for the thickness-tapered composite beams.

The parametric study is conducted on the mid-plane tapered composite beams. The material chosen is T300/5208 graphite-epoxy. The properties are listed in Table 4.1. The specifications of the composite laminate and the geometric properties are detailed in individual problems. All the problems are solved using both conventional and hierarchical finite element formulations.

The mid-plane tapered laminate is analyzed considering all types of variations: variations in the boundary conditions, variations in the stacking sequences and variation in taper angle. For each case, results for the lowest three natural frequencies are obtained and plotted in figures to elaborate on the interpretations. Where applicable, results are plotted for both the conventional and the hierarchical formulations and suitable comparisons are made. After each figure, appropriate interpretations are provided to explain how these variations affect the natural frequencies of the beams. For example, how the variations in the boundary conditions are related to the global degrees of freedom, and how this will effect the natural frequencies, how the variations in the inclination angles affect the natural frequencies through changes in the flexural rigidity of the laminate, and so on are detailed. Also, a comparison between the results obtained using both the formulations is done with the help of figures. Each subsection ends in a table that summarizes the results mentioned in it.

Table 4.1 Mechanical properties of unidirectional graphite-epoxy composite material [6]

Density (ρ , Kg/m^3)	1660.80
Longitudinal Modulus (E_1, GPa)	144
Transverse Modulus (E_2, GPa)	12.14
E_3	$(=E_2)$
In-Plane Shear Modulus (G_{12}, GPa)	4.48
Shear Modulus (G_{13}, GPa)	$(=G_{12})$
Out of Plane Shear Modulus (G_{23}, GPa)	4.90
Poisson's Ratio (ν_{12})	0.21
ν_{21}	0.017

Table 4.2 Mechanical properties of isotropic resin material

Elastic Modulus (E, GPa)	3.93
Shear Modulus (G, GPa)	1.034
Poisson's Ratio (ν)	0.37

Finally, overall conclusions that relate to the two kinds of formulations and changes within the mid-plane taper configuration are provided that serve as factors to be considered in design. These conclusions can guide the designer on the choice of the taper angle, and other parameters involved in the analysis such as the boundary conditions.

4.2 Parametric Study on Free Vibration of Mid-Plane Tapered Composite Beams

Problem Description:

A mid-plane tapered composite beam as the one shown in Figure 3.12 has the following geometric properties: height (H) = 1.219 mm; length (L) = 12.2 mm (L/H=10).
The configuration of the thick section of the beam is $[\pm 45_2]_s$ and that of the thin section is $[\pm 45]_s$. There are 8 plies in the thick section and 4 in the thin section. The angle of taper is equal to 1.43°. The mechanical properties of the graphite-epoxy and the resin are listed in Tables 4.1 and 4.2.

The lowest three natural frequencies are to be determined for all possible changes that can be performed on the composite beam such as, the change in the boundary conditions, the change in the inclination angle and the change in the fiber orientation. The natural frequencies are obtained using both the formulations, conventional and hierarchical as described in the previous chapters. Tables and Figures are provided for comparison and commenting purposes.

4.2.1 The Effect of Boundary Conditions on the Natural Frequencies

To consider the effects of different boundary conditions on the natural frequencies of the above-mentioned mid-plane tapered beam, values of the lowest three natural frequencies are obtained using the hierarchical finite element formulation.

Table 4.3 Frequencies ($\times 10^5$) for different boundary conditions for $[\pm 45_2]_s$ laminate

1	2.02	0.876	0.468	0.206
2	5.57	3.57	2.26	1.75
3	10.91	8.05	5.84	5.36

Table 4.1 gives us the detailed results for the lowest three natural frequencies for different boundary conditions for the above-mentioned example. One trigonometric hierarchical element with four internal degrees of freedom (1T4) is used to model the beam. As expected, there is a considerable variation in the values of the frequencies with change in the boundary conditions. The fixed-fixed type of support gives the highest value of natural frequencies, whereas the free-fixed type gives the lowest value (the frequency of the first mode of the fixed-fixed beam is nearly 900 % more than that of the

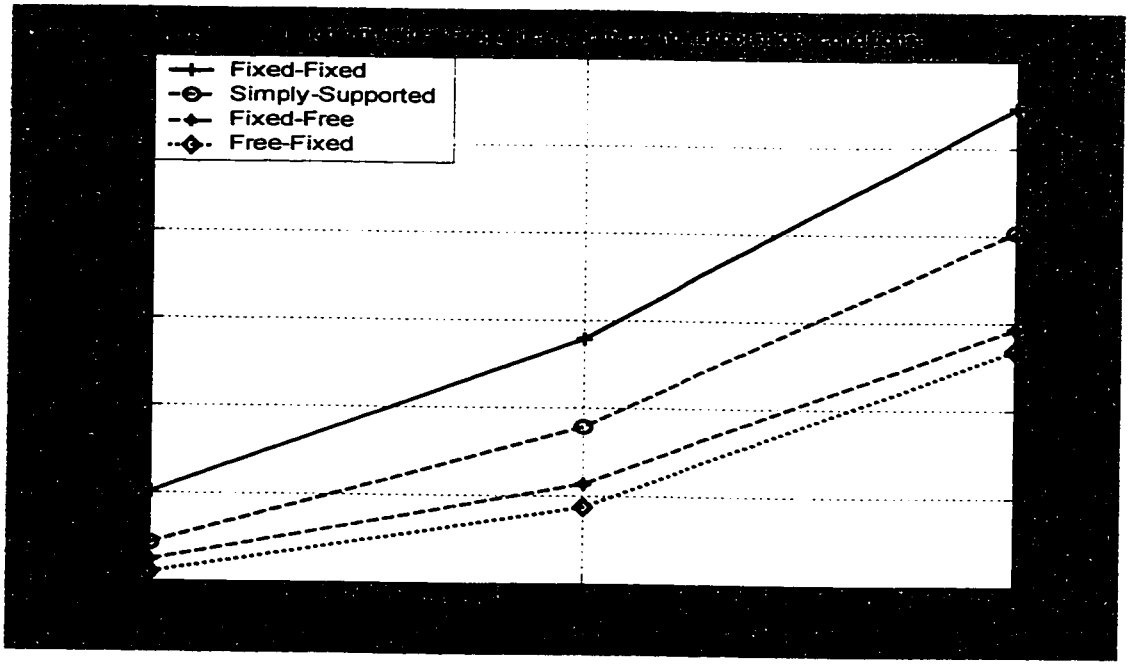

Figure 4.1 Natural frequencies of beams with different boundary conditions having $[\pm 45_2]_s$ configuration

first mode in the free-fixed support). The simply supported type comes as the second highest and the fixed-free is the third. An interesting observation with regard to the mid-plane taper is that changing the location of fixity from one end to another (i.e. making the fixed-free support as free-fixed), will significantly reduce the initial mode frequencies (more than 50% for the first mode). In general, the degree of restrain and the position of restrain affect the value of the natural frequency. Figure 4.1 gives the graphical representation of the variation of natural frequencies for different boundary conditions. The fixed –fixed beam having the maximum restraint has the highest values for the frequencies of successive modes of vibration. The other three cases under consideration, viz. simply-supported, fixed-free and free-fixed, all have two degrees of freedom restrained but vary in the manner of restrain. Restraining the displacements at both the ends of the beam, has the effect of increasing the values of natural frequencies compared to restraining both the displacement and rotation at one end.

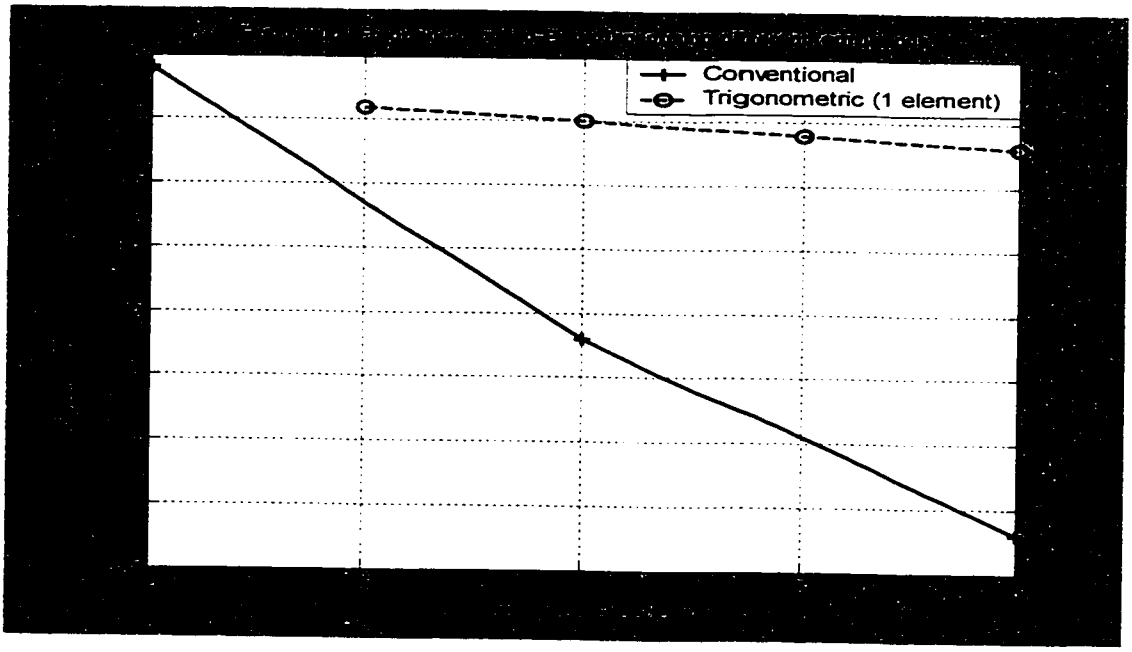

Figure 4.2 Fundamental frequency obtained using different formulations for the Fixed-Free mid-plane tapered composite beam

Figure 4.2 shows the convergence of the fundamental frequency for the mid-plane tapered composite beam under consideration. The trigonometric hierarchical formulation shows excellent convergence with just one element and increase in the degrees of freedom. In comparison, the conventional formulation uses more elements and does not converge to a value although having the same number of degrees of freedom.

4.2.2 The effect of laminate configuration on the natural frequencies

The same input data is used as in the last subsection, except that the kind of laminate configuration is chosen differently to see the effect of different fiber orientations on the natural frequencies of mid-plane tapered composite beams. The lowest three natural frequencies are determined for the following types of laminates, that have the following configurations at the thick sections are angle-ply $[\pm 45_2]_s$, cross-ply $[0/90]_{2s}$ and quasi-isotropic $[0/90/-45/45]_s$ laminates. The values are determined by trigonometric hierarchical finite element method using only one element to model the beam. The element has eight degrees of freedom including four internal degrees of freedom (1T4).

Table 4.4 Natural frequencies ($\times 10^5$) for different boundary conditions for $[0/90]_{2s}$ laminate

Mode	Fixed – Fixed	Simply- Supported	Fixed-Free	Free-Fixed
1	3.1843	1.3800	0.7217	0.3351
2	8.7776	5.6312	3.5113	2.7784
3	17.179	12.659	9.1541	8.4616

Tables 4.3, 4.4 and 4.5 give us the values of the lowest three frequencies for different boundary conditions for the mentioned laminates.

Table 4.5 Natural frequencies ($\times 10^5$) for different boundary conditions for $[0/90/-45/45]_s$ laminate

1	3.1097	1.3627	0.6950	0.3327
2	8.5824	5.5212	3.4378	2.7421
3	16.832	12.422	8.9659	8.3015

The results are shown graphically in Figures 4.3, 4.4, 4.5 and 4.6. As evident, for all types of boundary conditions the cross-ply laminate gives the highest values of the natural frequencies, followed by the quasi-isotropic and the angle-ply laminate configurations in the cases taken.

The nature of the values of natural frequencies for different laminate configurations can be explained by the Equation (3.54), which states that,

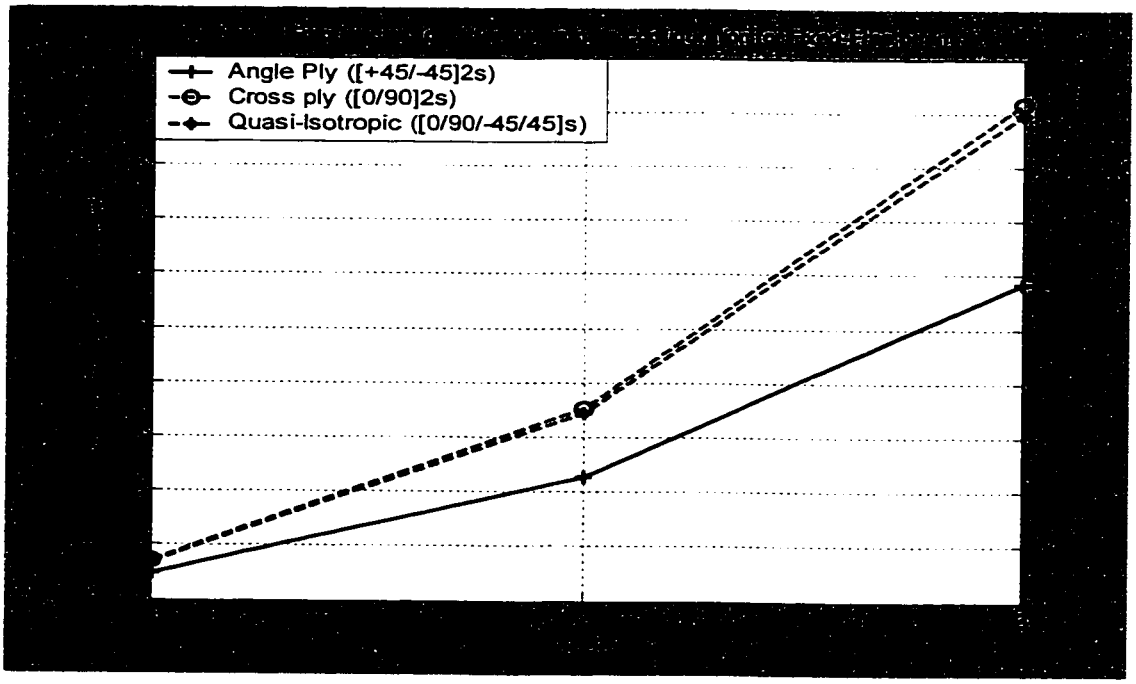

Figure 4.3 Natural frequencies obtained for different laminate configurations for the Fixed-Free mid-plane tapered composite beam

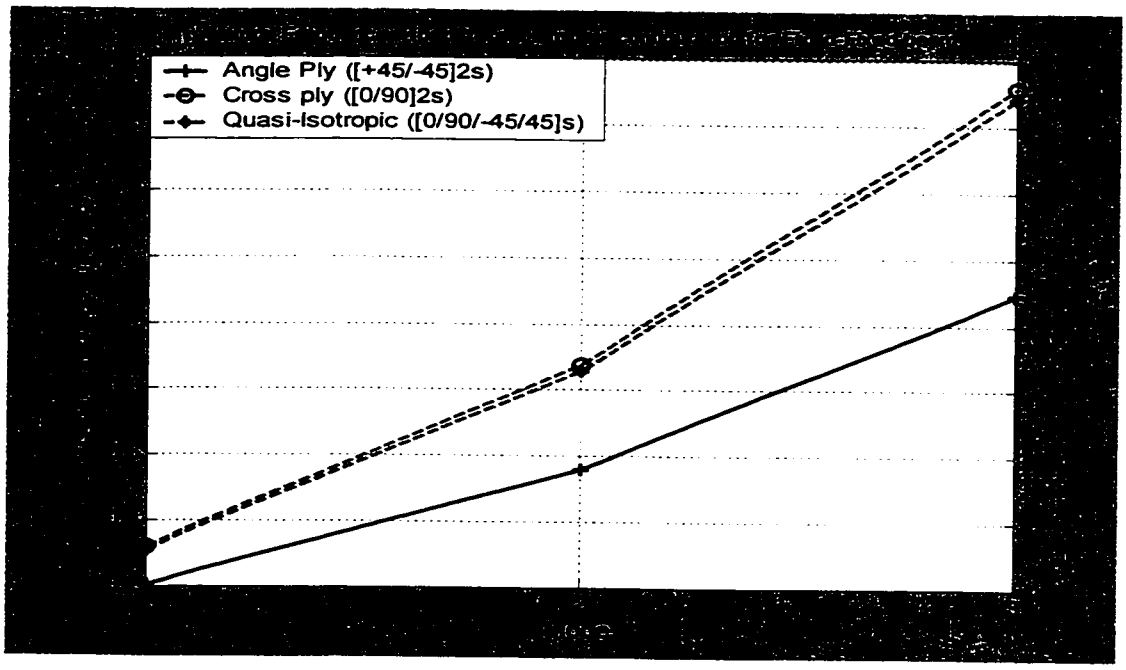

Figure 4.4 Natural frequencies obtained for different laminate configurations for the Fixed-Fixed mid-plane tapered composite beam

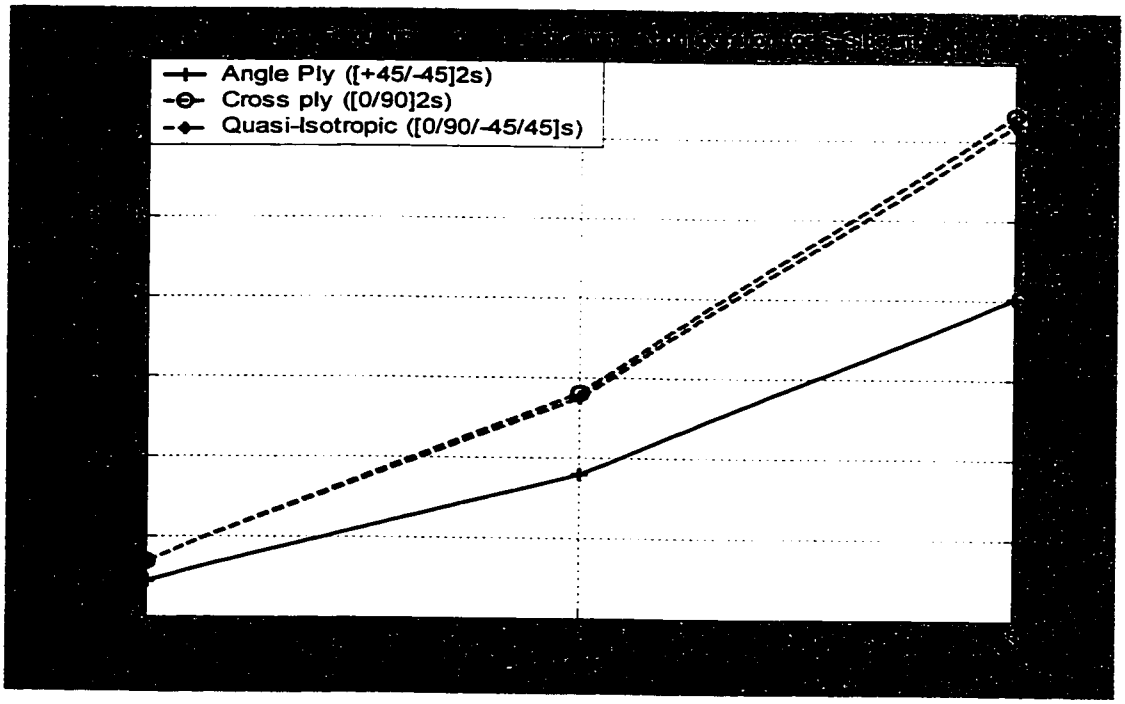

Figure 4.5 Natural frequencies obtained for different laminate configurations for the Simply-Supported mid-plane tapered composite beam

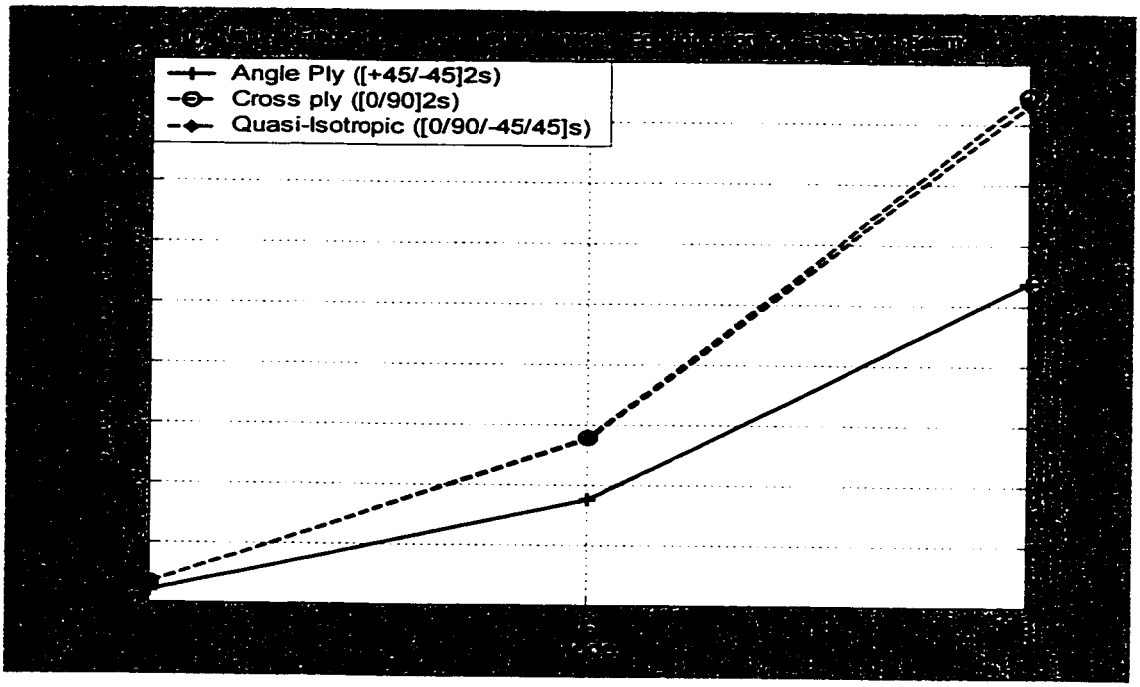

Figure 4.6 Natural frequencies obtained for different laminate configurations for the Free-Fixed mid-plane tapered composite beam

$$D_{11} = \sum_{p=1}^{m}\left[t_p \overline{Z}_p^2 + \frac{t_p^3}{12}\right](\overline{Q}_{11})_p \tag{4.1}$$

The change in the fiber orientation has a direct effect on the flexural rigidity of the laminate, bD_{11}, where D_{11} is the bending or flexural laminate stiffness relating the bending moment M_x to curvature κ_x. $(\overline{Q}_{11})_p$ is the transformed stiffness coefficient of a ply, which can be defined as:

$$(\overline{Q}_{11})_p = (\cos^4\theta)Q_{11} + (\sin^4\theta)Q_{22} + 2(\cos^2\theta)(\sin^2\theta)Q_{12} + 4(\cos^2\theta)(\sin^2\theta)Q_{33} \tag{4.2}$$

where Q_{11}, Q_{12}, Q_{22} *and* Q_{33} are coefficients of the ply stiffness matrix, and they are functions of the mechanical properties of the ply.

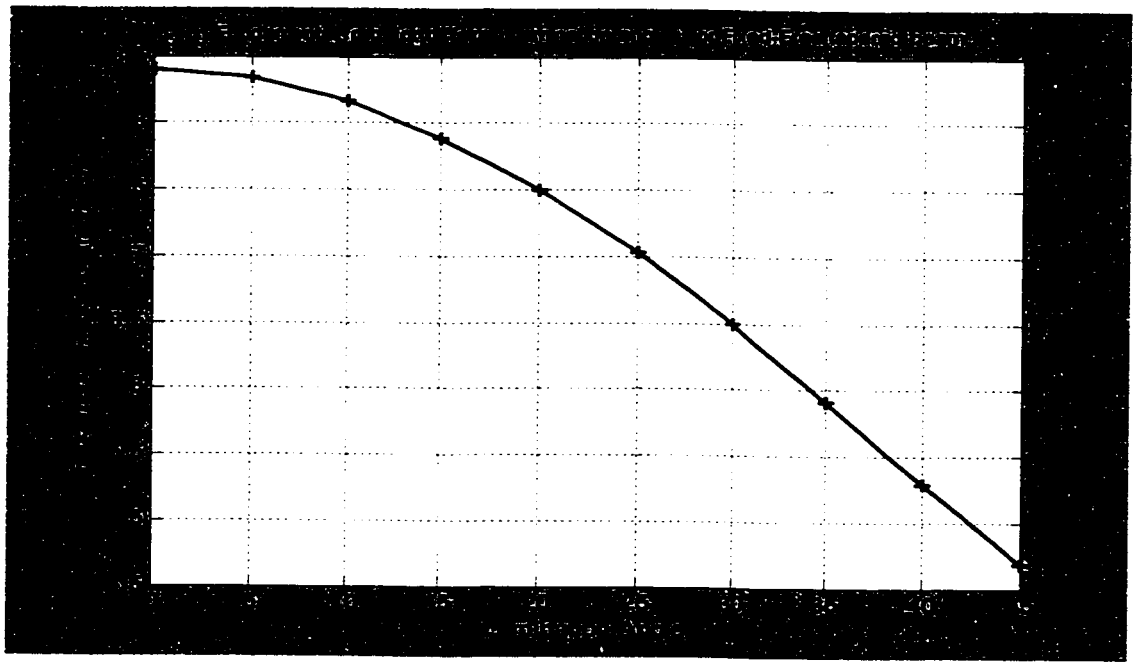

Figure 4.7 Fundamental frequency for various lamination angles ($\pm\theta$) for Fixed-Free tapered beam

It is obvious from Equations (4.1) and (4.2) that, the flexural rigidity of a ply, and consequently the laminate, is a function of ply orientation. In addition, the natural frequency is directly proportional to D_{11} and hence, there is a significant drop in the natural frequency for the lamination angles greater than $\pm\theta = 10^{\circ}$ (Figure 4.7). Results similar to those shown in Figure 4.7 are obtained for other taper angles as well.

4.2.3 The Effect of Taper Angle on the Natural Frequencies

We now intend to consider the effect of taper angle on the natural frequencies of the mid-plane tapered composite beams. The mechanical properties are as listed in Tables 4.1 and 4.2. The height (H) of the tapered beams considered here is 10.97 mm respectively.

The number of plies in the thick section of the tapered laminate are 72 and in the thin section are 24. The configurations for the thick and thin sections are respectively, $[0_4/\pm 45_4/\pm 45_8/-45_8]_s$ and $[0_4/\pm 45_4]_s$. Three taper angles have been selected for comparison, viz. 2, 4.29 and 6 degrees. The results will be obtained using the trigonometric hierarchical formulation (1T2) and the boundary conditions of the beam are Fixed-Free.

Table 4.6 Natural frequencies ($\times 10^5$) for different taper angles for a Fixed-Free mid-plane tapered composite beam

Mode	2° Taper Angle	4.29° Taper Angle	6° Taper Angle
1	0.0808	0.373	0.7319
2	0.3526	1.627	3.1943
3	0.9407	4.341	8.5218

Table 4.6 details the results for the comparison of natural frequencies for different taper angles. The tapered composite beam having an angle of 2 degrees has the lowest values for natural frequencies. The tapered beams having taper angles as 4.29 degrees and 6 degrees give the successive higher values.

Figure 4.8 illustrates these results for all the three taper angles that we have taken. The change in the taper angles affects directly the entries of the element stiffness and mass matrices. Generalizing from the results obtained above, the higher the taper angle, the higher the values of the natural frequencies. Equations (3.62)–(3.64) give a clear relationship stating that the stiffness matrix is a function of (the slope) the taper, and that they are in direct proportion. Hence, higher taper angle leads to a stiffer laminate, which eventually leads to higher values of the natural frequencies. This effect is similar to the

effect of the change in the fiber orientation. The change in the fiber orientations affects the flexural rigidity of the laminate, and hence, the element stiffness matrix. Also, it can be recalled from vibration analysis that the dynamic matrix, [a] is the product of the inverse of the mass matrix and the stiffness matrix. Hence, higher values of the stiffness matrix due to higher taper angles and lower values of the mass matrix due to decreasing value of the length of the taper for the case considered, lead to higher values of the coefficients of the dynamic matrix. Accordingly, this will lead to higher eigenvalues and consequently higher natural frequencies.

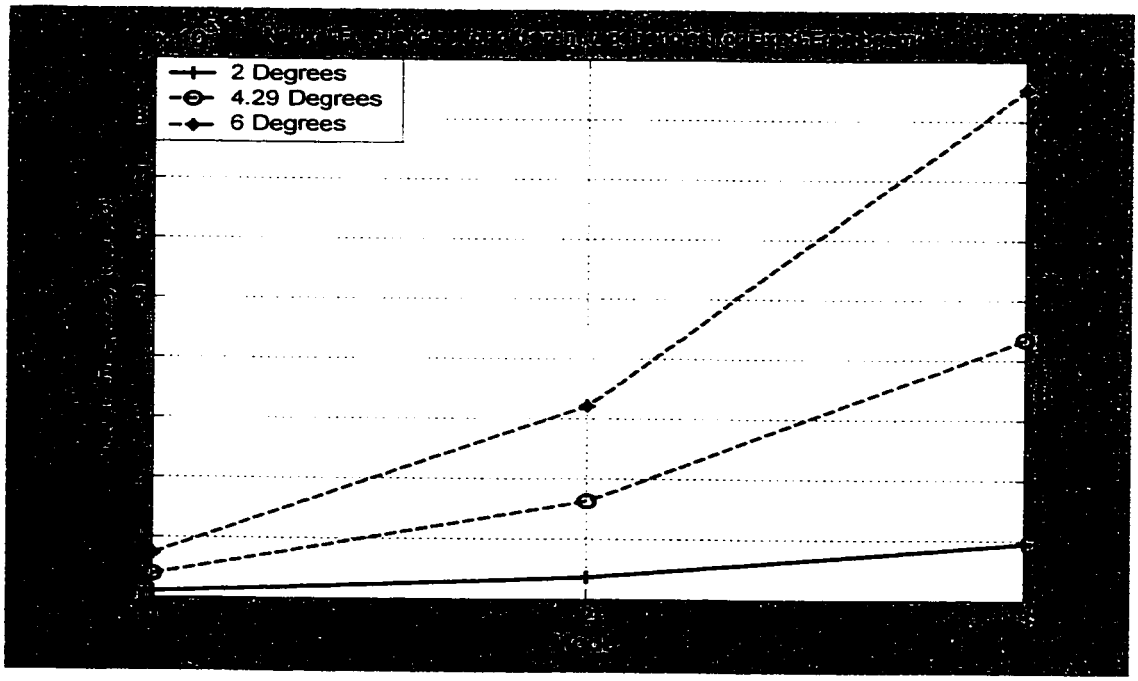

Figure 4.8 Natural Frequencies obtained using different taper angles for the Free-Fixed mid-plane tapered composite beam

4.2.4 The effect of internal DOF on natural frequency

We now intend to explore the effect of increasing the internal degrees of freedom in a trigonometric hierarchical element used here to model the mid-plane tapered composite beams.

The geometric specifications for the problem are: height (H) = 7.3152 mm; Length (L) = 36.6 mm. The laminate configuration at the thick section is $[0_4/\pm 45_4/\pm 45_4/-45_4]_s$ and at the thin section is $[0_4/\pm 45_4/\pm 45_4]_s$. There are 48 plies in the thick section and 24 in the thin section. The angle of taper is equal to 2.86°. The boundary conditions of the beam are Fixed-Free.

Table 4.7 Natural frequencies ($\times 10^{-4}$) obtained using different formulations for a Fixed-Free mid-plane tapered composite beam

Mode	1C (2 DOF)	2C (4 DOF)	1T1 (3 DOF)	1T2 (4 DOF)	1T3 (5 DOF)	1T4 (6 DOF)
1	4.49	4.47	4.47	4.47	4.47	4.47
2	26.80	24.36	22.40	22.03	22.03	22.03
3	-[1]	82.26	81.10	59.16	57.30	57.30

Table 4.7 gives the natural frequencies for the first three modes obtained using conventional and trigonometric hierarchical finite element formulations for the problem. In the conventional FEM, the accuracy of the solutions obtained, is increased by refining the mesh i.e. increasing the number of elements and consequently the nodal degrees of freedom. Hence, in the above case, when two elements (2C) are used to model the beam,

[1] For the case of fixed-free beam modeled by one element in the conventional formulation, there will be two degrees of freedom. Hence, there will be only two obtainable modes (two values of natural frequencies).

values of the natural frequencies are refined for more accuracy. But increasing the number of elements, especially in the case of tapered composite beams, can be numerically expensive and also it introduces more discontinuities in the curvature. HFEM on the other hand, offers an alternative by increasing the internal degrees of freedom and improving the accuracy of the solutions. As we have seen in previous examples as well, the HFEM formulation having the same number of system degrees of freedom as the conventional formulation (see for eg. 2C and 1T2 having 4 system DOF each in Table 4.7), gives more accurate results. In the trigonometric HFEM as well, increasing the internal degrees of freedom, gives more freedom to the inside of the element and it is able to represent the mode shapes more accurately. Hence, we see that the values of frequencies change till the system degrees of freedom in the trigonometric HFEM become 6 (1T4).

4.2.5 The effect of different taper types on the natural frequency

In the previous sections we have conducted detailed parametric studies on one of the types of tapered composite beam, i.e. mid-plane tapered composite beam. It would be interesting to learn as to what effect the parameters would have on other kinds of tapered composite beams. Hence, an overlapped-grouped tapered composite beam as described in Figure 4.9, will be analyzed for its free vibration characteristics in this section.

Botting et al. [77] and Fish and Vizzini [78] have shown that tapered laminates can be tailored for stiffness and strength by altering the internal ply-drop configuration.

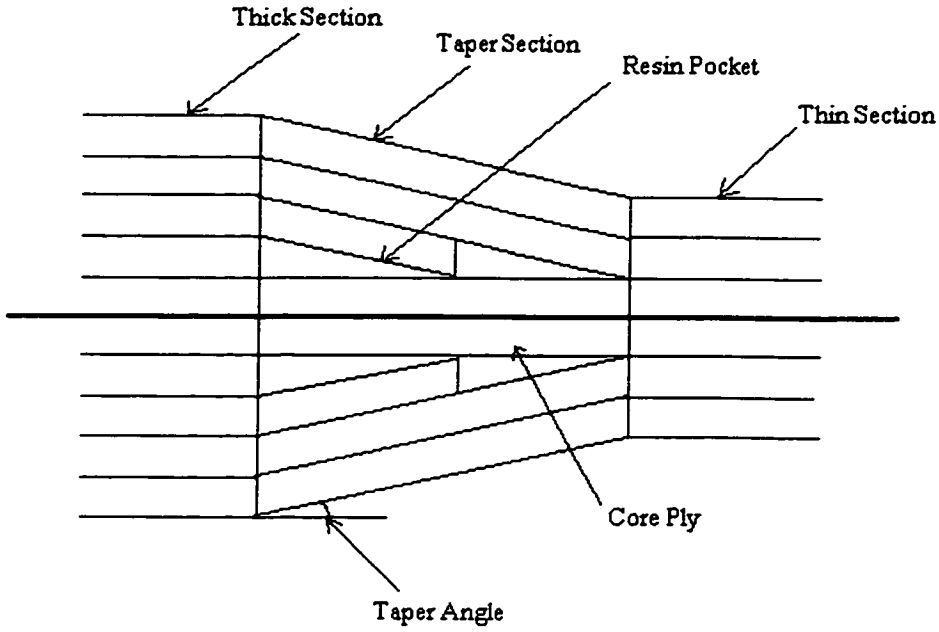

Figure 4.9 Schematic diagram of a composite internal taper beam (overlapped-grouped)

The overlapped–grouped structure (Figure 4.9) was one of the ply-drop configurations that they analyzed for delamination initiation and growth and damage tolerance. They applied the finite element method to different ply-drop configurations and showed that altering the ply-drop configuration could decrease the stress state at the ply-drop. Our concern in this study is to apply the HFEM to these internal tapered beams for their dynamic analysis and compare the results with those obtained for the mid-plane tapered beam.

Problem Description

An internally tapered composite beam as the one shown in Figure 4.9 has the following geometric properties: height (H) = 1.524 mm; length (L) = 12.2 mm (L/H=10).

The configuration of the thick section of the tapered beam is $[\pm 45_2/-45]_s$ and that of the thin section is $[\pm 45/45]_s$. There are 10 plies in the thick section and 6 in the thin section. The angle of taper is equal to 1.43°. The mechanical properties of the graphite-epoxy and the resin are listed in Tables 4.1 and 4.2.

Table 4.8 Natural frequencies ($\times 10^5$) for different types of tapers having different boundary conditions

Type of Condition	Natural Frequencies ($\times 10^5$)					
	Mid-Plane Taper			Overlapped-Grouped Taper		
	Mode No.			Mode No.		
	1	2	3	1	2	3
Fixed-Fixed	2.7124	7.4716	14.639	1.8304	5.0445	9.8956
Simply-Supp.	1.1866	4.7924	10.783	0.7901	3.2387	7.2913
Fixed-Free	0.5725	2.9316	7.7341	0.4409	2.0621	5.3011
Free-Fixed	0.3089	2.4280	7.2546	0.1778	1.5624	4.8325

Table 4.8 gives detailed results for the given problem for the internally tapered composite beam of Figure 4.9. Results for the mid-plane tapered composite beam for the same configuration of the laminate are also given for comparison. As seen in the case of the mid-plane taper, natural frequencies of different modes for different boundary conditions vary considerably for the internal taper as well. The ascendancy of the values of frequencies for different boundary conditions is also the same, being the maximum for fixed-fixed case and the minimum for free-fixed case. This is because the factors affecting the values of the natural frequencies, viz. the degree of restrain and the position

of restrain are the same. Another feature of importance is that for the same number of plies and the same ply configuration, the values of frequencies of different modes for the mid-plane tapered beam are higher than those of the overlapped-grouped tapered beams. The rearranging of the internal ply-drop in the laminates has an effect on the stiffness of the laminate and hence affects the values of the natural frequencies.

Table 4.9 Natural frequencies ($\times 10^5$) for different types of tapers having different laminate configurations

Ply Group	Natural Frequencies ($\times 10^5$)					
	Mid-Plane Taper			Overlapped-Grouped Taper		
	Mode No.			Mode No.		
	1	2	3	1	2	3
$[\pm 45_2]_s$ (Angle-Ply)	2.02	5.57	10.91	1.2838	3.5297	6.9011
$[0/90]_{2s}$ (Cross-Ply)	3.1843	8.7776	17.179	2.6528	7.3484	14.449
$[0/90/45/-45]_s$ (Quasi-Isotropic)	3.1097	8.5824	16.832	1.9458	5.3948	10.752

Table 4.9 gives a comparison of the values of natural frequencies for different ply-groups for the mid-plane and overlapped-grouped tapered composite beams. The boundary conditions of the beams are fixed-fixed. As in the case of the effect of boundary conditions on the frequencies of different modes, different ply-groups have the same effect on the overlapped-grouped tapered composite beams as they have on the mid-plane tapered composite beams. Hence, for the overlapped-grouped tapered composite beams,

the angle-ply configuration has the lowest values of natural frequencies for all the modes considered. The cross-ply laminate has the maximum value and the quasi-isotropic laminate has the intermediate value. The flexural rigidity of the laminate is a function of the ply orientation and hence is affected by any change in the laminate configuration. Consequently, the values of the natural frequencies show the corresponding change. A more detailed explanation has been given in section 4.2.2.

4.3 Parametric Study on Forced Vibration of Mid-Plane Tapered Composite Beams

In the previous section a detailed study was performed on the free vibration of mid-plane tapered composite beams. In the current section, we intend to extend the study to the forced vibration analysis of the mid-plane tapered composite beams.

A laminate that has a configuration of $[0_4/\pm 45_4/\pm 45_4/-45_4]_s$, i.e. having 48 plies in the thick section and 24 in the thin section ($[0_4/\pm 45_4]_s$) and having a taper angle of 2.86° is considered. The height (H) of the laminate is 7.3152 mm. The length (L) of the laminate is 36.6 mm. The boundary conditions of the laminate are fixed-free. The mechanical properties of the laminate are as detailed in Tables 4.1 and 4.2.

4.3.1 The effect of taper angle on the response of the mid-plane tapered composite beam

To consider the effect of the taper angle on the forced response of a tapered composite beam, a tapered beam having the specifications mentioned below is subjected

to the loading as given in Figure 4.10. The number of plies in the thick section of the tapered laminate is 72 and in the thin section is 24. The configurations for the thick and thin sections are respectively, $[0_4/\pm 45_4/\pm 45_8/-45_8]_s$ and $[0_4/\pm 45_4]_s$. Three taper angles have been selected, viz. 2, 4.29 and 6 degrees. The results will be obtained using the trigonometric hierarchical formulation (1T2) and the boundary condition of the beam is Fixed-Free.

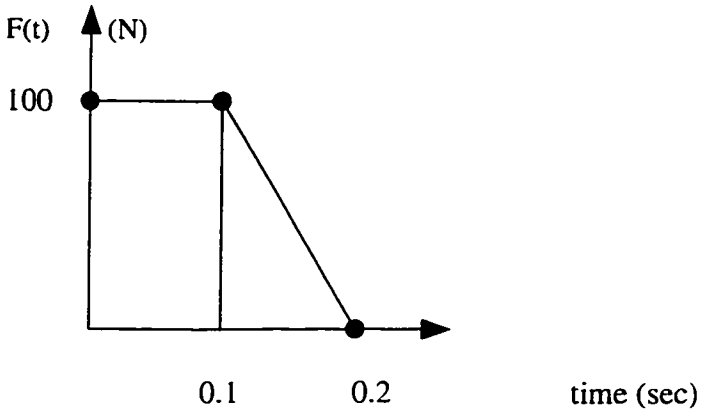

Figure 4.10 Force applied at the free end of the tapered composite beam

The height (H) of the tapered beams considered here is taken to be 10.97 mm.

Table 4.10 gives us the values of the maximum deflection of the degrees of freedom associated with the displacement and rotation at the free end of the fixed-free mid-plane tapered composite beam.

Table 4.10 Comparison of the forced response for different taper angles

DOF	2° Taper Angle	4.29° Taper Angle	6° Taper Angle
3	0.0019 (m)	0.0002 (m)	0.0001 (m)
4	0.0360 °	0.0078 °	0.0040 °

The forced vibration analysis for this problem is done using the direct integration technique of Newmark-β method. The results are compared with that obtained using the mode superposition technique and they are in excellent agreement. The deflection and the rotation at the free end, both decrease in value as the taper angle is increased. As discussed while considering the effect of the taper angle on the natural frequencies, Equations (3.54–3.56) illustrate clearly the direct relationship between the stiffness matrix and the taper angle.

We concluded that higher taper angle leads to a stiffer laminate. Hence, the maximum deformations, viz. deflection and rotation would consequently be less for a stiffer laminate (i.e. for a laminate having high taper angle).

4.3.2 The effect of laminate configuration on the response of the mid-plane tapered composite beam

To consider the forced response of different laminate configurations, we consider a tapered composite beam having the following geometric properties:

height (H) = 1.219 mm; length (L) = 12.2 mm (L/H=10).

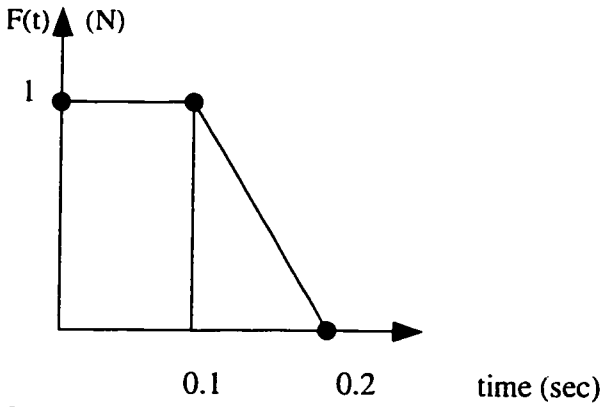

Figure 4.11 Force applied at the free end of the tapered composite beam

There are 8 plies in the thick section and 4 in the thin section. The angle of taper is equal to 1.43°. The mechanical properties of the graphite-epoxy and the resin are listed in Tables 4.1 and 4.2. The laminate configurations that are considered for the analysis here have the angle-ply $[\pm 45_2]_s$, cross-ply $[0/90_2]_s$ and quasi-isotropic $[0/90/-45/45]_s$ configurations at the thick section. The boundary condition of the beam are fixed-free. The stiffness and mass matrices for the problem are determined by trigonometric hierarchical finite element method using only one element to model the beam. The element has eight degrees of freedom (DOF) including four hierarchical DOF. The loading at the free end of the beam is as given in Figure 4.11.

Table 4.11 Comparison of the forced response of laminates with different configurations

DOF	Cross-Ply	Angle-Ply	Quasi-Isotropic
3	0.0001 (m)	0.0003 (m)	0.0001 (m)
4	0.0172°	0.0421°	0.0180°

Table 4.11 gives us the maximum response of the mid-plane tapered composite beam having different laminate configurations in the forced vibration problem. The degrees of freedom labeled 3 and 4 are the displacement and rotation at the free end of the fixed-free beam. The deformations are values of the maximum displacement and rotation at the free end. Angle-ply laminate has the maximum value of the deflection, quasi-isotropic laminate has an intermediate value and cross-ply laminate deflects the least.

Fundamentally, deflection is a function of the force applied and the stiffness of the structure. In the present case, the force applied is the same, hence the stiffness of the

beams with different laminate configurations is the differentiating factor. As mentioned before, according to Equations (4.1) and (4.2) the stiffness of a laminate is a function of the ply orientation. Hence from the direct relationship given by these two equations, the cross-ply laminate has the maximum stiffness and the angle-ply laminate has the minimum with quasi-isotropic laminate having an intermediate value. Consequently, the deflections are in the reverse order.

4.3.3 Response of mid-plane tapered beam to sinusoidal loading

In the previous subsections, we analyzed the forced response of mid-plane tapered composite beams when the loading was as shown in Figure 4.11. We will now analyze the response of the beams to sinusoidal loading.

The number of plies in the thick section of the tapered laminate considered for this problem is 72 and in the thin section is 24. The configurations for the thick and thin sections are respectively, $[0_4/\pm 45_4/\pm 45_8/-45_8]_s$ and $[0_4/\pm 45_4]_s$. Three taper angles as selected previously are chosen, viz. 2, 4.29 and 6 degrees. The results will be obtained using the trigonometric hierarchical formulation (1T2) and the boundary condition of the beam is Fixed-Free. The height (H) of the tapered beams is 10.97 mm. The loading at the free end of the beam is as given in Figure 4.12.

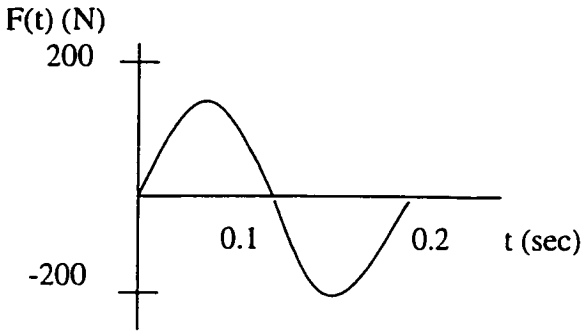

Figure 4.12 Force applied at the free end of the tapered composite beam

Table 4.12 Comparison of the forced response for different taper angles

DOF	2° Taper Angle	4.29° Taper Angle	6° Taper Angle
3	0.0019 (m)	0.0002 (m)	0.0001 (m)
4	0.0370°	0.0080°	0.0041°

Table 4.12 above gives a comparison of the deflections at the free end of the mid-plane tapered composite beams having different taper angles. As we had seen in section 4.3.1, the larger the taper angle is, the higher is the stiffness of the laminate. Hence, laminates having larger taper angles will have less deflection. Therefore, we see that the laminate having taper angle of 2° has the maximum deflection while a taper angle of 6° leads to minimum deflection.

Another important feature that is evident in this example of sinusoidal loading is that keeping the laminate and the taper angles same, the deflections at the free end of the fixed-free beam are nearly same in this case and in the example dealt with in section 4.3.1. The difference being that the magnitude of the maximum load applied at the free end in the sinusoidal case is twice than that in the previous case. Hence, the kind of loading has a profound effect on the values of deflection.

We will now analyze mid-plane tapered composite beams having different laminate configurations subjected to sinusoidal loading. We consider a tapered composite beam having the following geometric properties:

height (H) = 1.219 mm; length (L) = 12.2 mm (L/H=10).

There are 8 plies in the thick section and 4 in the thin section. The angle of taper is equal to 1.43°. The mechanical properties of the graphite-epoxy and the resin are listed in Tables 4.1 and 4.2. The laminate configurations that are considered for the analysis here are angle-ply $[\pm 45_2]_s$, cross-ply $[0/90_2]_s$ and quasi-isotropic $[0/90/-45/45]_s$. The boundary condition of the beam is fixed-free. The stiffness and mass matrices for the problem are determined by trigonometric hierarchical finite element method using only one element to model the beam. The element has eight degrees of freedom (DOF) including four hierarchical DOF (1T4). The loading at the free end of the beam is as given in Figure 4.13.

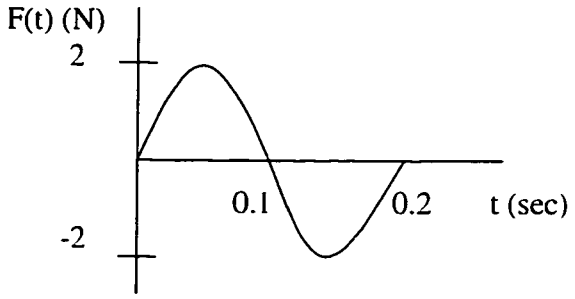

Figure 4.13 Force applied at the free end of the tapered composite beam

Table 4.13 Comparison of the forced response of different laminate configurations

DOF	Cross-Ply	Angle-Ply	Quasi-Isotropic
3	0.0001 (m)	0.0003 (m)	0.0001 (m)
4	0.0176°	0.0431°	0.0184°

Table 4.13 gives the values of deflection at the free end of the fixed-free mid-plane tapered composite beams. As in the previous case, the angle-ply configuration has the maximum values of the deflections and the cross-ply has the minimum. Since the loading is sinusoidal in nature, the maximum value of the load applied is twice that in the previous case (section 4.3.2).

4.4 Overall Conclusions

Based on the results obtained in the preceding sections for different variations in the tapered composite beams, we can summarize some key conclusions to aid the designer in making informed decisions in the design process of tapered composite beams.

1) The hierarchical formulation developed in this thesis is much more efficient than the conventional formulation. In numerous examples throughout the thesis, we have seen that the HFEM uses far less number of elements than the conventional FEM and gives more accurate answers much faster. In terms of the system degrees of freedom (DOF) of the structure, the HFEM gives more accurate answers than the conventional FEM having the same number of system DOF. The inclusion of the internal degrees of freedom in the HFEM, lends more freedom to the inside of the element thereby increasing its efficiency to model the structure. Hence, more accurate results are obtained much faster using less number of elements and degrees of freedom.

2) In modeling thickness-tapered composite beams, the HFEM offers the critical ability to model them with minimum number of elements and still get more accurate answers and speedy convergence.

3) The trigonometric HFEM formulation is more efficient than the polynomial HFEM. Also, the trigonometric functions offer the ease of manipulation as compared to higher order polynomials.

4) The natural frequencies of the mid-plane tapered composite beams are always higher than the corresponding values for overlapped-grouped tapered composite beams, regardless of the method of formulation applied.

5) With regard to the boundary conditions, the free-fixed boundary conditions give the lowest values of the natural frequencies for both the types of tapers. Likewise the fixed-fixed type gives the highest values of the frequencies for both kinds of tapers.

6) With regard to the fiber orientations, the angle-ply group minimizes the values of the natural frequencies in both types of tapers. This is because the angle-ply laminates have the maximum stiffness.

7) The higher the taper angle is, the higher is the value of the natural frequencies as explained in section (4.2.3).

8) The nature of loading in forced vibration affects the values of deflection.

4.5 Summary

In this chapter, a thorough parametric study on the mid-plane tapered composite beams is conducted. The composite beams chosen are practical in terms of mechanical

properties and geometric description. The overlapped-grouped configuration of the internally tapered composite beams is also studied and suitable conclusions are made.

All possible variations in the thickness-tapered composite beams are made to make a comprehensive analysis of their dynamic behavior. Variations in boundary conditions, laminate configurations and taper angles are made. For each variation, the results for the lowest three natural frequencies are obtained and plotted in figures to elaborate on the interpretations. Suitable comparisons are made between the conventional and the hierarchical formulations to establish the advantages of the new method. Each subsection ends in a table that summarizes the results mentioned in it. In the last section overall conclusions are provided that would serve the design process.

Chapter 5

Summary

5.1 Conclusions

In the present thesis the hierarchical finite element formulations for the analysis of composite beams have been developed. The developed formulations have been adapted so as to be applicable and appropriate to thick and thin composite beams. The vibration analysis of uniform-thickness and variable-thickness composite beams has been conducted using the developed formulations. Two sub-formulations of the Hierarchical Finite Element Method (HFEM), viz. trigonometric and polynomial formulations, have been considered and their applications to uniform-thickness and variable-thickness composite beams have been made.

Prior to the introduction of the HFEM formulation, the conventional finite element formulation has been derived in detail to systematically bring out the efficiency, accuracy and the advantages of the HFEM formulation. This has been done to make evident the basic aspects of the conventional method and the enhancements that are made in it through the HFEM.

The conventional finite element model for the beam structure considers two degrees of freedom per node, viz. displacement and slope so as to satisfy the geometric boundary conditions. The hierarchical formulation enhances the capability of the element by making the degree of the approximating function to tend to infinity. This is done by making use of trigonometric and polynomial functions. The four cubic displacement modes used in the conventional formulation are retained. The higher order modes are selected from a variety of polynomial and trigonometric functions. Accordingly, the stiffness and mass matrices are set up.

The programming, involving symbolic computation, is done using MATLAB® and MATHEMATICA® software. At the end of each formulation, suitable problems on the free and forced vibration have been solved and the results are validated with the exact solutions. A comparison between the results obtained using the conventional and the hierarchical formulations is inherent in all the problems. The HFEM is also applied to the static analysis of composite beams to highlight specific points of the method. To elaborate on the analysis in the present thesis, a parametric study using both the types of formulations is provided.

The parametric study considers various changes in the composite laminates to demonstrate their influences on the natural frequencies and the maximum response to forced vibration. These changes include the change in the boundary conditions, change in

the laminate configuration, change in the internal degrees of freedom, change in the taper angle and finally change in the type of internal taper. The difference in the composite laminate's responses is remarkable for each change within the same type of taper.

The study done in this thesis is of great importance to the mechanical designer, who designs and develops composite structures to withstand dynamic loads. The important and principal conclusions are:

1) The hierarchical finite element method increases element effectiveness by adding internal degrees of freedom to the element. This is achieved by adding trigonometric or polynomial functions to the approximating function. The trigonometric sub-formulation is more accurate than the polynomial sub-formulation as demonstrated in this thesis.

2) Both the hierarchical sub-formulations perform better than the conventional formulation, both in terms of accuracy and speed of convergence. Also significant is that both the sub-formulations use less number of elements and system degrees of freedom to arrive at a more accurate answer.

3) The parametric study performed on the variable-thickness composite beams gives a comprehensive understanding of their behavior under different physical conditions. Values of the natural frequencies and the maximum response to forced vibration for beams having different taper

angles, boundary conditions, laminate configurations and types of internal tapers allow the designer to develop appropriately the optimum design.

5.2 Contributions

The primary contributions have been mentioned in respective chapters and are summarized as follows:

1) The trigonometric hierarchical finite element method has been proposed and applied to the analysis of variable-thickness composite beams.

2) A set of polynomials is proposed for the polynomial hierarchical formulation that fares better than the conventional FEM formulation.

3) Both the forms of hierarchical formulations, viz. trigonometric and polynomial sub-formulations have been applied to the static analysis of uniform-thickness composite beams subjected to a uniformly varying load.

4) Forced vibration analysis of uniform and variable-thickness composite beams is carried out using both the sub-formulations.

5.3 Recommended Future Work

The following recommendations may be considered for future studies:

i) The HFEM considered in this thesis can be extended to other types of internally tapered variable-thickness composite beams.

ii) The HFEM can be applied to the stress analysis of the tapered composite beams.

iii) For the polynomial sub-formulation, other suitable polynomials could be chosen that are more efficient than the present one.

iv) The hierarchical formulation could be extended to the analysis of composite plates.

v) The effect of damping has not been considered in this analysis. Further work can be done to include this effect in the free and forced vibration of composite beams and plates.

References

[1] Abarcar, R. B. and Cunniff, P. F., "The Vibration of Cantilevered Beam of Fiber Reinforced Material", Journal of Composite Materials, Vol. 6, 1972, pp. 504-516.

[2] Teoh, L. S. and Huang, C. C., "The Vibration of Beams of Fiber Reinforced Material", Journal of Sound and Vibration, Vol. 51, 1977, pp. 467-473.

[3] Teh, K. K. and Huang, C. C., "Effects of Fiber Orientation on Free Vibrations of Composite Beams", Journal of Sound and Vibration, Vol. 69, 1980, pp. 327-337.

[4] Kapania, R. K. and Raciti, S., "Recent Advances in Analysis of Laminated Beams and Plates, Part II: Vibrations and Wave Propagation", AIAA Journal, Vol. 27,1989, pp. 935-946.

[5] Miller, A. K. and Adams, D. F., "An Analytical means of determining the Flexural and Torsional Resonant Frequencies of generally Orthotropic beams", Journal of Sound and Vibration, Vol. 41, 1975, pp. 433-449.

[6] Vinson, J. R. and Sierakowski R. L., *The Behavior of Structures composed of Composite Materials*, 1986, Boston, U. S. A, pp. 139-144, Martinus Nijhoff Publishers.

[7] Chen, A. T. and Yang, T. Y., "Static and Dynamic formulation of Symmetrically Laminated Beam Finite Element for Microcomputer", Journal of Composite Materials, Vol. 19, 1985, pp. 459-475.

[8] Chandrashekhara, K., Krishnamurthy, K., and Roy, S., "Free Vibrations of Composite beams including Rotary Inertia and Shear Deformation", Composite Structures, Vol. 14, 1990, pp. 269-279.

[9] Chandrashekhara, K. and Bangera, K. M., "Free Vibration of Composite Beam using a Shear Flexible Beam Element", Computers and Structures, Vol. 43(4), 1992, pp. 719-727.

[10] Chandrashekhara, K. and Bhimareddi, A., "Some observations on the modeling of Laminated Composite Beams with general Lay-ups", Composite Structures, Vol. 19, 1991, pp. 371-380.

[11] Abramovich, A., "Shear Deformation and Rotary Inertia Effects of Vibrating Composite Beams", Composite Structures, Vol. 20, 1992, pp.165-173.

[12] Singh, M. P. and Abdelnasser, A. S., "Random Response of Symmetric Cross-Ply Composite Beams with Arbitrary Boundary Conditions", AIAA Journal, Vol. 30(4), 1992, pp. 1081-1088.

[13] Krishnaswamy, S., Chandrashekhara, K., and Wu, W. Z. B., "Analytical Solutions to Vibration of Generally Layered Composite Beams", Journal of Sound and Vibration, Vol. 159(1), 1992, pp. 85-99.

[14] Abramovich, H. and Livshits, A., "Free Vibrations of Non-Symmetric Cross-Ply Laminated Beams", Journal of Sound and Vibration, Vol. 176(5), 1994, pp. 596-612.

[15] Khedeir, A. A., and Reddy, J, N., "Free Vibrations of Cross-Ply Laminated Beams with Arbitrary Boundary Conditions", International Journal of Engineering Science, Vol. 32(12), 1994, pp. 1971-1980.

[16] Eisenberger, M., Abramovich, H., and Shulepov, O., "Dynamic Stiffness Analysis of Laminated Beam Using a First Order Shear Deformation Theory", Composite Structures, Vol. 31, 1995, pp. 265-271.

[17] Abramovich, H., Eisenberger, M., and Shulepov, O., "Vibrations of Multi Span Non-Symmetric Composite Beams", Composites Engineering, Vol. 5(4), 1995, pp. 397-404.

[18] Zappe, J. A., and Lesieutre, G. A., "Vibration Analysis of Laminated Beams using an Iterative Smeared Laminate Model", Journal of Sound and Vibration, Vol. 199(2), 1997, pp. 275- 284.

[19] Yuan, F. and Miller, R. E., "A New Finite Element for Laminated Composite Beams", Computers and Structures, Vol. 14, 1989, pp. 731-745.

[20] Yuan, F. and Miller, R. E., "A Higher-Order Finite Element for Laminated Composite Beams", Computers and Structures, Vol. 31, 1990, pp. 125-150.

[21] Manjunatha, B. S. and Kant, T., "New Theories for Symmetric / Unsymmetric Composite and Sandwich Beams with C° Finite Element", Composite Structures, Vol. 23, 1993, pp. 61-73.

[22] Lee, C. and Liu, D., "An Interlaminar Stress Continuity Theory for Laminated Composite Analysis", Computers and Structures, Vol. 42, 1992, pp. 69-78.

[23] Shi, G. and Lam, K. Y., "Finite Element Vibration Analysis of Composite Beams based on Higher Order Beam Theory", Journal of Sound and Vibration, Vol. 219(4), 1999, pp. 707-721.

[24] Shi, G., Lam, K. Y., and Tay, T. E., "On Efficient Finite Element Modeling of Composite Beams and Plates Using Higher Order Theories and an Accurate Composite Beam Element", Composite Structures, Vol. 41(2), 1998, pp. 159-165.

[25] Hodges, D. H., Atilgan, A. R., Fulton, M. V., and Rehfield, L. W., "Free Vibration Analysis of Composite Beams", Journal of American Helicopter Society, Vol. 36(3), 1991, pp. 36-47.

[26] Karabelis, D. L., and Beskos, D. E., "Static, Dynamic and Stability Analyses of Structures Composed of Tapered Beams", Computers and Structures, Vol. 16, 1983, pp. 731-748.

[27] Venkatesh, A., and Rao, K. P., "A Laminated Anisotropic Curved Beam and Shell Stiffening Finite Element", Computers and Structures, Vol. 15(2), 1982, pp. 197-201.

[28] Nabi, M. S., and Ganesan, N., "Generalized Element for the Free Vibration Analysis of Composite Beams", Computers and Structures, Vol. 51(5), 1994, pp. 607-610.

[29] Oral, S., "A Shear Flexible Finite Element for Non-Uniform Laminated Composite Beams", Computers and Structures, Vol. 38(3), 1991, pp. 353-360.

[30] Rao, S. R., and Ganesan, N., "Dynamic Response of Tapered Composite Beams using Higher Order Shear Deformation Theory", Journal of Sound and Vibration, Vol. 187(5), 1995, pp.737-756.

[31] Rao, S. R., and Ganesan, N., "Dynamic Response of Non-Uniform Composite Beams", Journal of Sound and Vibration, Vol. 200(5), 1997, pp.563-577.

[32] He, K., Hoa, S. V., and Ganesan, R., "The Study of Tapered Laminated Composite Structures: A Review", Composites Science and Technology, Vol. 60(14), 2000, pp. 2643-2657.

[33] Zienkiewicz, O. C., *The Finite Element Method*, 1979, New York, McGraw-Hill.

[34] Peano, A. G., "Hierarchies of Conforming Finite Elements for Plane Elasticity and Plate Bending", Computers and Mathematics with Applications, Vol. 2, 1976, pp. 211-224.

[35] Babuska, I., Szabo, B. A., and Katz, I. N., "The p-version of the Finite Element Method", SIAM Journal of Numerical Analysis, Vol. 18(3), 1981, pp. 515-545.

[36] Bardell, N. S., "Free Vibration Analysis of a Flat Plate using the Hierarchical Finite Element Method", Journal of Sound and Vibration, Vol. 151(2), 1991, pp. 262-289.

[37] Zienkiewicz, O. C., Irons, B. M., Scott, F. C., and Campbell, J., "Three Dimensional Stress Analysis", University of Liege Press, Proc. IUTAM Symp. On High Speed Computing of Elastic Structures, 1971, pp. 413-433.

[38] Zienkiewicz, O. C., Owen, D. R. J., Philips, D. W., and Nayak, G. C., "Finite Element Methods in the Analysis of Reactor Vessels", Nuclear Engineering Design, Vol. 20, 1972, pp. 507-541.

[39] Szabo, B. A., and Mehta, A. V., "P-Convergent Finite Element Approximations in Fracture Mechanics", International Journal of Numerical Methods in Engineering, Vol. 12, 1978, pp. 551-560.

[40] Basu, P. K., Szabo, B. A., and Taylor, B. D., "Theoretical Manual and Users Guide for Comet-XA. Rep. WV/CCM-79/2", Center for Computational Mechanics, Washington University, 1979.

[41] Zienkiewicz, O. C., Kelly, D. W., Gago, J. P. de S. R., and Babuska, I., "Hierarchical Finite Element Approaches, Adaptive refinement and Error Estimates", Proc. MAFELAP 1981.

[42] Kelly, D. W., Gago, J. P. De S. R., Zienkiewicz, O. C., and Babuska, I., "A Posteriori Error Analysis and Adaptive Processes in the Finite Element Method: Part I – Error Analysis", International Journal of Numerical Methods in Engineering, Vol. 19, 1983, pp. 1593-1619.

[43] Gago, J. P. De S. R., Kelly, D. W., Zienkiewicz, O. C., and Babuska, I., "A Posteriori Error Analysis and Adaptive Processes in the Finite Element Method: Part II – Adaptive Mesh Refinement", International Journal of Numerical Methods in Engineering, Vol. 19, 1983, pp. 1621-1656.

[44] Szabo, B. A., "Mesh Design for the p-version of the Finite Element", Computer Methods in Applied Mechanics and Engineering, Vol. 55, 1986, pp. 181-197.

[45] MSC/NASTRAN Application Manual for the McNeal Schwendler Corporation. Version 66, 1983.

[46] Han, W., and Petyt, M., "Linear Vibration Analysis of Laminated Rectangular Plates using the Hierarchical Finite Element Method – I: Free Vibration Analysis", Computers and Structures, Vol. 61, 1996, pp. 705-712.

[47] Han, W., and Petyt, M, "Linear Vibration Analysis of Laminated Rectangular Plates using the Hierarchical Finite Element Method – II: Forced Vibration Analysis", Computers and Structures, Vol. 61, 1996, pp. 713-724.

[48] Han, W., and Petyt, M., "Geometrically Non-Linear Vibration Analysis of Thin, Rectangular Plates using the Hierarchical Finite Element Method – I: The Fundamental Mode of Isotropic Plates", Computers and Structures, Vol. 63, 1997, pp. 295-308.

[49] Han, W., and Petyt, M., "Geometrically Non-Linear Vibration Analysis of Thin, Rectangular Plates using the Hierarchical Finite Element Method – II: 1st Mode of Laminated Plates and Higher Modes of Isotropic and Laminated Plates", Computers and Structures, Vol. 63, 1997, pp. 309-318.

[50] Rebeiro, P., and Petyt, M., "Non-Linear Vibration of Plates by the Hierarchical Finite Element and Continuation Methods", International Journal of Mechanical Sciences, Vol. 41, 1999, pp. 437-459.

[51] Rebeiro, P., and Petyt, M., "Non-Linear Vibration of Composite Laminated Plates by the Hierarchical Finite Element Method", Composite Structures, Vol. 46, 1999, pp.197-208.

[52] Rebeiro, P., and Petyt, M., "Non-Linear Vibration of Beams with Internal Resonance by the Hierarchical Finite Element Method", Journal of Sound and Vibration, Vol. 224, 1999, pp.591-624.

[53] Bardell, N. S., Dunsdon, J. M., and Langlay, R. S., "Free Vibration of Thin, Isotropic, Open, Conical Panels ", Journal of Sound and Vibration, Vol. 217, 1998, pp. 297-320.

[54] West L. J., Bardell, N. S., Dunsdon, J. M. and Loasby, P. M., "Some Limitations Associated with the use of K-Orthogonal Polynomials in Hierarchical Versions of the Finite Element Method", Structural Dynamics: Recent Advances (editors, Ferguson, N. S., Wolfe, H. F. and Mei, C.), The Institute of Sound and Vibration Research, Southampton, 1997, pp. 217-227.

[55] Houmat, A., "An Alternative Hierarchical Finite Element Formulation Applied to Plate Vibration", Journal of Sound and Vibration, Vol. 206, 1997, pp. 201-215.

[56] Leung, A. Y. T., and Chan, J. K. W., "Fourier p-elements for the Analysis of Beams and Plates", Journal of Sound and Vibration, Vol. 212, 1998, pp. 179-185.

[57] Beslin, O., and Nicholas, J., "A Hierarchical functions set for predicting very high order plate bending modes with any boundary conditions", Journal of Sound and Vibration, Vol. 202, 1997, pp. 633-655.

[58] Pian, T. H. H., "Derivation of Element Stiffness Matrices", AIAA Journal, Vol. 2, 1964, pp. 576-577.

[59] Krahula, J. L., and Polhemus, J. F., "Use of Fourier Series in the Finite Element Method", AIAA Journal, Vol. 6, 1968, pp. 726-728.

[60] Thomus, J., and Documaci, E., "Improved Finite Elements for Vibration Analysis of Tapered Beams", Aeronautical Quarterly, Vol. 24, 1973, pp. 39-46.

[61] Dawe, D. J., "Finite Strip Models for Vibration of Mindlin Plates", Journal of Sound and Vibration, Vol. 59, 1978, pp. 441-452.

[62] Barrette, M., Berry, A., and Beslin, O., "Vibration of Stiffened Plates Using Hierarchical Trigonometric Functions ", Journal of Sound and Vibration, Vol. 235(5), 2000, pp. 727-747.

[63] Han, W., Petyt, M., and Hsiao, K. M., "An Investigation into Geometrically Non-Linear Analysis of Rectangular Laminated Plates Using the Hierarchical Finite Element Method", Finite Element Analysis and Design, Vol. 18, 1994, pp. 273-288.

[64] Cook, R. D., Malkus, D. S., and Plesha, M. E., *Concepts and Applications of Finite Element Analysis*, 1989, New York, U. S. A., Wiley Publishing Company

[65] Reddy, J. N., *An Introduction to Finite Element Method,* 1993, New York, U. S. A., McGraw-Hill Inc.

[66] Bathe, K. J., *Finite Element Procedures,* 1996, New Jersy, U. S. A., Princeton Hall.

[67] Weaver, W. Jr., Timoshenko, S. P., and Young, D. H., *Vibration Problems in Engineering,* 1990, New York, U. S. A., Wiley Publishing Company.

[68] Yang, T. Y., *Finite Element Analysis of Structures,* 1985, New York, U. S. A., Wiley Inc.

[69] Paz, M, *Structural Dynamics – Theory and Computation,* 1997, New York, U. S. A., Chapman & Hall Inc

[70] Abd EL-Maksoud, Mohamed A, "Dynamic analysis and buckling of variable-thickness laminated composite beams using conventional and advanced finite element formulations", M. A. Sc. Thesis, 2000, Concordia University.

[71] Whitney, J. M., and Ashton, J. E., *Structural Analysis of Laminated Anisotropic Plates,* 1987, Lancaster, Pa., U. S. A., Technomic Publishing Company.

[72] Berthelot, J. M., *Composite Materials – Mechanical Behavior and Structural Analysis,* 1999, U. S. A, Springer Verlag, New York Inc.

[73] Reddy, J. N., *Mechanics of Laminated Composite Plates - Theory and Analysis,* 1997, U. S. A., CRC Press

[74] Gere, J. M., and Timoshenko, S. P., *Mechanics of Materials,*1990, Boston, U. S. A., PWS-Kent Publishing Company.

[75] Kim, D. H., *Composite Structures for Civil and Architectural Engineering,* 1995, U. S. A., E & FN Spon.

[76] Meirovitch, L., and Bahruh, H., "On the inclusion principle for the hierarchical finite element method", International Journal of Numerical Methods in Engineering, Vol. 19, 1983, pp. 281-291.

[77] Botting, A. D., Vizzini, A. J., and Lee, S.W., "Effect of ply-drop configuration on delamination strength of tapered composite structures", AIAA Journal, Vol. 34(8), 1996, pp. 1650-1656.

[78] Fish, J. C., and Vizzini, A. J., "Tailoring concepts for improved structural performance of rotorcraft flexbeams", Composites Engineering, Vol. 2(5), 1992, pp. 303-312.

APPENDIX - I

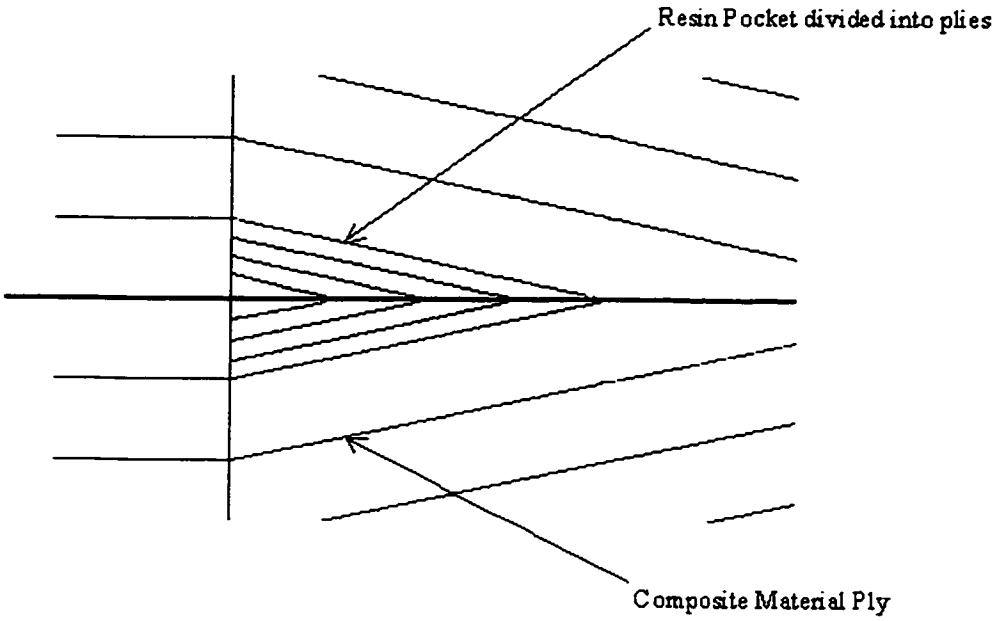

Figure AI.1 Division of resin pocket into plies for analysis

For composite materials,

$$(\overline{Q}_{11})_p = (\cos^4\theta)Q_{11} + (\sin^4\theta)Q_{22} + 2(\cos^2\theta)(\sin^2\theta)Q_{12} + 4(\cos^2\theta)(\sin^2\theta)Q_{33} \qquad \text{(AI.1)}$$

where,

$$Q_{11} = \frac{E_1}{1-\upsilon_{12}\upsilon_{21}}; \qquad Q_{12} = \frac{\upsilon_{12}E_2}{1-\upsilon_{12}\upsilon_{21}}; \qquad Q_{21} = Q_{12}; \qquad Q_{22} = \frac{E_2}{1-\upsilon_{12}\upsilon_{21}};$$

and $Q_{33} = G_{12}$

For the case of an isotropic material, $\overline{Q}_{11} = Q_{11} = \frac{E}{1-\upsilon^2}$

APPENDIX - II

The calculation of the stiffness matrix of the tapered composite beam by the trigonometric hierarchical finite element method would involve modeling the whole beam by one element and increasing the number of trigonometric terms in the element. Since there is a continuous drop in the number of plies over the length of the beam, the value of the bending coefficient, D_{11}, which is dependent on the number of plies, will also vary over the length of the beam. Hence we would consider sections of the beams where the number of plies are the same. This would also necessitate that we split the integration for the calculation of the stiffness matrix into as many parts as the number of sections of the beam. Each section would have a different expression for the bending coefficient, D_{11}, and the expression for the stiffness for the tapered beam of Figure AII.1 would be as follows,

$$K_{ij} = \frac{1}{l^3}\left(\int_0^{1/2} \left(b(D_{11}(\xi))_I \frac{d^2N_i}{d\xi^2}\frac{d^2N_j}{d\xi^2} \right) d\xi + \int_{1/2}^{1} \left(b(D_{11}(\xi))_{II} \frac{d^2N_i}{d\xi^2}\frac{d^2N_j}{d\xi^2} \right) d\xi \right) \qquad \text{(AII.1)}$$

where $(D_{11}(\xi))_I$ and $(D_{11}(\xi))_{II}$ are the expressions for the bending coefficient, D_{11}, for the two sections . The calculation of the expressions for D_{11} for individual section is details as follows. We will take a section that has a resin pocket in it so that we can see how we take the influence of the resin pocket into account.

The expression for the bending coefficient, D_{11}, is as given in Equation (AII.2), where m1 is the number of plies in the section considered, m is the slope of the taper and

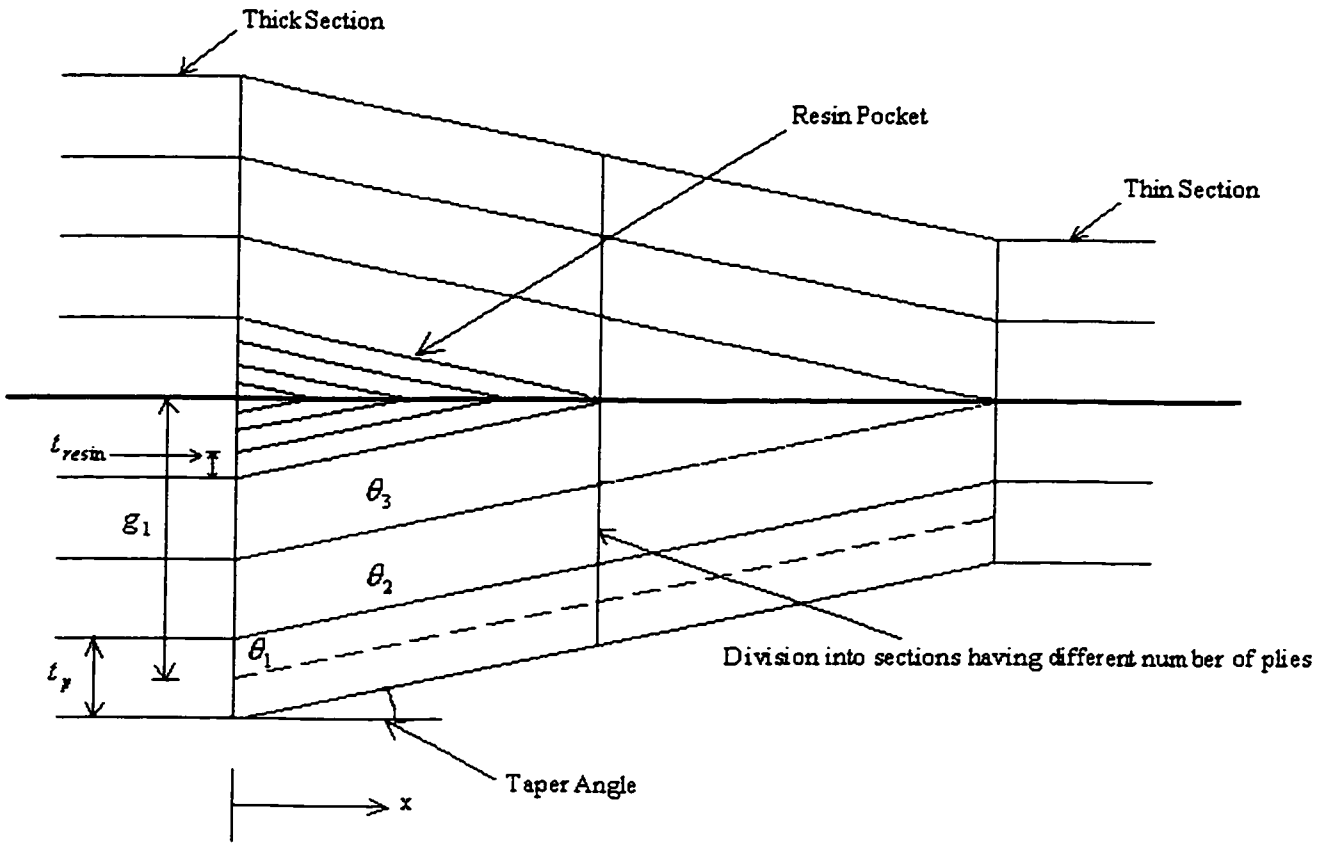

Figure AII.1 Schematic of a composite mid-plane tapered beam showing the division into different sections

$$D_{11} = \sum_{p=1}^{m1}\left[t_p(mx+g)_p^2 + \frac{t_p^3}{12}\right](\overline{Q}_{11})_p \qquad \text{(AII.2)}$$

g is the intercept on the y-axis. Considering one ply at a time, the expression of D_{11} for the ply having an angle of θ_1 will be as follows (see Figure AII.1),

$$D_{11}(\theta_1) = \left[t_p(mx+g_1)^2 + \frac{t_p^3}{12}\right](\overline{Q}_{11}(\theta_1)) \qquad \text{(AII.3)}$$

where,

$$(\overline{Q}_{11}(\theta_1)) = (\cos^4\theta_1)Q_{11} + (\sin^4\theta_1)Q_{22} + 2(\cos^2\theta_1)(\sin^2\theta_1)Q_{12} + 4(\cos^2\theta_1)(\sin^2\theta_1)Q_{33} \quad \text{(AII.4)}$$

and the values of the coefficients Q_{11}, Q_{22}, Q_{12}, Q_{33} are given in Appendix-I.

Similarly, expressions of D_{11} for other plies having angles, θ_2 *and* θ_3, can also be obtained and summed to obtain the final expression for, D_{11}, of the given section. In the case of the resin pocket, the resin pocket is divided into a number of plies and each ply is again considered in the same manner as done for composite plies. As given in Figure AII.1, the expression for D_{11} for the resin pocket will be,

$$D_{11}(re\sin) = \left[(t_{re\sin})(mx + g)^2 + \frac{t_{re\sin}^3}{12} \right] \left(\overline{Q}_{11}\ (re\sin) \right) \quad \text{(AII.5)}$$

where,

$\overline{Q}_{11}(re\sin) = Q_{11} = \dfrac{E}{1-\upsilon^2}$ and $t_{re\sin}$ is as given in the Figure AII.1.

The program developed in MATLAB® has provision to detect the presence of a resin pocket and calculate the $D_{11}(re\sin)$ as given in Equation (AII.5). It then adds the calculated $D_{11}(re\sin)$ to the D_{11} obtained for other composite plies. Hence we obtain the final expression for the coefficient, D_{11}, for the considered section. Similarly, the expressions of D_{11} for all the sections are obtained by the program and used in the calculation of the stiffness matrix.